DISSERTATION

WESTERN EQUINE ENCEPHALITIS VIRUS: NEUROINVASION, PATHOGENESIS, AND IMMUNOMODULATORY TREATMENT STRATEGIES

Submitted by

Aaron Timothy Phillips

Department of Microbiology, Immunology, and Pathology

In partial fulfillment of the requirements

For the Degree of Doctor of Philosophy

Colorado State University

Fort Collins, Colorado

Fall 2013

Doctoral Committee:

Advisor: Kenneth Olson

Carol Blair Brennan
Tawfik Aboellail
Ronald Tjalkens

ABSTRACT

WESTERN EQUINE ENCEPHALITIS VIRUS: NEUROINVASION, PATHOGENESIS AND IMMUNOMODULATORY TREATMENT STRATEGIES

Western equine encephalitis virus (WEEV; *Alphavirus*) is a mosquito-borne virus that can cause severe encephalitis in humans and equids. WEEV is closely-related to eastern equine encephalitis virus (EEEV) and may model similar pathogenesis in a mouse model. Previous studies have shown that intranasal infection of outbred CD-1 mice with the WEEV McMillan (McM) strain result in high mortality within 4 days of infection, thus providing a model of exposure to airborne encephalitic alphavirus. In addition, WEEV McM causes high mortality within 5-7 days following peripheral inoculation of mice. Therefore, WEEV McM may be used to model infection following exposure to infected mosquitos. The route of WEEV entry into the central nervous system (CNS) is not well-understood. In the studies presented here, bioluminescence (BLM) imaging and recombinant reporter viruses based on WEEV McM were applied to detect and track virus in mice following intranasal or subcutaneous inoculation, and used to determine correlation between BLM and viral titer. Additionally, histopathology analysis was guided by corresponding BLM images and used to identify specific CNS regions affected during infection.

The major findings from these studies indicate that WEEV McM uses a different route for entry into the CNS for each of the two inoculation methods (intranasal or footpad). Intranasal challenge resulted in neuroinvasion occurring primarily through cranial nerves, mainly in the olfactory tract. Olfactory bulb neurons were initially infected followed by spread of the infection into different regions of the brain. WEEV distribution was confirmed by immunohistochemistry

as having marked neuronal infection but very few infected non-neuronal glial cells. Axons displayed infection patterns consistent with viral dissemination along the neuronal axis. The trigeminal nerve served as an additional route of neuroinvasion showing significant FLUC expression within the brainstem. Neuroinvasion from footpad inoculation demonstrated a consistent pattern in the spatiotemporal distribution of virus among the imaged brains, none of which involved the olfactory bulb. These studies support the hypothesis that neuroinvasion of WEEV likely occurs in areas of the CNS where the blood-brain barrier is naturally absent. These areas include the median eminence of hypothalamus (hypothalamic output), posterior pituitary, pineal body, and the area postrema.

There are no antiviral therapies against alphaviral disease and current vaccine strategies target only a single alphavirus species. In an effort to develop new tools for a broader response to outbreaks, a novel alphavirus vaccine comprised of cationic-lipid-nucleic acid complexes (CLNCs) and the ectodomain of WEEV E1 protein (E1ecto) was designed and tested. Interestingly, the CLNC component alone had therapeutic efficacy as it increased survival of CD-1 mice following lethal WEEV infection. Immunization with the CLNC-WEEV E1ecto mixture (lipid-antigen-nucleic acid complexes; LANACs) using a prime/boost regimen provided strong protection in mice challenged with WEEV subcutaneously, intranasally, or via mosquito. In addition, the LANAC immunization protocol significantly increased survival of mice following intranasal or subcutaneous challenge with EEEV, indicating potential as a ‘pan-alphavirus’ vaccine candidate. Mice immunized with LANAC mounted a strong humoral immune response, but did not produce neutralizing antibodies.

ACKNOWLEDGMENTS

I would like to thank my advisor, Dr. Kenneth Olson, for the faith and unwavering support he provided throughout my graduate studies. I have learned an immense amount while under his tutelage and am grateful for the opportunity. I would like to extend my gratitude to my committee members, Drs. Carol Blair Brennan, Tawfik Aboellail, and Ronald Tjalkens. Your guidance throughout the various stages of my studies was invaluable. I would like to thank Todd Bass for histological preparation of specimens, Dr. Eric Mossel and Cori Mossel for technical assistance, Amber Rico for imaging assistance, Lab Animal Resources at Colorado State University for excellent care of our mice, and Dr. Anna D. Fails for helpful neuroanatomy consultation. I would like to thank Dr. Steve Dow for providing the liposomes, Dr. Richard Bowen for performing the EEEV challenge experiments, Lab Animal Resources (Colorado State University) for outstanding care of the animals used in these studies, Dr. Gerald Callahan for assistance in writing, Dr. C. Brandon Stauft for generating 'McFire', Dr. David Piwnica-Worms for providing the transgenic mice, Monica Heersink for care and maintenance of mosquitoes, and Tach Costello and Susan Rogers for superior administrative support. I would also like to thank the National Institutes of Health and the Rocky Mountain Regional Center of Excellence for Biodefense and Emerging Infectious Diseases for providing the support for these studies.

DEDICATION

I dedicate this dissertation to Wendy, Ava, and Lola. Your love and support mean the world to me and I appreciate the sacrifices you have made throughout my studies. I could not have done it without you. You are the wind in my sails.

TABLE OF CONTENTS

LIST OF TABLES

LIST OF FIGURES

CHAPTER 1: LITERATURE REVIEW

Introduction

Arthropods are invertebrate animals belonging to the phylum *Arthopoda*, a name referencing the articulated nature of the jointed appendages characteristic of these animals. Examples of arthropods include insects, arachnids, and crusteans. A sub-group of arthropods are considered to be hematophagous, meaning that, at some stage during their life cycle, the arthropod feeds on the blood of a live vertebrate host. Well-known hematophagous arthropods include mosquitoes, biting flies, ticks, kissing bugs, fleas, and lice.

A group of viruses, known as arthropod-borne viruses or 'arboviruses', exist by means of a biological transmission-cycle involving hematophagous arthropods and vertebrate hosts (amphibians, reptiles, birds, and mammals). Arboviruses, therefore, represent an important collection of viruses capable of inducing viremia in a vertebrate host, and virus replication in the vector. Transmission between arthropods or between vertebrates has been reported for some arboviruses. For example, the pathogenic arbovirus, LaCrosse virus, can be transovarially transmitted by *Aedes triseriatus* mosquitoes and overwinters in diapausing eggs (Reese, Mossel et al. 2010). This phenomenon is known as vertical transmission. Tick-borne viruses may be transmitted to tick offspring via vertical transmission, but transmission may also occur between co-feeding ticks, a phenomenon known as horizontal transmission (Havlikova, Lickova et al. 2013). Evidence for person-to-person transmission of an arbovirus can be found in a report in which Zika virus was transmitted, possibly through sexual intercourse, from an infected individual during the convalescent stage of Zika-induced disease (Foy, Kobylinski et al. 2011). However, life-cycle maintenance of arboviruses primarily involves two alternating transmission

events: 1) arthropod-to-vertebrate transmission through infectious virus excretion in arthropod salivary gland secretions, resulting in infection of vertebrate tissue, and 2) vertebrate-to-arthropod transmission through arthropod ingestion of viremic blood from an infected vertebrate host, resulting in virus infection of an arthropod's digestive tract tissue. In both these cases, transmission involves hematophagous activity by the arthropod.

Arboviruses are distributed globally and are responsible for emerging and re-emerging infectious disease (Weaver and Barrett 2004; Dash, Bhatia et al. 2013). Most arboviruses are represented by four families of RNA viruses: *Togaviridae, Flaviviridae, Bunyaviridae* and *Reoviridae* (Table 1.1). Importantly, not all virus species belonging to these families are arboviruses. Hepatitis C virus is a member of the family Flaviviridae, but is not transmitted by arthropod vectors. Some members of these virus families are vectored by arthropods but infect plants, such as Tomato spotted-wilt virus in the family Bunyaviridae. Highly pathogenic arboviruses that are transmitted by mosquitoes include dengue virus (DENV), West Nile virus (WNV), chikungunya virus (CHIKV). Highly pathogenic arboviruses that are transmitted by ticks include and Crimean-Congo hemorrhagic fever virus (CCHFV) and tick-borne encephalitis virus (TBEV) (Metz and Pijlman 2011).

Arboviruses can cause a variety of diseases in humans, including hemorrhagic fever, hepatitis and encephalitis. These human diseases result in hundreds of thousands of deaths each year (Whitehead, Blaney et al. 2007). Additionally, epizootic outbreaks can occur which domesticated animals. Important arboviruses affecting these animals include Venezuelan equine encephalitis virus (VEEV), Rift Valley fever virus (RVFV), and bluetongue virus (BTV). These viral agents cause dramatic losses of livestock in short periods of time, especially in cases when

prophylactic or therapeutic treatments are not available (Savini, MacLachlan et al. 2008; Paessler and Weaver 2009).

Table 1.1 Arboviruses of medical importance. Adapted from (Metz and Pijlman 2011).

Family/genus	Species	Vector		Clinical symptoms	Geographical distribution
Togaviridae					
Alphavirus	Eastern equine encephalitis virus (EEEV)	Mosquito	Culiseta sp.	Febrile illness, encephalitis	N/S-America
	Western equine encephalitis virus (WEEV)	Mosquito	Culex sp.	Febrile illness, encephalitis	N/S-America
			Culiseta sp.		
	Venezuelan equine encephalitis virus (VEEV)	Mosquito	Culex sp.	Febrile illness, encephalitis	N/S-America
	Sindbis virus (SINV)	Mosquito	Culex sp.	Febrile illness, arthritis	Africa, Asia, Australia, Asia, Europe
	Semliki Forest virus (SFV)	Mosquito	Aedes sp.	Febrile illness, arthritis	Africa, Asia
	Chikungunya virus (CHIKV)	Mosquito	Aedes sp.	Febrile illness, arthritis	Africa, Asia, Europe
	O'nyong nyong virus (ONNV)	Mosquito	Anopheles sp.	Febrile illness, arthritis	Africa
	Ross River virus (RRV)	Mosquito	Culex sp.	Febrile illness, arthritis	Australia
Flaviviridae					
Flavivirus	Dengue 1-4 (DENV)	Mosquito	Aedes sp.	Febrile illness, hemorrhagic fever	N/S-America, Asia, Australia, Africa
	Yellow fever virus (YFV)	Mosquito	Aedes sp.	Hepatitis, hemorrhagic fever	N/S-America, Africa
	Japanese encephalitis virus (JEV)	Mosquito	Culex sp.	Febrile illness, encephalitis	SE Asia
	West Nile virus (WNV)	Mosquito	Culex sp.	Febrile illness, encephalitis	N-America, Africa, M-East, Europe
	St.Louis encephalitis virus (SLEV)	Mosquito	Culex sp.	Encephalitis	N/S-America
	Tick-borne encephalitis virus (TBEV)	Tick	Ixodes sp.	Encephalitis	Europe, Asia
Bunyaviridae					
Nairovirus	Crimean-Congo hemorrhagic fever virus (CCHFV)	Tick	Hyalomma sp.	Hemorrhagic fever	Africa, Asia, Europe
Orthobunyavirus	La Crosse virus (LACV)	Mosquito	Aedes sp.	Encephalitis	N-America
Phlebovirus	Rift valley fever virus (RVFV)	Mosquito	Aedes sp.	Hemorrhagic fever, encephalitis	Africa
Reoviridae					
Orbivirus	Bluetongue virus (BTV)	Midge	Culicoides sp.	Febrile illness, cyanosis	N/S-America, Africa, Asia, Europe
	African horse-sickness virus (AHSV)	Midge	Culicoides sp.	Respiratory failure, fever	Africa, M-East, Europe
	Colorado tick fever virus (CTFV)	Tick	Dermacentor sp.	Febrile illness, malaise	N-America

Among the 500 known arboviruses, 63 were first isolated in North America (Calisher 1994). Six of these viruses are human pathogens: western equine encephalitis virus (WEEV), eastern equine encephalitis virus (EEEV), St. Louis encephalitis virus (SLEV), Powassan (POW) virus, LaCrosse virus (LACV), and Colorado tick fever virus (CTFV). All but one of the arboviral pathogens can cause encephalitis; only CTFV does not (Calisher 1994). The designers of offensive biological warfare programs recognized the potential of some American arboviruses to be weaponized. The alphaviruses (EEEV, WEEV, and VEEV) were determined to provide the greatest potential for weaponization due to their ease of production, stability when lyophilized, and high morbidity or mortality rate when transmitted through methods involving airborne virus (Steele, Reed et al. 2007). Thus, alphaviruses are considered to be among the most medically important arboviruses (Hollidge, Gonzalez-Scarano et al. 2010).

Alphaviruses

Of the 29 mosquito-borne viral species that belong to the *Alphavirus* genus of the family *Togaviridae*, at least 16 are known to cause disease in humans and other animals (Karabatsos 1985; Calisher 1994; Del Piero, Wilkins et al. 2001; Griffin, Byrnes et al. 2004). Although arthritis, acute flu-like illness, and rash are attributable to many alphaviral infections, some alphavirus species lead to CNS infection and encephalitis. Alphaviruses most often associated with CNS infection are limited to the Americas, and include strains of EEEV, VEEV, and WEEV (Steele, Reed et al. 2007).

WEEV is normally maintained in a transmission cycle involving *Culex tarsalis* mosquitoes and passerine birds (Hardy 1987). Equids and humans can be infected but do not contribute to the maintenance cycle, and are referred to as 'dead-end' hosts. In fact, WEEV was initially isolated during an epizootic outbreak of equine encephalitis in the San Joaquin Valley of California. This particular outbreak affected almost 6,000 horses and was associated with an equine mortality rate of 50% (Meyer, Haring et al. 1931). Enzootic activity of WEEV in the western U.S. is detected most summers using serological surveillance of sentinel animals or through vector surveillance programs (Reisen, Hardy et al. 1995). According to the USDA, epizootics have been reported in horses (Canada 1975), turkeys (California 1993–1994; Nebraska 1957), and emus (Texas and Oklahoma 1992). These findings highlight the potential for a WEEV outbreak in humans. Naturally-acquired WEEV infection of humans has been estimated to yield fatality rates of 8% to 15% (Steele, Reed et al. 2007). Human patients may present clinically with symptoms ranging from an acute febrile illness to fulminant encephalitis. Neurologic sequelae may be present in survivors, particularly children and infants (Finley, Longshore et al. 1955). Thankfully, there has been a recorded decrease in WEEV activity in

North America over the past 20–30 years, resulting in no recent human cases. The reason behind the decline in WEEV cases in humans is not known. Evaluation of 10 WEEV strains, representing a variety of isolation locations, hosts, and all decades from the 1940's to the 1990's, failed to show evidence of a decline in virulence (Forrester, Kenney et al. 2008). Additionally, a study evaluating the growth kinetics of WEEV strains isolated over the past 60 years found minimal differences in in vitro growth patterns among these strains, despite their genetic differences and separation in time and space (Reisen, Fang et al. 2008).

Despite the lack of evidence for a decrease in virulence among WEEV isolates over the past 60 years, a consistent finding is that WEEV isolates exhibit a broad range of virulence in mice regardless of the decade in which they are collected. Experimental evidence suggests that WEEV strains can be categorized into high and low mortality phenotypes in mice (Nagata, Hu et al. 2006; Forrester, Kenney et al. 2008; Logue, Bosio et al. 2009). Among the high mortality phenotypes, WEEV McMillan strain (McM) induces rapid and lethal encephalitic disease in a mouse infection model and is the basis of the studies presented throughout this dissertation. The McM strain was isolated from a human case from Canada in 1942, but the details regarding its passage history are unknown. Among the low mortality phenotypes, WEEV Imperial-181 strain (IMP) was reported to be essentially avirulent in mice (Logue, Bosio et al. 2009). Perhaps the most informative study regarding the mechanism behind the decline in human cases of WEEV-induced encephalitis comes from a study in which a panel of chimeric viruses was generated from McM and IMP strains (Mossel, Ledermann et al. 2013). Testing revealed that a single amino acid at position 214 within the E2 protein was important for neurovirulence and mosquito-infectivity and that the two phenotypes (neurovirulent infection of the vertebrate host or disseminated infection in the vector) were mutually exclusive.

Molecular virology of alphaviruses

All alphaviruses have an enveloped nucleocapsid containing a single-stranded, positive-sense RNA genome with a 5′ methylated cap and 3′ polyadenylated termini. The 5′ end of the viral genome is translated into 4 nonstructural proteins (nsP 1–4) that form viral replication complexes. A negative-strand RNA replication intermediate is generated and contains a subgenomic promoter (SGP) or internal initiation site that initiates transcription of the 26S subgenomic RNA. The 26S subgenomic RNA encodes the structural proteins (capsid, E3, E2, 6K, and E1) used in the assembly of new virions. We will now review the alphavirus proteins individually to determine their role(s) during infection.

Nonstructural protein 1 has both guanine-7-methyltransferase and guanylyltransferase enzymatic activities, and functions to synthesize the cap structure to viral RNA (Cross 1983; Mi and Stollar 1991; Laakkonen, Hyvonen et al. 1994). The nonstructural protein 2 has multiple known enzymatic activities and roles, including helicase activity required for RNA duplex unwinding during RNA replication and transcription (Gomez de Cedron, Ehsani et al. 1999), RNA triphosphatase and nucleoside triphosphatase activity (Rikkonen, Peranen et al. 1994; Vasiljeva, Merits et al. 2000), and protease activity for cleaving the viral nonstructural polyprotein into intermediate and final component proteins (Strauss, De Groot et al. 1992).The function of nonstructural protein 3 is not well-understood. Reports indicate that nsP3 is required for minus-strand and subgenomic RNA synthesis (Hahn, Strauss et al. 1989; Lemm, Rumenapf et al. 1994; Shirako and Strauss 1994), and may play a role in modulation of pathogenicity in mice (Tuittila and Hinkkanen 2003; Park and Griffin 2009). The nsP3 was also shown to possess both ADP-ribose 1-phosphate phosphatase activity and RNA-binding activity, important in the induction of apoptosis in infected cells (Malet, Coutard et al. 2009). The final nonstructural

protein, nonstructural protein 4, functions as the RNA-dependent RNA polymerase (RdRP) (Kamer and Argos 1984; Hahn, Grakoui et al. 1989).

The alphavirus structural proteins are translated as a polyprotein from the subgenomic RNA (Raju and Huang 1991). The capsid protein is translated first and is cleaved from the polyprotein by autoproteolysis. Release of the capsid protein from the nascent polypeptide chain allows a signal sequence at the N-terminus to be recognized. This signal sequence prompts the translocation of the remaining sequence across the ER membrane (Garoff, Huylebroeck et al. 1990). Within the ER, E1 and pE2 undergo post-translational modifications, including glycosylation (Metz and Pijlman 2011). Dimerization of pE2 and E1 is required for the transport of the glycoproteins to the cell surface (Johnson, Schlesinger et al. 1981). Prior to arrival at the cell membrane, pE2 is cleaved by furin to form E3 and E2 (Gaedigk-Nitschko and Schlesinger 1990). This cleavage event is required for maturation to allow entry into and fusion with new host cells (Salminen, Wahlberg et al. 1992; Heidner, McKnight et al. 1994).

Assembly of new virions begins with a single copy of the RNA genome being encapsidated within 240 copies of capsid protein, which together form the nucleocapsid core of the mature virion (Jose, Snyder et al. 2009). The molecular mechanism for encapsidation involves a nucleation event in which capsid (amino acids 81 to 112) recognizes an encapsidation signal on the genomic RNA (Weiss, Nitschko et al. 1989; Weiss, Geigenmuller-Gnirke et al. 1994; Linger, Kunovska et al. 2004). The budding of virions from the plasma membrane is the final stage of the virus life-cycle. The nucleocapsid cores, which are assembled in the cell cytoplasm, diffuse or actively transit to the plasma membrane. At the plasma membrane, nucleocapsid cores are bound by the cytoplasmic domain of E2, but not E1 (Kail, Hollinshead et al. 1991; Zhao and Garoff 1992; Liu and Brown 1993; Liu and Brown 1993; Strauss, Strauss et

al. 1995). This interaction seeds the formation of the envelope as the virus buds from the host cell.

Alphavirus expression systems

Alphavirus genomic RNA is fully infectious when transfected into permissive cells. Consequently, alphavirus genomes are readily manipulated in the laboratory using cDNA synthesis and traditional cloning techniques followed by *in vitro* transcription of the viral genome. During this process, the virus genome is *in vitro* transcribed from a linearized IC plasmid using bacteriophage RNA polymerase such as T7 polymerase. The resulting RNA can be electroporated (or chemically-transfected) into permissive cells. The result is the production of infectious virus particles.

Importantly, recombinant alphaviruses have been developed in which the SGP sequence is duplicated to drive expression of heterologous genes during infection (RaymsKeller, Powers et al. 1995; Olson, Myles et al. 2000; Cook and Griffin 2003; Foy, Myles et al. 2004; Vanlandingham, Tsetarkin et al. 2005; Ryman, Gardner et al. 2007; Ryman, Gardner et al. 2007; Foy and Olson 2008; Patterson, Poussard et al. 2011; Ziegler, Nuckols et al. 2011). Other authors have referred to these engineered recombinant viruses as 'alphavirus expression systems' (AES) (Foy and Olson 2008). Most AESs which have been developed to date have been based on Old World alphaviruses such as Sindbis (Higgs, Powers et al. 1993; Higgs, Olson et al. 1995; RaymsKeller, Powers et al. 1995; Powers, Kamrud et al. 1996; Olson, Myles et al. 2000; Cook and Griffin 2003; Foy, Myles et al. 2004; Ryman, Gardner et al. 2007; Ryman, Gardner et al. 2007; Zhang, Burke et al. 2007), Semliki Forest (Liljestrom and Garoff 1991), O'nyong-nyong (Brault, Foy et al. 2004), or chikungunya viruses (Ziegler, Nuckols et al. 2011). Although these

AESs have significantly enhanced our understanding of virus-vector and virus-host interactions, reports of AESs based on propagating New World encephalitic alphavirus isolates are less prevalent in the literature (Caley, Betts et al. 1997; Gardner, Ebel et al. 2011; Patterson, Poussard et al. 2011). To our knowledge, there have been no reports describing an infectious WEEV-based AES.

A more complete understanding of the alphavirus infection patterns in vertebrates is crucial to characterizing the pathogen-host relationship. The technology of in vivo imaging promises to streamline the process of investigating infectious agents in an animal model. Firefly luciferase (FLUC) is a commonly used *in vivo* as a BLM reporter. FLUC catalyzes the oxidation of its substrate, luciferyl adenylate (luciferin), with the products being light, in the form of a photon, and oxyluciferin (Hopkins, Seliger et al. 1967). Firefly luciferase (FLUC) and its substrate, luciferin, were first used to describe the distribution of bacteria in a living host (Contag, Spilman et al. 1997) and the system has subsequently been used to describe infection in mice for herpesvirus type-I (Luker, Bardill et al. 2002), a neurovirulent strain of Sindbis virus (Cook and Griffin 2003; Ryman, Gardner et al. 2007; Ryman, Gardner et al. 2007; Gardner, Burke et al. 2008), VEEV (Patterson, Poussard et al. 2011), EEEV (Gardner, Burke et al. 2008; Gardner, Ebel et al. 2011), and human immunodeficiency virus (HIV) gene expression (Contag, Spilman et al. 1997). Research applying *in vivo* imaging technology to analyze vaccinia virus infection has shown potential for predicting lethality of virus infection based on luminescence (Zaitseva, Kapnick et al. 2009).

The studies presented in this dissertation include the use of recombinant WEEV virus engineered to express luciferase (McFire and McFly) or to induce the expression of luciferase in a transgenic animal (Tg UAS-LUC) through the viral expression of the transactivator GAL4-

VP16 (McGal). A diagram illustrating the layout of the respective virus genomes are presented in Figure 1.1. Collectively, this panel of recombinant WEEV McM viruses comprises an important set of tools, which provide the researcher with a convenient method for monitoring infection progress. The resulting data are important to the development of an animal model of WEEV infection.

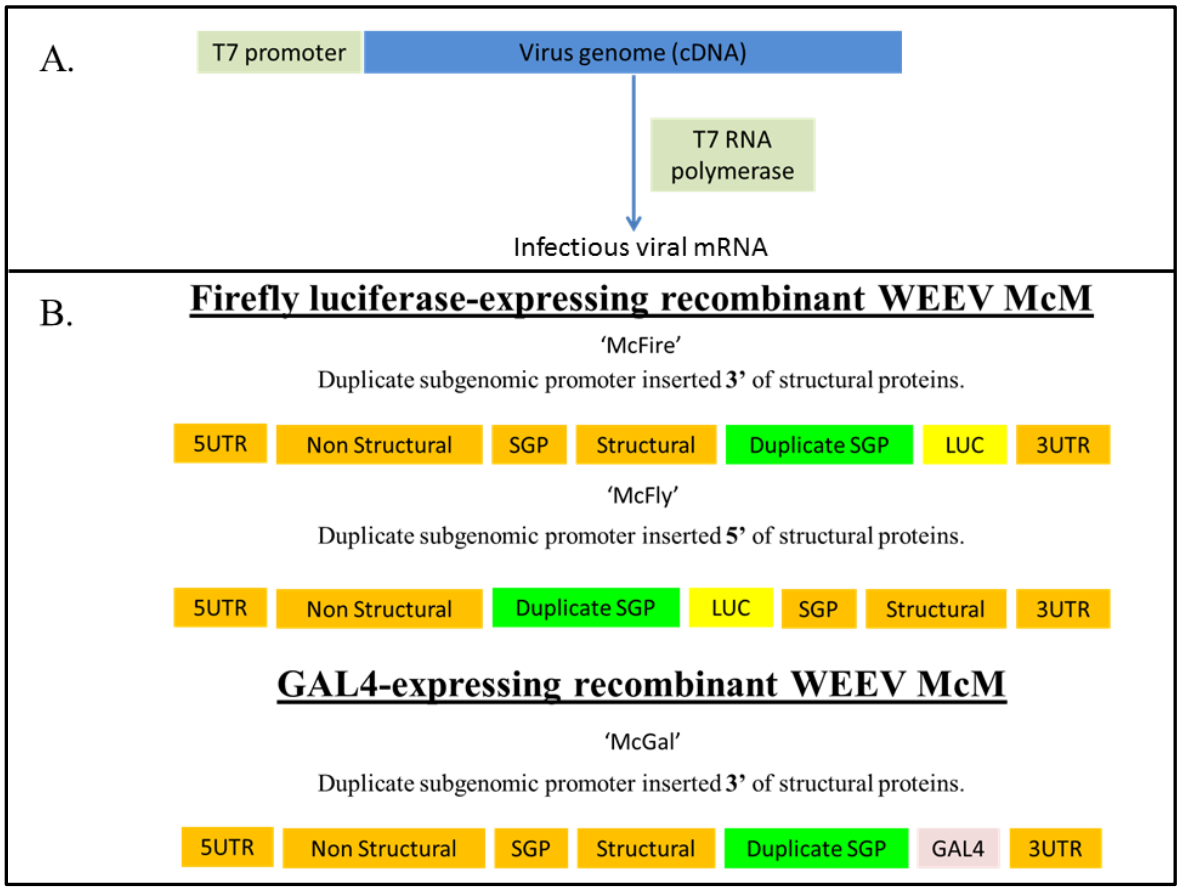

Figure 1.1 Diagram of recombinant western equine encephalitis viruses used throughout this dissertation. A) Diagram illustrating the *in vitro* generation of infectious viral mRNA from the infectious clone plasmid using the bacteriophage T7 promoter and polymerase. B) Schematic diagram illustrating the layout of the genome for each recombinant virus used in these studies. subgenomic promoter (SPG), untranslated region (UTR).

A well-characterized animal model is a crucial component of antiviral research. This is especially true when considering pathogens such as WEEV, in which the target cells (neurons) are difficult to work with in culture. Additionally, components of the CNS, such as the blood-brain-barrier and multiple cell types, are absent from *in vitro* model systems. Outbred CD-1 mouse model of McM infection has been developed and used to characterize the infection using traditional methods (Logue, Phillips et al. 2010). Pro-inflammatory chemokines and cytokines, such as MCP-1 and interferon-gamma, increased significantly in infected brain tissue (Logue, Phillips et al. 2010). Immunopathology may contribute to alphavirus-associated neuropathogenesis. This is supported in studies with VEEV, which have shown extended mean time to death of mice treated with anti-thymocyte serum (Woodman, McManus et al. 1975). In the case of neurovirulent Sindbis virus, neuronal death is due to inflammatory and excitotoxic insults or apoptosis depending on the strain of virus, age of the mouse, and specific neuroanatomical location (Griffin 2005).

Protective host-immune responses against infection with encephalitic alphavirus

The host-immune response to alphavirus infection has been well-studied. Early studies demonstrated that antibodies, which are not necessarily neutralizing to infectious virus particles, are capable of facilitating recovery from alphavirus infection of the CNS (Griffin and Johnson 1977). In these studies, intracerebral inoculation with neuroadapted Sindbis virus (NSV) was successfully treated by passive transfer of homologous immune serum at 24 hours post-infection. The protective component within the serum was determined to be Sindbis-specific IgG. This work was extended in a later study using severe combined immunodeficient (SCID) mice – a model of persistent alphavirus encephalomyelitis. Adoptive transfer of hyperimmune serum into persistently infected mice was sufficient to clear infectious virus and virus RNA from the

nervous system. Interestingly, adoptive transfer of sensitized T cells had no effect on viral clearance (Levine, Hardwick et al. 1991). Furthermore, Levine et al., demonstrated that the capability of an antibody to clear virus from either NSV-infected SCID mice or from NSV-infected primary rat neuron cultures was not related to the neutralization of infectious virus. These important studies indicate that there is a non-cytolytic mechanism of antibody action which is independent of MHC class I expression, as neurons do not express MHC-I molecules and therefore are not subject to CD8+ cell-mediated lysis. Additionally, Levine et al. showed that the mechanism of protection and clearance was independent of complement-dependent cell lysis. In those studies, neither treatment with cobra venom factor (to deplete the third component of complement), nor treatment with cyclo-phosphamide (to suppress natural killer cell function) prevented antibody-mediated clearance of virus from infected mice. Importantly, viral clearance from neurons occurred without any evidence of cellular lysis. CNS neurons are terminally-differentiated and are not replaced in the event that they are lost. A mechanism for viral clearance which preserves the function of the cell is of intense interest.

Treatments preventing encephalitic disease following infection with alphaviruses

Currently, no specific therapies are available for alphaviral infections. Unlicensed live attenuated and inactivated vaccines are available against some alphaviruses, but they can have significant side effects. VEEV TC-83 is an attenuated vaccine but all others are inactivated. The response rate to TC-83 immunization is 82%, and a single boost with formalin-inactivated C-84 vaccine increases the response rate to over 90%; however, adverse events are reported in 23% of recipients (Engler, Mangiafico et al. 1992). Thus, TC-83 is considered reactogenic and moderately effective as measured by neutralizing antibody. The formalin-inactivated WEEV TSI-GSD-210 vaccine produced neutralizing antibodies in fewer than half of subjects, thus is poorly

immunogenic (Pittman 1999). A formalin-inactivated EEEV vaccine (strain PE-6) induces neutralizing antibodies in less than 80% of those who receive two doses (Strizki and Repik 1995; Pittman 1999). Finally, immune interference has been reported with same-day administration of the two formalin inactivated WEEV and EEEV vaccines in humans (Reisler, Gibbs et al. 2012). Clearly, better vaccines and/or adjuvants are needed for New World alphaviruses.

Alphaviruses have two envelope glycoproteins, E2 and E1, which function in viral adsorption and penetration, respectively. Subunit vaccines consisting of recombinant forms of WEEV E2 or E1 have been reported to induce significant protection in animal models (Das, Gares et al. 2004; Wu, Barabe et al. 2007; Gauci, Wu et al. 2010). Although E2 is the major neutralizing antigen, E1 is more highly conserved among alphaviruses (Hahn, Lustig et al. 1988; Netolitzky, Schmaltz et al. 2000). One report, which investigated a panel of monoclonal antibodies specific to SINV structural proteins, showed anti-SINV E2 antibodies to be highly-neutralizing yet specific only to Sindbis virus antigen, while anti-SINV E1 antibodies were determined to be non-neutralizing yet cross-reactive to WEEV (McM strain) as well as VEEV (strain TC-83) and EEEV (New Jersey strain) (Roehrig, Gorski et al. 1982). Thus, E1 is an excellent vaccine candidate because it might offer broader ("pan-alphavirus") protection against fatal encephalitis. While antibodies targeting alphavirus E1 glycoprotein often fail to neutralize extracellular virus, non-neutralizing antibodies raised to the prototypic alphavirus (SINV) E1 glycoprotein are highly protective in an animal model of infection (Schmaljohn, Johnson et al. 1982). Possible mechanisms of protection resulting from anti-alphavirus E1 antibodies binding to infected cells are discussed later in this chapter.

The studies within this dissertation include the development of a vaccine candidate based on WEEV McM E1 glycoprotein. Adjuvants, which induce rapid antiviral protection from

innate-immune activation, are attractive platforms for development of a pan-alphavirus vaccine (Logue, Phillips et al. 2010). Cationic liposome-nucleic acid complexes (CLNCs) are potent activators of the innate immune system and are currently under investigation as vaccine adjuvants. The nucleic acid component of CLNCs, unmethylated CpG oligodeoxynucleotides (ODN) or the dsRNA analog polyinosinic:polycytidylic acid (PIC) are agonists of Toll-like receptor 9 (TLR9) and Toll-like receptor 3 (TLR3), respectively. Treatment with ODN or PIC results in strong cytokine/chemokine induction, establishing an antiviral state within the host. Accordingly, ODN or PIC have been used as components of vaccine formulations to enhance the host's immune response (von Hunolstein, Mariotti et al. 2001; Xie, Gursel et al. 2005; Sloat and Cui 2006; Fogg, Americo et al. 2007; Kumar, Koyama et al. 2008; Tewari, Flynn et al. 2010) and further studies have shown that adjuvants containing both ODN and PIC can enhance the immunogenicity of vaccines (Kasturi, Skountzou et al. 2011; Kidner, Morton et al. 2012). Although ODN and PIC can each induce an antiviral immune response within the host, the responses differ in expression profile, cellular localization, and signaling pathways (Kawai and Akira 2007). Importantly, WEEV, EEEV, and VEEV are exquisitely sensitive to experimental immunomodulation with ODN or PIC (Julander, Siddharthan et al. 2007; Logue, Phillips et al. 2010; Patterson, Poussard et al. 2011).

A promising treatment strategy for post-exposure control of alphavirus infection of the CNS is the passive-transfer of anti-alphavirus antibodies into the infected host. There have been multiple reports in which passive-immunotherapy used to successfully treat alphavirus infections of the CNS of mice (Phillpotts, Jones et al. 2002; Phillpotts 2006; Hunt, Bowen et al. 2011), and some specifically examining protection against WEEV (Olitsky, Schlesinger et al. 1943; Zichis and Shaughnessy 1945). One study reported that antibodies to the E1 protein of SINV, a member

of the WEEV antigenic complex of viruses, were also cross-protective against virus from a different antigenic complex, SFV of the SFV antigenic complex of viruses (Wust, Nicholas et al. 1989). Additionally, the antibodies used in this study were non-neutralizing to infectious virus. This finding suggests the possibility that antibodies targeting the E1 of an alphavirus could be developed to protect animals from multiple alphavirus species, regardless of virus neutralization capacity of the antibody. Protective isotypes were determined to be IgG class. IgM class antibodies failed to provide protection in these studies. As mentioned previously, anti-SINV E1 antibodies were determined to be cross-reactive with WEEV (McM), VEEV (TC-83), and EEEV (New Jersey) (Roehrig, Gorski et al. 1982). The development of a pan-alphavirus immunotherapeutic treatment would greatly benefit biodefense efforts and the general public health. Perhaps a combination of innate immunoactivation, immunization, and passive immunotherapy could provide rapid and long-lasting protections, especially in the event of intentional release scenarios, where individual dose amounts of virus could be meaningfully large.

Virus infections of the central nervous system

It is instructive to review what is known regarding neuroinvasion and pathogenesis of WEEV and other encephalitic viruses, as this information serves to better identify gaps in knowledge, as well as potential commonality among virus mechanisms of neuropathogenesis. Viruses affecting the human nervous system can lead to a broad-range of clinical outcomes. Affected regions of the brain can vary depending upon the species of virus, and in many cases, the specific virus sub-type or strain. Additionally, survivors of CNS infection can develop neurological sequelae, as indicated above for WEEV, and during the poliovirus epidemics of the 1940's and 50's (Trevelyan, Smallman-Raynor et al. 2005). At its peak (1950–1954),

poliomyelitis resulted in the paralysis of approximately 22,000 persons in the United States each year (Langmuir 1963).

Rapid onset of neurological symptoms during an acute viral infection can allow for timely virological investigations that link a viral isolate with a specific disease, as was the case for WEEV's initial isolation (Meyer, Haring et al. 1931). Causal relationship between virus and disease can be confirmed according to Koch's postulates. It is more difficult to link a viral species to diseases that manifest symptoms subsequent to viral clearance from the host. However, considerable evidence now implicates viral CNS infections as playing a role in some long-term and progressive neurodegenerative diseases (Mattson 2004). Following the 1918 "Spanish Flu" pandemic, nearly every patient who had an acute episode of encephalitis lethargica went on to develop post-encephalitic Parkinsonism (Dourmashkin 1997; Reid, McCall et al. 2001). Also, a number of neurotropic mosquito-borne viruses, including West Nile virus (WNV), Japanese encephalitis virus (JEV), and St. Louis encephalitis virus can cause PD-like symptoms in humans or rodents (Jang, Boltz et al. 2009). Older reports indicate that WEEV, also a mosquito-borne virus, may be capable of causing Parkinsonism in humans following encephalitic infection (Mulder, Parrott et al. 1951; Palmer and Finley 1956). Residual neurological defects can occur long after the WEEV infection has subsided and include tremor, intellectual deterioration, and cog-wheel rigidity. In a more recent report, 6 of 25 patients from a Colorado epidemic of WEEV presented with a 'parkinsonian syndrome' in the form of severe, progressive neurological sequelae (Schultz, Barthal et al. 1977). Furthermore, the 'spreading pathogen' hypothesis is supported by the asymmetry typically observed in certain neurodegenerative diseases such as PD (Hobson 2012).

Encephalitic viruses and their entry into the CNS

Virus mechanisms of neuroinvasion have been well-studied and involve at least one of two general mechanisms: 1) direct invasion of peripheral nerves (including cranial nerves), and subsequent spread of virus along the neuronal axis and into the CNS, or 2) virus (blood-borne or within infected cells) overcoming the blood-brain-barrier (BBB) of the host, to infect CNS tissue (Koyuncu, Hogue et al. 2013). For many of the arboviral encephalitides, the specific mechanisms of neuroinvasion remain unknown. Very few reports are available which have investigated, in detail, the spatio-temporal distribution of WEEV within the CNS. The latter point is further complicated by the fact that there are two, distinct routes of virus challenge used among published studies of WEEV (discussed in later sections), each exhibiting different disease phenotypes. Therefore, it is worthwhile to review what is currently known regarding virus mechanisms of neuroinvasion, and to consider the possibility that WEEV may behave similarly.

Direct invasion of peripheral nerves

Viruses are capable of directly infecting peripheral nervous tissue, and in doing so, may gain access to the CNS. Some viruses infect peripheral nerves as part of their natural maintenance cycle, as occurs with rabies virus or herpes viruses (Koyuncu, Hogue et al. 2013). Other neurotropic viruses demonstrate efficient neuroinvasion independent of any selective pressure to do so, as is the case with alphavirus infection of 'dead-end' hosts. Interestingly, many viruses share general mechanisms of neuroinvasion despite dramatic differences in virus genome characteristics (ssRNA, dsRNA, DNA, etc.), virion composition (enveloped or non-enveloped), and ecology. Table 1.1 summarizes the known or suspected routes of neuroinvasion for the viruses that are capable of causing neuropathological changes in animals, including humans.

Table 1.2 CNS entry routes for medically important viruses.

Genome	Virus Family	Naked/Enveloped	Viruses	CNS entry
dsDNA	Adenoviridae	Naked	MAV-1[1]	BBB and BMVECs
	Herpesviridae	Enveloped	alpha herpesvirus[2]	sensory nerve endings and ORN
			HSV-1, HSV-2, VZV, PRV, and BHV	
			beta herpesvirus[3]	BBB and BMVECs
			HCMV	
			gamma herpesvirus[4]	BBB and BMVECs
			EBV	
	Polyomaviridae	Naked	JCV[5]	BBB and BMVECs
dsRNA	Reoviridae	Naked	T3[6]	BBB and peripheral nerve
(+)ssRNA	Coronaviridae	Enveloped	MHV[7]	peripheral nerve and ORN
	Flaviviridae	Enveloped	WNV[8], JEV[9], and TBEV[10]	BBB, perpheral nerve, ORN and BMVECs
	Picornaviridae	Naked	poliovirus[11], EV71[12], and TMEV[13]	NMJ and BBB
	Togaviridae	Enveloped	EEEV[14], VEEV[15], WEEV[16], SINV[17], and SFV[18]	ORN, TGN, BBB(proposed)
(-)ssRNA	Arenaviridae	Enveloped	LCMV[19]	BBB
	Bornaviridae	Enveloped	BDV[20]	ORN
	Bunyavirdae	Enveloped	LACV[21,22]	ORN, BBB(proposed)
	Orthomyxoviridae	Enveloped	Influenza A[23]	perpheral nerve, ORN, TGN, and VGN
	Paramyxoviridae	Enveloped	morbilivirus[24]	BBB
			MV	
			rubulavirus[25]	BBB
			MuV	
			henipavirus[26]	BBB, ORN(proposed)
			HeV and Nipah	
	Rhabdoviridae	Enveloped	RabV[27] and VSV[20]	NMJs and ORN
ssRNA-RT	Retroviridae	Enveloped	HIV[28] and HTLV[28]	BBB
Key to abbreviations:				
BBB = blood-brain-barrier			HSV-2 = herpes simplex type-2	RabV = rabies virus
BDV = Borna disease virus			JCV = JC virus	SFV = Semliki Forest virus
BHV = bovine herpes virus			JEV = Japanese encephalitis virus	SINV = Sindbis virus
BMVECs = brain microvascular endothelial cells			LACV = LaCrosse virus	T3 = reovirus T3
EBV = Epstein-Barr virus			LCMV = lymphocytic choriommeningitis virus	TBEV = tick-borne encephalitis virus
EEEV = eastern equine encephalitis virus			MAV-1 = mouse adenovirus 1	TGN = trigeminal nerve
EV71 = enterovirus 71			MHV = mouse hepatitis virus	TMEV = Theiler's murine encephalomyelitis virus
HCMV = human cytomegalovirus			MuV = mumps virus	VEEV = Venezuelan equine encephalitis virus
HeV = Hendra virus			MV = measles virus	VGN = vagus nerve
HIV = human immunodeficiency virus			NMJs = neuromuscular junctions	VZV = varicella zoster virus
HTLV = human T-lymphotropic virus type 1			ORN = olfactory receptor neuron	WEEV = western equine encephalitis virus
HSV-1 = herpes simplex type-1			PRV = pseudorabies virus	WNV = West Nile virus
[1]Gralinski et al (2009)			[11]Ohka et al (2004)	[20]Mori et al (2005)
[2]Tirabassi et al (1998)			[12]Solomon et al. (2010)	[21]Johnson (1983)
[3]Fish et al (1998)			[13]Tsunoda and Fujinami (2010)	[22]Bennett et al (2008)
[4]Casiraghi et al (2011)			[14]Vogel et al (2005)	[23]Park et al (2002)
[5]Boothpur and Brennan (2010)			[15]Charles et al (1995)	[24]Schneider-Schaulies et al (2003)
[6]Richardson-Burns et al (2002)			[16]Reed et al (2005)	[25]Watanabe et al (2013)
[7]Bergmann et al (2006)			[17]Cook and Griffin (2003)	[26]Dups et al (2012)
[8]Verma et al (2010)			[18]Dropulic and Masters (1990)	[27]Ugolini (2011)
[9]Lai et al (2012)			[19]Bonthius (2012)	[28]Kaul et al (2001)
[10]Ruzek et al (2011)				

The specifics regarding each route, and the viruses known or suspected to use each route, are detailed in the following sections. The peripheral nervous system (PNS) is in direct contact with peripheral tissue and is not isolated from circulating blood by a barrier similar to the BBB. Therefore, peripheral nerves are relatively more accessible to invading viruses (Koyuncu, Hogue et al. 2013). Some viruses can enter the PNS by binding to receptors located at the axon terminus on sensory and autonomic nerves. Most alphaherpesviruses, belonging to the family *Herpesviridae*, utilize this method for neuroinvasion (Smith 2012). Representative alphaherpesviruses affecting humans include herpes simplex type-1 (HSV-1), herpes simplex type-2 (HSV-2), and varicella zoster virus (VZV). Other important alphaherpesviruses affecting animals other than humans include pseudorabies virus (PRV) and bovine herpes virus (BHV). The alphaherpesvirus infection process involves entry of virus into the axon termini of pseudo-unipolar sensory neurons by membrane fusion (Lycke, Hamark et al. 1988). In neurons, virus-plasma membrane fusion appears to be facilitated by the expression of the host protein Nectin-1, a member of the immunoglobulin superfamily. Subsequent to membrane fusion and entry, alpha herpesvirus capsid-inner tegument complexes interact with the intracellular-transport machinery of the host neuron, and are efficiently transported, in a retrograde direction, to the cell body. The molecular interactions responsible for the hijacking of neuronal transport machinery are thought to involve the viral protein VP1/2 and its recruitment of dynein motors (Zaichick, Bohannon et al. 2013). The alpha herpesviruses have evolved a method of maintaining quiescent infections in host PNS neurons, a unique feature among neurotropic viruses (Kramer, Cook et al. 2003). The quiescent state of the virus, also known as latency, can be reversed by stress-inducing stimuli, leading to the rapid production of virus progeny. Post-replication transport of alphaherpesviruses can occur in either retrograde or anterograde directions, a characteristic that very few neurotropic

viruses possess. The molecular details regarding the post-replication transport of virus are not completely understood and are the subject of some debate (Diefenbach, Miranda-Saksena et al. 2008; Smith 2012). In general, anterograde transport of virus may involve several viral proteins (gE, gI, and US9) and their recruitment of neuron-specific microtubule motor kinesin-3/KIF1A (Kramer, Greco et al. 2012; Smith 2012). In nature, spread of alphaherpesviruses into the CNS is rare in immune-competent hosts. This point is surprising, since infected neurons of the PNS ganglia share synaptic connections with neurons of the CNS. Nonetheless, herpesvirus infections typically remain limited to the PNS ganglia involved and the dermatome innervated by those infected neurons. HSV-1 infects the trigeminal ganglia and, accordingly, causes lesions around the oral cavity. HSV-2 infects the lumbar-sacral ganglia, and, accordingly, causes lesions in and around the genitals region (Margolis, Imai et al. 2007). However, when CNS invasion does occur, neuropathological changes can be debilitating (Tirabassi, Townley et al. 1998). In fact, herpes simplex encephalitis is one of the most severe virus diseases affecting the temporal lobe of humans (Hafezi and Hoerr 2013) and may rarely affect other regions such as the limbic system (Sokolov and Reincke 2012). Typical symptoms associated with herpesvirus encephalitis include fever, headache, and altered mental function.

Another route for the direct virus invasion of peripheral nerves is known to occur at neuromuscular junctions (NMJs). NMJs are specialized synapses that act to interface motor neurons with the muscles they control. Rabies virus (RABV), belonging to the *Lyssavirus* genus of the family *Rhabdoviridae*, and poliovirus, belonging to the *Enterovirus* genus of the family *Picornavirdae*, are known to invade the CNS through NMJs (Ohka, Matsuda et al. 2004; Ugolini 2011). RABV can infect many mammals including skunks, raccoons, bats, foxes, coyotes and dogs (Dyer, Wallace et al. 2013). RABV, which can be present in saliva of infected animals, can

come into contact with NMJs of a host via bites or scratches (Racaniello 2006). In humans, untreated RABV infection of the CNS almost always results in fatal acute myeloencephalitis. RABV enters the motor neurons at the NMJs by binding to nicotinic acetylcholine receptors and neural cell-adhesion molecules (Ugolini 2011). Spread of virus occurs exclusively along the neuronal axis and in a retrograde direction. Once RABV reaches the brain, a range of behavioral and neurological symptoms begin, to include insomnia, confusion, slight or partial paralysis, excitation, anxiety, agitation, hallucinations, hypersalivation, and hydrophobia. Specific brain regions that replicate virus and show neuropathological changes include the hippocampus, limbic regions, medulla and cerebellum. Death occurs within days of the onset of these symptoms.

Poliovirus typically enters the host through the fecal-oral-route. Poliovirus comes into contact with NMJs following ingestion of viral particles and initial replication of virus in intestinal mucosa (Racaniello 2006). A resulting transient viremia seeds other sites of replication such as reticulo-endothelial tissue and skeletal muscle. The host protein CD155, an immunoglobulin-superfamily member enriched on axonal membranes, is thought to be the receptor for poliovirus entry into motor neurons at NMJs (Ren and Racaniello 1992). Typically, the cell body of a motor neuron resides in the spinal cord and can be in synaptic contact with neurons within motor centers of the brain. Poliovirus infection progresses, in a retrograde direction, along motor neurons of the spinal cord to motor-associated nuclei of the brain. A study which examined brain lesions observed in autopsies of 158 polio patients indicated the following regions, in descending order of prevalence: reticular formation, vestibular nuclei, cerebellar fastigial nuclei, periaqueductal gray, hypothalamic nuclei, substantia nigra, and thalamic nuclei (Howe and Bodian 1942). Paralytic poliomyelitis is not typical and is estimated to occur in only 1-2% of poliovirus infections.

Virus invasion of cranial nerves is a well-represented mechanism of neuroinvasion among encephalitic viruses (see Table 1.1). Cranial nerves reported to be utilized as routes for virus invasion into the CNS include the first cranial nerve (olfactory nerve), the fifth cranial nerve (trigeminal nerve), and the tenth cranial nerve (vagus nerve). As previously discussed, HSV-1 infects the fifth cranial nerve (trigeminal nerve), but typically remains limited to the trigeminal ganglia in immune competent hosts. Other viruses are known to infect the trigeminal nerve and include influenza A virus (Park, Ishinaka et al. 2002) and VEEV (Charles, Walters et al. 1995). Influenza virus is also reported to neuroinvade through cranial nerve ten (vagus nerve), sympathetic nerves, and cranial nerve one (olfactory nerve) (Park, Ishinaka et al. 2002).

Direct invasion of cranial nerves

Virus invasion of the CNS through the olfactory nerves is a well-recognized route to encephalitis. The olfactory nerves are the only cranial nerves that originate from the telencephalon. The telencephalon is the anterior subdivision of the embryonic forebrain, which also gives rise to the cerebrum. Additionally, the olfactory nerve is one of only two cranial nerves that do not join with the brainstem, the other being cranial nerve two, the optic nerve. The olfactory nerves consist of sensory neurons which connect at the olfactory bulb. The olfactory bulb is the most rostral region of the CNS in most vertebrates and is supported by the cribiform plate of the ethmoid bone. Olfactory sensory neurons (OSN) are bipolar neurons that form specialized epithelial structures with their dendrites. This specialized structure is known as the olfactory neuroepithelium. The axons of OSNs extend through the natural perforations of the cribiform plate and synapse onto neurons within the glomerular layer of the olfactory bulb, within the CNS proper.

New World alphavirus strains readily cause encephalitis after aerosol or intranasal exposure in animal models, making these alphaviruses potential biodefense agents requiring efficacious therapeutic and vaccine-based responses. Previous studies have shown that following respiratory routes of inoculation, neuroinvasion occurs preferentially through the olfactory tract by initial infection of neuroepithelia (Ryzhikov, Ryabchikova et al. 1995; Vogel, Abplanalp et al. 1996; Roy, Reed et al. 2009). Responsible for sensing odorants, neuroepithelial tissue is in direct contact with the environment and easily subject to initial infection by these routes. Viral dissemination into the CNS likely occurs through the long axonal projections of OSNs, which converge upon the olfactory bulb of the CNS (Figure 1.2).

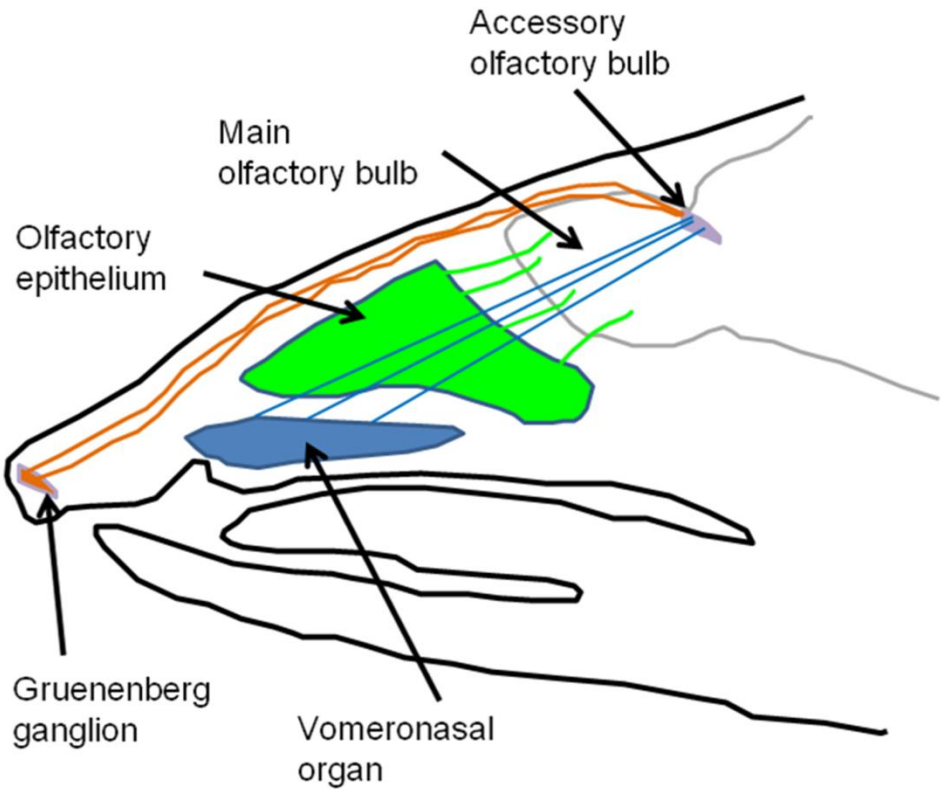

Figure 1.2 Diagram of odorant-sensing tissues of the mouse. The Gruenenberg ganglion is thought to be responsible for detecting odorants involved in suckling and these neurons synapse at the accessory olfactory bulb. The vomeronasal organ is responsible for detecting

pheromones and also synapses at the accessory olfactory bulb. The olfactory sensory neurons within the olfactory epithelium, depicted here as green lines, synapse at the main olfactory bulb.

Histological evidence supports this proposed mechanism (Roy, Reed et al. 2009). However, published characterizations are few. Notably, reports characterizing WEEV infection in an animal model are rare (Liu, Williams et al. 2000; Reed, Larsen et al. 2005). Additionally, WEEV is a naturally-occurring recombinant virus generated from ancestral EEEV- and Sindbis-like virus (Figure 1.3) (Hahn, Lustig et al. 1988). As EEEV and Sindbis virus have markedly different disease phenotypes in humans, a better description of WEEV pathogenesis is needed to identify infection patterns. For example, neuroadapted Sindbis virus (NSV), engineered to express a bioluminescent reporter, was observed to infect spinal segments of mice, a feature not associated with EEEV infection (Cook and Griffin 2003). However, it was not clear from these studies if NSV had spread into the spinal segment from the brain or from the spinal nerves. Anterograde spread of virus was clearly shown, however, as NSV within the spinal segments followed intra-cerebral inoculation of mice. Additionally, the structural proteins of WEEV are derived mostly from Old World alphavirus, except for the capsid protein, which is derived from New World alphavirus. Importantly, capsid protein was reported to be responsible for the potent host-macromolecular synthesis shutdown known to occur during infection with New World alphaviruses (Atasheva, Fish et al. 2010). The naturally-occurring recombination event which led to the formation of WEEV may be important to vaccine strategies aimed at providing protection from multiple alphaviruses. As mentioned previously, anti-SINV E1 antibodies were cross-reactive to multiple alphaviruses. As WEEV is within the same serocomplex as SINV, WEEV

may also contain immunogenic epitopes that induce cross-protections, a highly-desired feature of anti-alphavirus vaccines.

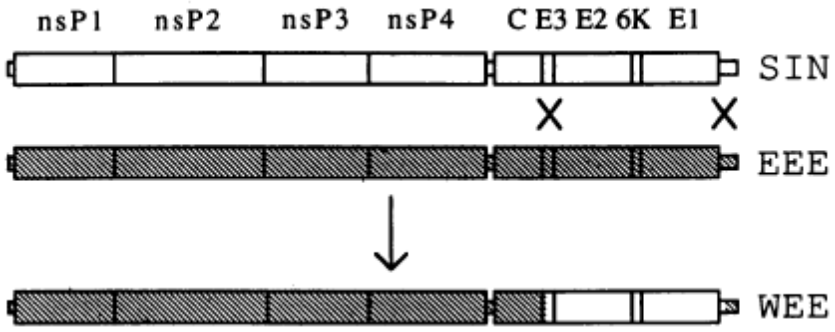

Figure 1.3 Schematic representation of the recombination event that produced western equine encephalitis virus. The crossover points to produce WEEV are indicated. SIN, Sindbis virus; EEE, EEEV. (Hahn, Lustig et al. 1988).

Several virus species belonging to the family *Paramyxovirdae* are known to enter the CNS following challenge with airborne virus. Nipah virus was shown to enter the CNS via the olfactory route in a hamster model of infection (Munster, Prescott et al. 2012). Similarly, Hendra virus (HeV) was reported to use the olfactory system to enter the CNS in a mouse model of infection (Dups, Middleton et al. 2012). LaCrosse virus (LACV), belonging to the family *Bunyavirdae*, is another example of a mosquito-borne virus which can enter the CNS. Interestingly, LACV entry into the brain occurs by infection of olfactory neuroepithelium following intraperitoneal inoculation of mice (Bennett, Cress et al. 2008). However, the route of LACV invasion of the CNS following the bite of an infected mosquito is poorly understood. Reports indicate that RABV, Borna disease virus (BDV), vesicular stomatitis virus (VSV), influenza virus, parainfluenza virus, SLEV, and HSV-1 can enter the CNS through the olfactory nerve (Monath, Cropp et al. 1983; Mori, Nishiyama et al. 2005; Ugolini 2011). Additionally,

prions have been suggested to use the olfactory route to enter the CNS (Mori, Nishiyama et al. 2005; Detje, Meyer et al. 2009). Lastly, mouse hepatitis virus (MHV), a betacoronavirus belonging to the family *Coronaviridae*, may also use peripheral nerves and olfactory sensory neurons as a route for entry into the CNS (Bergmann, Lane et al. 2006).

Virus entry into CNS by routes other than trans-neuronal spread from peripheral nerves

The BBB is a physiological separation of circulating blood from the extracellular fluid within the CNS, which is imposed, in part, by the tight-junctions characteristic of brain microvascular endothelial cells (BMVECs) (Figure 1.4). The BBB is responsible for maintaining homeostasis of the CNS, and does so by regulating the chemical environment, immune cell transport, and the entry of xenobiotics (Abbott, Patabendige et al. 2010). The BMVECs regulate paracellular transport of immune cells through tight-junctions and transcellular transport of moleules by specialized transporters, pumps, and receptors (Wong, Ye et al. 2013). Virus mechanisms for breaching the BBB are reviewed in the following sections.

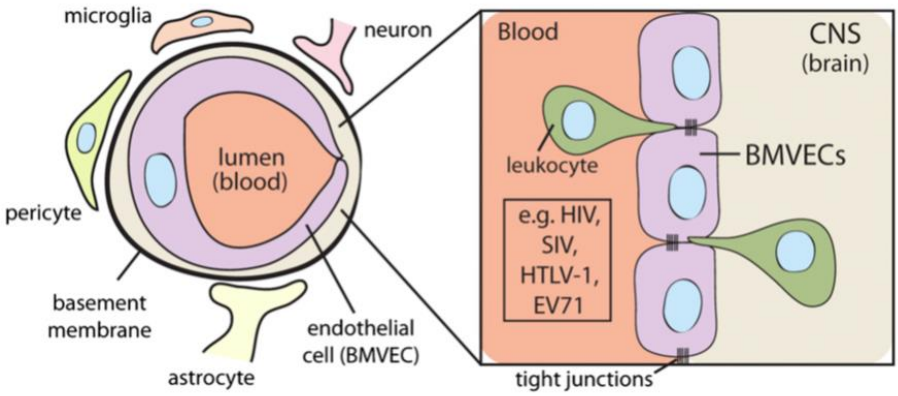

Figure 1.4 Diagram showing the composition of the BBB. Virus can traverse the BMVECs either through infecting BMVECs or by traversing the BBB in infected leukocytes (Koyuncu, 2013).

Virus invasion via circulating infected leukocytes

Another important route of virus invasion into the CNS involves infected circulating leukocytes, which then migrate into the CNS (McGavern and Kang 2011). This route of neuroinvasion is characteristic of viruses belonging to the family *Retroviridae* such as human immunodeficiency virus (HIV), simian immunodeficiency virus (SIV), and human T-lymphotropic virus type 1 (HTLV) (Kaul, Garden et al. 2001). Approximately 10%-20% of people suffering from HIV infection exhibit HIV-associated dementia. In the case of HIV infection, migration of infected memory T-cells or infected monocyte/macrophage precursors can introduce virus particles into the CNS, where microglia and astrocytes can become infected. HIV primarily targets CD4+ T-lymphocytes but can infect microglia and astrocytes because both of these cells express the receptor CD4+ and chemokine co-receptors (Martin, Wyatt et al. 1997; Schweighardt and Atwood 2001). Enterovirus 71 (EV71), belonging to the family *Picornavirdae*, and JC virus, a human polyoma virus belonging to the family *Polyomavirdae*, are also known to enter the CNS via infected leukocytes (Boothpur and Brennan 2010; Solomon, Lewthwaite et al. 2010).

Invasion by infection of brain microvascular endothelial cells (BMVEC)

The BBB is imposed by the selectivity of the BMVECs tight junctions and transport proteins. However, replicating virus within the BMVECs can allow for exit of virus into the basal lamina. Astrocytes, supportive cells within the brain parenchyma, are known to form end-feet processes around BMVECs, which serve to stimulate the BMVECs to form tight-junctions as well as provide other molecular communications to BMVECs. This second barrier is known as the *glia limitans*. Virus entry into the glia limitans may result in infection and/or disruption of

astrocyte function, thus disrupting the BBB. Furthermore, the *glia limitans* consists of gap-junctions, readily allowing the passage of material into the brain parenchyma. Therefore, once through the BMVEC-layer, virus may encounter CNS neurons directly after passing through the *glia limitans*.

Many RNA virus species can infect BMVECs. Well-known examples include West Nile virus (WNV) (Verma, Kumar et al. 2010), hepatitis C virus (HCV) (Fletcher, Wilson et al. 2012), and HTLV-1 (Afonso, Ozden et al. 2008). Many DNA viruses can also infect BMVECs, including JC virus (JCV) (Chapagain, Verma et al. 2007), Epstein-Barr virus (EBV) (Casiraghi, Dorovini-Zis et al. 2011), human cytomegalovirus (HCMV) (Fish, Soderberg-Naucler et al. 1998), and mouse adenovirus 1 (MAV-1) (Gralinski, Ashley et al. 2009). Additionally, Japanese encephalitis virus (JEV) and Semliki Forest virus (SFV) may enter the CNS through BMVEC-perturbations (Dropulic and Masters 1990; Lai, Ou et al. 2012).

Most BMVEC-infecting viruses overcome the BBB through interactions between virus proteins and tight-junction proteins (Afonso, Ozden et al. 2008; Gralinski, Ashley et al. 2009) However, in the case of WNV, infection induces the loss of tight-junction proteins in BMVECs (Xu, Waeckerlin et al. 2012). Additionally, WNV infection can induce the expression of matrix metalloproteinases, which degrade the extracellular matrix and result in BBB permeability. The metalloproteinase-induced BBB-permeability attracts leukocytes, leading to further BBB compromise by cytokine-induced mechanisms, mostly involving TNF-α (Wang, Town et al. 2004).

Invasion via virally-induced immune-mediated BBB perturbations

Virus infection of cells other than BMVECs can also result in the expression and secretion of pro-inflammatory cytokines/chemokines. Monocyte chemoattractant protein-1 (MCP-1) expression can be induced during viral infection and result in the disruption of tight-junction proteins, thus compromising the BBB (Deshmane, Kremlev et al. 2009). WEEV infection induces expression of inflammatory cytokines and chemokines (MCP-1, IL-12, IFN-γ, and TNF-α) within the brains of mice (Logue, Phillips et al. 2010) (Figure 1.5). Immune-mediated mechanisms of viral neuropathogenesis represent an important feature of encephalitic disease. In the following sections, we will review the host-immune response to alphavirus infection, with a focus on protective immune responses.

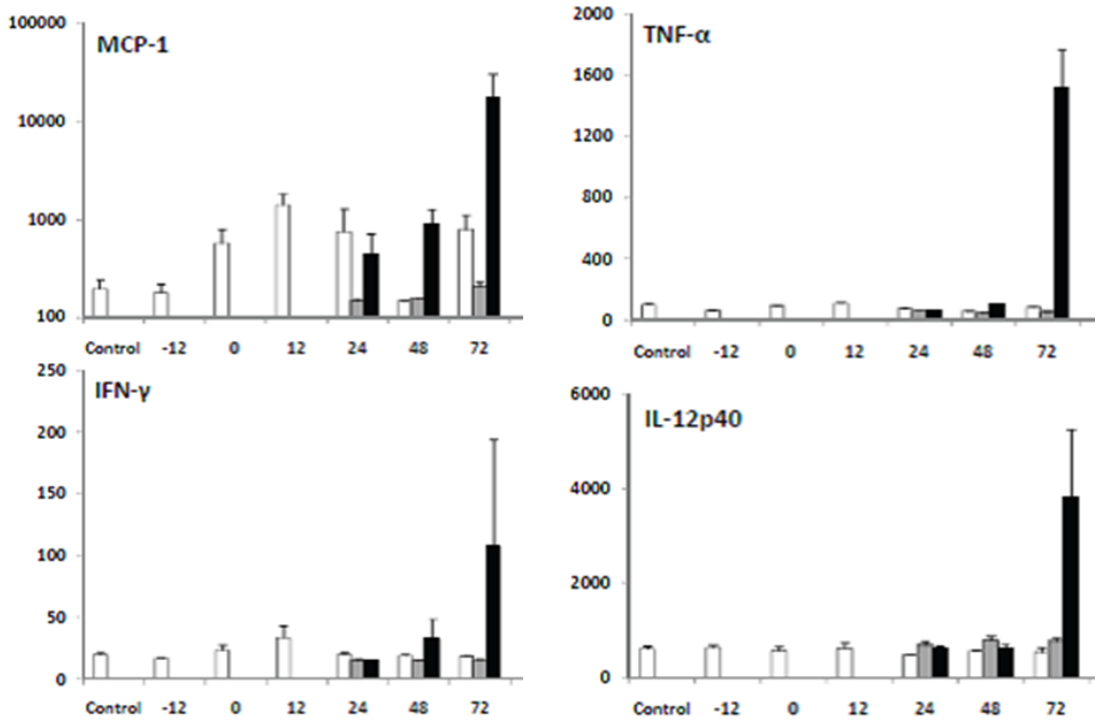

Figure 1.5 Cytokine expression following exposure to CLDC and/or WEEV. CD-1 mice were treated with CLDC and challenged with 1×10^3pfu WEEV-McM at 24 hours after the

CLDC treatment (grey bars), or challenged without CLDC treatment (black bars), or only treated and not challenged (white bars). Whole brains were extracted and homogenized and serum was collected at −12, 0, 12, 24, 48, 72, and 96h relative to virus inoculation. IFN-γ, TNF-α, MCP-1, and IL-12 concentrations (pg/g tissue) were determined by either ELISA or cytometric bead assay and flow cytometry. (Taken from Logue, Phillips, et al. 2010).

Paramyxoviruses, such as measles virus (MV), and mumps virus (MuV) can also cause serious CNS infections. MV and MuV infections typically begin in the upper respiratory tract, leading to infection of lymphoid tissue, which then causes viremia and spread of infection to other tissues. MuV is highly neurotropic and, like WEEV, can cause acute encephalopathy in children with high incidence (Koyuncu, Hogue et al. 2013). Prior to the widespread use of an effective vaccine, was a leading cause of viral meningitis and the most common cause of unilateral acquired sensorineural deafness in children (Dayan and Rubin 2008). Virus neuroinvasion is thought to occur through virally-induced immune-mediated perturbation of the BBB. During acute encephalitic infection with MuV, elevated levels of multiple cytokines can be detected in cerebrospinal fluids of children (Watanabe, Suyama et al. 2013). Encephalitic infection with MV is more rare than for MuV and is approximated to occur in 0.1% of the cases (Buchanan and Bonthius 2012). Neurological disease resulting from MV infection, however, can be devastating, and can include a fatal form of sclerosing panencephalitis, which can manifest weeks or years after initial infection (Buchanan and Bonthius 2012). How MV gains access into the CNS is not well-understood. It has been previously proposed that MV spreads into the brain by infecting BMVECs (Esolen, Takahashi et al. 1995) and/or via migration of infected leukocytes (Okamoto, Vricella et al. 2012). The molecular mechanisms of encephalitic infection

with MuV or MV are poorly understood, but may involve virus-induced disruption of Th1/Th2 balance and subsequent defective T cell proliferation (Schneider-Schaulies, Meulen et al. 2003).

Viruses such as tick-borne encephalitis virus (TBEV), Theiler's murine encephalomyelitis virus (TMEV), lymphocytic choriommeningitis virus (LCMV), and LaCrosse virus (LACV) are all thought to gain access to the CNS through infection-induced BBB perturbation (Johnson 1983; Bennett, Cress et al. 2008; Tsunoda and Fujinami 2010; Ruzek, Salat et al. 2011; Bonthius 2012). A reovirus, known as type 3 (T3), may also perturb the BBB to gain access to the CNS, however additional mechanisms may involve peripheral nerves (Richardson-Burns, Kominsky et al. 2002).

Other hypothesized mechanisms for virus-induced neuropathogenesis

Although activation of the host immune response may significantly contribute to neuronal death, viruses may also induce neuropathogenesis directly through the expression of viral proteins. Several of the viruses associated with encephalitic or neurodegenerative disease share a common characteristic, which is the expression of viral proteins known to impart permeability in host-cell membranes. These viral pores or 'viroporins' have been extensively studied. Influenza virus matrix protein M2 has proton- and cation-transport activity (Pinto, Holsinger et al. 1992). Interestingly, influenza virus induces both ER stress and the unfolded-protein-response during infection (Roberson, Tully et al. 2012). Additionally, virus-induced influx of Ca^{2+} is required for efficient WNV replication, and possibly for virus-induced rearrangement of the endoplasmic reticulum (ER) membrane (Scherbik and Brinton 2010). Alphaviruses like WEEV may be especially well-suited for neuropathogenesis because they express the viroporin 6K. The protein 6K forms Ca^{2+}-permeable ion-pores in the ER, releasing

calcium-stores and sustaining elevated intracellular calcium concentrations $[Ca^{2+}]_i$ (Antoine, Montpellier et al. 2007).

Pathological changes resulting from sustained increases in $[Ca^{2+}]_i$ include increased reactive-oxygen species and reactive-nitrogen species formation, altered bioenergetics, and mitochondrial morphological abnormalities; all of which are known characteristics of neurodegenerative diseases such as PD. In fact, mitochondrial pathology, including altered mitochondrial bioenergetics, perturbed calcium homeostasis and impaired organelle turnover have been deemed potentially critical mechanisms involved in the cell death that characterizes PD (Schapira, Cooper et al. 1989; Schapira, Mann et al. 1990). This realization has promoted intense research efforts for developing therapeutic strategies aimed at restoring dysfunctional mitochondrial processes in PD (Pienaar and Chinnery 2013). Importantly, alphaviral infection results in perturbations in mitochondrial bioenergetics (Silva da Costa, Pereira da Silva et al. 2012), supporting the viroporin-associated neuropathogenesis hypothesis. Viroporins may also be important to the induction of neurodegeneration, particularly in basal and brainstem nuclei. Neurons in these areas are reported to have high energy demands and perturbations in $[Ca^{2+}]_i$ could result in increased susceptibility to pathological changes.

Summary and goals

Alphavirus encephalitides present a public health problem and several are considered to be emerging infectious diseases. The public health problem is further complicated by the fact that some encephalitic alphaviruses are highly-infectious via respiratory challenge and, thus, may be conceived as bioweapons. There are significant gaps in our understanding of WEEV neuropathogenesis. For example, it is not clear where WEEV enters the brain following olfactory or non-olfactory challenge in mice. While olfactory pathways are likely for airborne challenge

with virus, data have not been reported indicating this route for mice. Furthermore, virus neuroinvasion following peripheral inoculation, a model for mosquito transmission, is less understood.

A major goal of the studies presented in this dissertation was to characterize in detail the spatiotemporal spread of WEEV in a mouse following either olfactory or non-olfactory challenge routes. In doing so, these studies may contribute previously unknown details regarding the pathogenesis of WEEV-induced encephalitis. This new knowledge may be useful to research aimed at developing protective treatment strategies. Accomplishing the aforementioned goal involved testing two hypotheses: (1) Luciferase activity resulting from infection with recombinant McFly can be used to monitor infection progress following intranasal inoculation of CD-1 mice, (2) Luciferase activity resulting from infection with recombinant McFire or McGal can be used to monitor infection progress following footpad inoculation of CD-1 mice.

Currently, no specific therapies are available for alphaviral infections. Unlicensed live attenuated and inactivated vaccines are available against some alphaviruses, but they can have significant side effects and/or are not cross-protective to multiple alphaviruses, thus limiting their usefulness during an epizootic outbreak, accidental exposure, or intentional release scenario. The second goal of these studies is to test a novel immunomodulatory strategy protein for protective activity against challenge with WEEV or EEEV. Specifically, we sought to test the hypothesis that vaccines based on WEEV E1 can provide protection against multiple alphaviruses and the effect on infection can be monitored using the in vivo imaging tools developed in the first two aims. Through a combination of innate and adaptive immune responses in the host, these treatments may provide a new avenue for the development of anti-alphavirus therapies.

CHAPTER 2: BIOLUMINESCENT IMAGING AND HISTOPATHOLOGIC CHARACTERIZATION OF WEEV NEUROINVASION IN OUTBRED CD-1 MICE

Introduction

Sections of the following chapter have been peer-reviewed and published in an open-access journal (Phillips, Stauft et al. 2013). As discussed in the previous chapter, the route(s) of virus neuroinvasion and CNS dissemination of WEEV is poorly understood. This chapter focuses on the development of recombinant WEEV reporter constructs and their use to detect and track experimental infection of mice. The major goals of these studies were to: 1) better characterize the process of neuroinvasion and CNS dissemination of WEEV in a mouse model of infection, and 2) use BLM imaging to detect and track experimental infection and identify sub-anatomic regions of high-level virus replication. These studies aim to better understand WEEV neuroinvasion and to compare the routes of viral entry into the CNS among different inoculation routes (intranasal or footpad inoculation).

We used *ex-vivo* imaging to identify specific brain regions where viral replication was occurring. We found a consistent pattern in the spatiotemporal distribution of virus among the imaged brains and extended these studies by performing histological analysis on the imaged tissues to characterize, in detail, the brain regions most affected by the experimental infections. As expected, virus neuroinvasion following i.n. challenge route occurs through olfactory pathways. However, in the case of footpad inoculation, there was no evidence of virus neuroinvasion involving the olfactory pathways. We find that non-olfactory neuroinvasion of WEEV likely occurs in areas of the CNS where the blood-brain barrier is naturally absent. These areas, all of which are circumventricular organs, include the organum vasculosum of the

lamina terminalis (hypothalamic output), median eminence of hypothalamus (hypothalamic output), posterior pituitary, pineal gland, and the area postrema.

Additionally, BLM activity resulting from infection with recombinant WEEV can be measured and used to evaluate the efficacy of treatment strategies. In the next chapter, we extended our studies by using the recombinant viruses developed in this chapter to evaluate the efficacy of an experimental treatment strategy. In summary, we show that the McM-based AES is capable of producing a conveniently measured marker of infection and, in doing so, provides a system for visualizing the progress of infection following virus challenge.

Materials and Methods

Virus Construction

A full-length infectious cDNA clone (IC) of the McMillan strain of WEEV (pMcM) was a kind gift of Dr. Thomas Welte (Colorado State University), was derived from virus obtained from the Arbovirus Reference Collection at the Center for Disease Control and Prevention in Fort Collins, CO, USA, and has been previously studied (Logue, Bosio et al. 2009). A full-length IC of 5'dsWEEV.McM.FLUC (McFire) was a kind gift from Dr. Brandon Stauft (Colorado State University). Detailed descriptions of the molecular cloning methods to engineer McFire have been previously published (Stauft 2012) and is freely-available online through Colorado State University Library digital depository.

Detailed descriptions of the molecular cloning methods used to engineer 3'dsWEEV.McM.FLUC (McFly) and 3'dsWEEV.McM.GAL4 (McGal) are provided in detail below. To summarize, SGP sequence (nucleotides 7341–7500 of viral genome) was duplicated immediately downstream of the last nucleotide of the E1 gene. FLUC from pGL3 Luciferase

Reporter Vector (Promega, Madison, WI) was inserted immediately downstream of the new SGP. The duplicated SGP was used to initiate transcription of FLUC encoded on the second subgenomic mRNA. Full details now follow.

McFly construction - A PCR fragment (fragment #1) was generated using the following primers (GCA CCG AAC GCA ACG GTA CCC ACA GCA TTA GC and CTG ACC GGT GCT CTT CGT CAT CTA CGT GTG TTT ATA AGC ATA GAG CTG CAG ACC AAC ACT ATA AGT CCA) from pMcM. A second PCR fragment (fragment #2) was generated from pMcM using the following primers (CAG ACC GGT CT GAG CGC GGC CAC TGA CAT AGC GGT AAA ACT CGA TGT ACT TC and CAG TCT AGA AAT ATT ATT GAA GCA TTT ATC AGG GTT ATT GTC TCA TGA GCG GAT AC). Fragment #1 was digested with KpnI and AgeI while fragment #2 was digested with AgeI and XbaI. The resulting digested fragments were gel purified and inserted (via two-step ligation) into a modified pUC19 plasmid which had the SapI sites removed via site-directed mutagenesis and which had been digested with KpnI and XbaI. The resulting intermediate plasmid was digested with SapI and AgeI. The following commercially synthesized oligonucleotide pair was mixed in equal molar amounts, heated to 90º C, and allowed to cool slowly and anneal: CCA GGC TCT TCG TGA TCC AGA TAC GAG ATC ATA CTG GCA GGC CTG ATC ATC ACG TCC CTT TCC ACG TTA GCC GAA AGC GTT AAG AAC TTC AAG AGC ATA AGA GGG AAC CCA ATC ACC CTC TAC GGC TGA CCT AAA TAG GTG ACG TAG TAG ACA CGC ACC TAC CCA CCG CCA AAA GGC CGG CCA CCG GTG ACC; GGT CAC CGG TGG CCG GCC TTT TGG CGG TGG GTA GGT GCG TGT CTA CTA CGT CAC CTA TTT AGG TCA GCC GTA GAG GGT GAT TGG GTT CCC TCT TAT GCT CTT GAA GTT CTT AAC GCT TTC GGC TAA CGT GGA AAG GGA CGT GAT GAT CAG GCC TGC CAG TAT GAT CTC GTA TCT GGA

TCA CGA AGA GCC TGG. The annealed double stranded oligonucleotides were also digested with SapI and AgeI. The digested products were ligated to form a new intermediate plasmid which contains a duplication of the subgenomic promoter immediately after the last nucleotide of the E1 gene. Following the duplicated subgenomic promoter are the engineered FseI and AgeI sites. These two sites act as the insertion site for transgene to be expressed from the final construct. Firefly luciferase was cloned into the Age1 and FseI sites of the intermediate plasmid by engineering FseI and AgeI sites at the 5' and 3' ends (respectively) of the PCR fragment generated from pGL3 pGL3 Luciferase Reporter Vector (Promega, Madison, WI). Once the transgene was determined to be appropriately inserted and accurate in terms of sequence, the intermediate plasmid was digested with KpnI and MfeI, gel purified, and ligated into the KpnI and MfeI digested and dephosphorylated full-length infectious clone. Final plasmids were sequenced to validate proper insertion orientation.

McGal construction – The plasmid pGAL4-VP16 was a kind gift from Dr. David Pwinica-Worms (Washington University). GAL4-VP16 was cloned into the Age1 and FseI sites of the intermediate plasmid (used to generate McFly) by engineering FseI and AgeI sites at the 5' and 3' ends (respectively) of the PCR fragment generated from pGAL4-VP16 plasmid. Virus expression of GAL4-VP16 was confirmed by infection of cells transfected with pUAS-FLUC. Expression was validated by luciferase activity imaging.

Rescue of Virus from Infectious Clone

Using SspI (New England Biolabs, Ipswich, MA), ICs were linearized and subsequently purified by QIAprep Spin MiniPrep Kit (Qiagen, Valencia, CA USA) and IC genomic RNA was *in vitro* transcribed using a bacteriophage T7 RNA Polymerase and MAXIscript™ kit (Life

Technologies, Grand Island, NY USA). BHK cells (2×10^7 cells in 400 µL) were electroporated with 20 µL of genomic RNA using an ECM 630 electroporator (BTX Harvard Apparatus, Holliston, MA USA). Two pulses of 450 V, 1200 Ω, and 150 µF were administered. Medium was taken from electroporated cells immediately and passaged once in BHK cells to make a stock virus. Supernatant was collected at 48 hpi and stored at −80°C. This stock was quantified using plaque titration in Vero cells and used for subsequent experiments.

Plaque Titrations

Virus titrations were performed in duplicate and plaque assays were performed as previously described (Liu, Voth et al. 1970). Briefly, 200µL each of 10-fold serial dilutions of sample are used to inoculate the wells of a 12-well tissue culture plate containing confluent Vero cells. After 1 hour, 40° C growth medium/agar overlay is applied to each well and allowed to cool to room temperature and solidify (approximately 20 minutes). Plates are incubated at 37° C for 3 days. Then, 200 µL of 3 mg/mL MTT (3-(4,5-dimethylthiazol-2-yl)-2,5-diphenyltetrazolium bromide; USB) was added to each well of the plates. Plates were incubated at 37°C for an additional 12-24 hours prior to being read.

Mouse Infection and Imaging

All animal protocols used in these experiments were reviewed and approved by the Animal Care and Use Committee at Colorado State University (Protocol approval #11-2605A). Mice were handled in compliance with the PHS Policy and Guide for the Care and Use of Laboratory Animals. Female 4–5 week old CD-1 mice (Charles River Labs, Wilmington, MA USA) were used in this study. Intranasal inoculation was conducted at a dose of 1×10^4 PFU of McM or WEEV.McM.FLUC in a volume of 20 µL delivered drop-wise onto the nostrils of

lightly anesthetized animals. For subcutaneous challenge studies, lightly anesthetized mice received 20 µL containing of 1×10^4 PFU of indicated virus into the footpad. For studies using GAL4-VP16 transactivator-expressing virus (McGal), transgenic (Tg) UAS-FLUC mice were used instead of CD-1 mice. A breeding colony of Tg UAS-FLUC mice were established from a breeding pair of Tg UAS-FLUC mice which were a kind gift from Dr. David Piwnica-Worms (Washington University). The Tg UAS-FLUC reporter mouse strain expresses FLUC under the regulatory control of a concatenated GAL4 promoter (UAS). For information on the generation and characterization of Tg UAS-FLUC mice, please see the corresponding published report (Pichler, Prior et al. 2008).

Imaging was performed after 150 mg/kg of luciferin (30 mg/mL stock diluted in PBS) was injected subcutaneously dorsal to the cervical spine of each infected animal. Administration of luciferin via this route has been shown to result in more consistent signal compared to intraperitoneal administration (Inoue, Kiryu et al. 2009). Each animal was imaged 10–15 minutes after injection of substrate. Uninfected mice were used as an imaging control to adjust for background. Mice were anesthetized by administration of isoflurane (Minrad Inc, Bethlehem, PA USA) through an XGI-8 anesthesia system (Caliper Life Sciences) connected to the IVIS 200 camera during imaging. Exposure time was kept to 3 minutes under standard settings for the camera. Living Image 3.0 software (Caliper Life Science) was used to analyze and process images taken using the IVIS 200 camera. A threshold for significant BLM was established using negative imaging controls at a total flux of 5×10^3 p/s/cm^2/sr. Total light emission from each mouse was determined by creating a region of interest of standard size for each mouse and collecting light emission data using the software.

Sagittal whole head sections of infected mice were imaged by injecting mice with 150 mg/kg of luciferin (30 mg/mL stock diluted in PBS) at the indicated time point (post-infection). After 10 minutes, mice were injected with another dose of luciferin, and promptly euthanized via inhalation of a lethal dose of isoflurane. Animals were decapitated and whole heads bisected along the medial sagittal plane. Resulting sections were briefly rinsed with PBS and promptly imaged.

Chemokine Quantification

Three i.n. inoculated animals were euthanized at each of three time points (24, 48, and 72 h.p.i.) after obtaining BLM images. Brains were harvested and assayed as previously described (Logue, Phillips et al. 2010). Briefly, whole brains were harvested, homogenized in buffered medium, which was clarified by centrifugation. Supernatant was collected and divided into aliquots. Single aliquots were used to assay for immunological markers (MCP-1 and IP-10, R&D Systems) or virus quantification by plaque assays as described above.

Immunohistochemistry

Paraffin -embedded formalin fixed tissue was rehydrated, treated with Tris-EDTA pH 9.0 at 90°C for 15 minutes, and blocked with SuperBlock T20 (Thermo, Rockford, IL), and incubated with biotinylated polyclonal rabbit anti-FLUC antibody (Abcam, Cambridge, MA) at 1:1000 dilution overnight at 4°C. Brain sections were washed 3 times with Tris-buffered saline containing 0.03% Tween 20(TBST). Secondary antibody was conjugated strepavidin-horseradish peroxidase (Rockland, Gilbertsville, PA) and was used at a 1:6000 dilution and incubated with sections for 30 minutes at room temperature. Slides were again washed three times with TBST. 3,3'-diaminobenzidine (DAB) was added to the slides and allowed to develop color for 5

minutes. Hematoxylin was used to counterstain. Hyperimmune horse serum generated against WEEV Fleming strain (CDC, Fort Collins, CO) was used for anti-WEEV immunohistochemistry at 1:600 dilution. Secondary antibody was HRP-conjugated rabbit polyclonal antibody to horse IgG heavy and light chains (Abcam, Cambridge, MA) used at a 1:3500 dilution. All other conditions remained unchanged relative to anti-FLUC immunohistochemistry staining.

Statistics

All titration data were $\log_{10}$ transformed and compared using unpaired Student's t test. In determining the correlation of PFU with BLM, curves were analyzed using Pearson correlation with 95% confidence interval. For chemokine quantification comparisons, unpaired t test was used. Analysis was conducted using statistical analysis software (SAS) version 9.2. Survival curves were subjected to Kaplan-Meier (log rank test) analysis using Prism version 4.00 for Windows (GraphPad). Quantitative analysis of BLM in the assessment of vaccine efficacy was conducted using two-tailed t-test.

Results

Recombinant FLUC-expressing WEEV Phenotype in CD-1 Mice

McFly infection of CD-1 mice was characterized after administering virus by the intranasal route. McFly virus expressed FLUC throughout infection (Figure 2.1A–C) where signal was restricted to the head. To determine if FLUC signal in other anatomical regions was potentially masked by signal from the head, mice showing signs of disease and strong luciferase signal in the head region were euthanized, decapitated, and imaged again with an opened visceral cavity. No signal was detected outside the head region (data not shown). Exponential increases in BLM signal (photons/second/centimeter^2/steradian) were observed from day 2 to day 3 post-

inoculation (Figures 2.1B, C, & E). Infection progressed from the nasal cavity toward more caudal regions and was symmetrical with respect to the sagittal axis. A 0% survival rate was observed for both WEEV.McM and McFly in animals (n = 10) inoculated by the intranasal route and a comparison of mouse survival showed no significant difference between the two viruses (Figure 2.1D) (P value = 0.4795). We compared FLUC activity to measured infectious virus titers from whole brain homogenates (Figure 2.1E–G). WEEV.McM virus replicated to 100- fold PFU/mL higher titer than WEEV.McM.FLUC within the first 24 hpi. McFly virus titer was statistically similar to WEEV.McM virus titer by 72 hpi. Comparison of total flux (p/s) for each McFly -inoculated mouse with viral titer measured within the whole brain (Figure 2.1G), showed a strong correlation (Pearson R = 0.9903 and R2 = 0.9807). As expected, uninfected control animals receiving daily luciferin injections did not show any signs of disease.

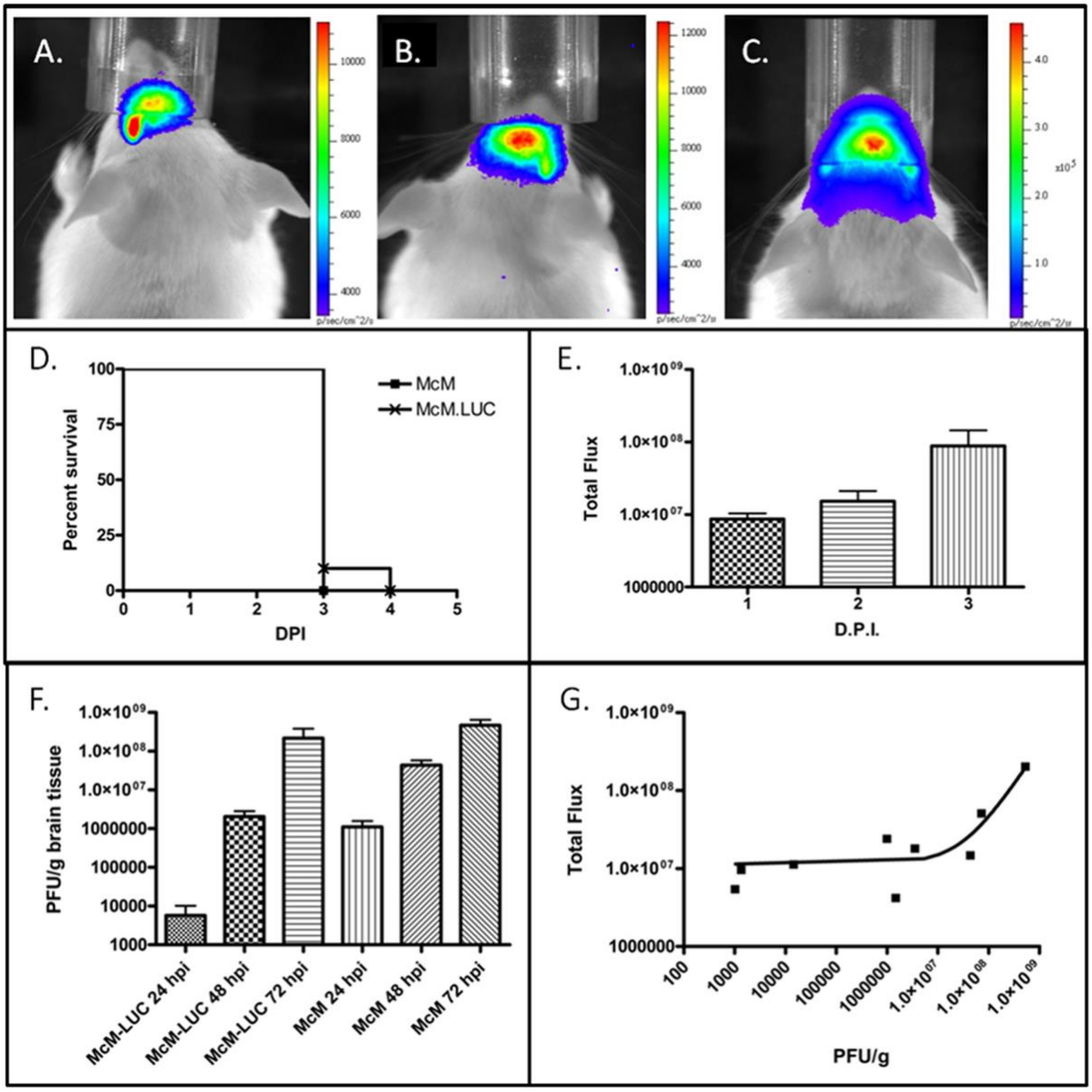

Figure 2.1. *In vivo* BLM imaging of infection progress using WEEV.McM.FLUC (McFly).

A: 24 hpi, B: 48 hpi, C: 72 hpi, D: Survival analysis of mice infected with WEEV.McM.FLUC and wild-type virus (WEEV.McM) after intranasal virus challenge. Note uniform lethality resulted from intranasal exposure by WEEV.McM.FLUC. E: FLUC activity was quantitatively measured in each animal at 1, 2, and 3 d.p.i. Results from BLM analysis demonstrate robust FLUC activity as infection progressed with the greatest

increase observed between days 2 and 3 post-infection. F: Brains of animals infected with WEEV.McM attain a higher viral titer more rapidly when compared with WEEV.McM.FLUC. WEEV.McM.FLUC titers approach those of McM by 72 h.p.i. G: Regression analysis of viral titer versus FLUC activity. Linear regression line appears curved due to log10 scaling of axes as required to clearly depict all data points (R2 = 0.9807).

Localization of Virus by ex vivo Imaging of Medial Sagittal Cross-sections

Neuroinvasion and CNS dissemination *in situ* were detected in CD-1 mice intranasally inoculated with McFly and sacrificed at various time points. These animals were euthanized, decapitated, and whole heads were separated along the medial sagittal plane. Representative images are presented (Figure 2.2A–D) which illustrate the course of dissemination into the CNS. BLM signal was initially observed in the nasal turbinates and olfactory bulb. The infection proceeded along the lateral olfactory tract and ultimately progressed through CNS regions consistent with olfactory sensory neuronal connectivity. Infection was invariably bilateral and intensified in regions consistent with basal nuclei, thalamus, and hypothalamus. Ultimately, FLUC expression was detected in neocortical regions and the brainstem by day 3 PI. Luciferase activity in the brainstem was separated into two distinct regions. The midbrain expression of FLUC appeared continuous with basal nuclei, thalamus, and hypothalamus and it was here that the greatest BLM was observed. BLM signal within the pons was discontinuous with signal from superior regions and failed to approach levels seen within basal nuclei, thalamus, hypothalamus, or cerebrum. Interestingly, the cerebellum was consistently spared from infection despite high BLM activity within posterior pons (cerebellum's site of attachment).

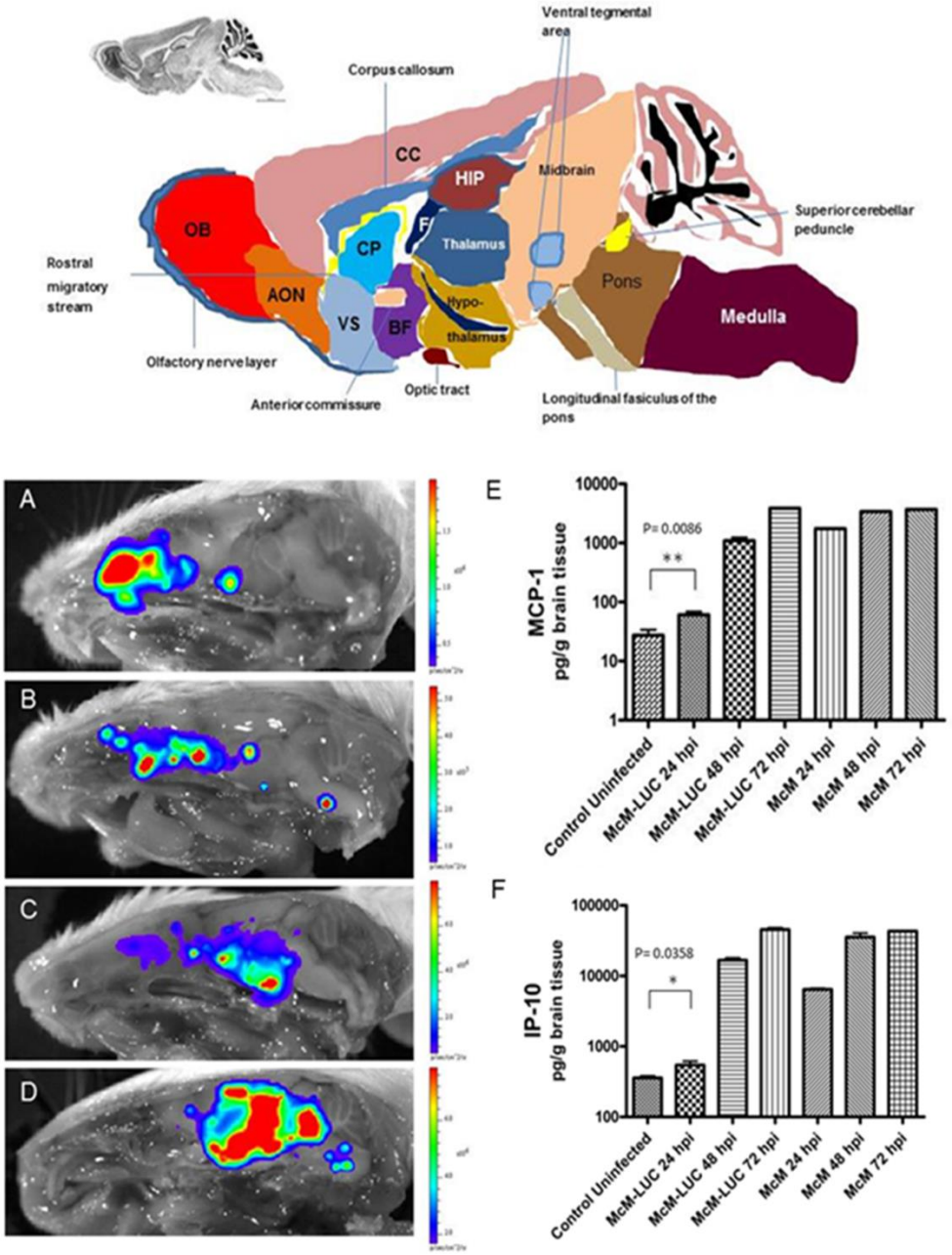

Figure 2.2 (Top) Schematic depiction of anatomical organization of mouse brain in medial sagittal view. AON: anterior olfactory nucleus, BF: basal forebrain, CC: cerebral cortex (isocortex), CP: caudate putamen, F: fornix, HIP: hippocampus, OB: olfactory bulb, VS: ventral striatum. Progress of infection with WEEV after intranasal inoculation (A–D). Whole heads were bisected along sagittal midline and imaged at 24 hpi (A), 48 hpi (B), 60 hpi (C) and 72 hpi (D). Luciferase activity pattern is consistent with dissemination along

olfactory pathways. Regions consistent with initial infection of the nasal turbinates show pronounced FLUC activity at 24 hpi. However, nasal turbinate BLM activity is exceeded by signal from areas consistent with infection proceeding through olfactory information processing within the CNS, including the lateral olfactory tract, anterior olfactory nucleus, basal ganglia, thalamus, and cerebrum. Lateral olfactory tract corresponds to the olfactory nerve layer of the diagram. Basal ganglia include VS, BF, sub-thalamic and midbrain areas. The cerebrum is the pink and purple structure caudal to the midbrain in the above diagram. Immunological markers of disease (MCP-1 and IP-10) resulting from WEEV.MCM.FLUC are strongly induced and comparable to WEEV.McM at 3 d.p.i. (E–F).

Characterization of Chemokine Induction Resulting from Infection with McFly

Chemokines associated with severe CNS inflammation (Carpentier, Williams et al. 2007) and previously shown to be highly induced during McM infection (Logue, Phillips et al. 2010) were measured in whole brain homogenates to compare the inflammatory responses within the CNS between WEEV.McM and WEEV.McM.FLUC (Figure 2.2E–F). Robust expression of both MCP-1 and IP-10 was observed in both infected groups of mice. Although WEEV.McM.FLUC was found to be attenuated when compared to wild-type McM in terms of PFU/g brain tissue (Figure 2.1F) and chemokine induction (Figure 2.2E-F), manifestation of clinical disease was comparable. This is supported by mean time to death measurements (3.0 days vs. 3.1 days) and signs of disease exhibited in both groups. Early events indicated that inflammatory markers resulting from WEEV.McM.FLUC infection were significantly less than those observed in McM infected animals at 24 hpi, but levels rapidly approached those of McM by the following day.

Clinical Signs

All infected mice (n = 10) showed variably severe clinical signs, namely depression and motor deficits culminating at 48–72 hours post infection (PI). Most affected animals developed ataxia, with rhythmic raising and lowering of front limbs alternatively. Reduced stride length was visually observed in affected animals during voluntary movement. Animals in this intermediate stage of the disease did not appear to have visual impairment as they remained responsive to visual stimulation. In a later stage of disease (as indicated by severity of clinical signs which required animal to be euthanized), animals were unresponsive to visual stimuli, but were typically responsive to touch. Mice showed unresponsiveness during handling only in the latest stage of disease (≥72 hpi). Lateral recumbency with tachypnea was characteristic of this terminal stage of the disease.

Pathology and Immunohistochemistry

Sagittal sections of the head were prepared to facilitate viewing the nasal mucosa and olfactory nerve as it crosses the cribriform plate and connects to the bulb to help determine anatomic locations of the brain lesions (Figure 2.2 diagram). Pathologic lesions were observed in histological specimens prepared from imaged mice and in mice receiving WEEV.McM. WEEV.McM and WEEV.McM.FLUC produced comparable lesions. Serial sections were stained using immunohistochemical methods (anti-FLUC and anti-WEEV for recombinant virus while only anti-WEEV was used for wt virus infections) to demonstrate viral expression at the affected sites. Lesions and luciferase immunopositivity were observed to follow the same pattern as the imaged FLUC activity (Shown in Figures 2.3, 2.4, and 2.5). IHC staining of both WEEV antigen and luciferase revealed that infection was almost exclusively limited to neurons and that

dissemination was likely through the neuronal connectivity. Histopathologic alterations encountered within the nasal cavity and brain are summarized as follows:

Phase I: extraneural viral lesions.

Twenty four hours PI: luminal aggregates of moderate numbers of neutrophils and fewer lymphocytes were detected in the nasal cavity with focal deciliation of respiratory mucosa corresponding to the areas of inflammation. In markedly immunopositive animals there was a focal erosion/ulceration (full thickness necrosis) of the respiratory mucosa and extension of the inflammatory exudate into the adjacent congested submucosa (Figure 2.3A). IHC (anti-FLUC) revealed immunoreactivity of variable numbers of neuroepithelial cells (Figure 2.3B). The numbers of positive cells increased with the severity of the clinical symptoms. The terminal of the olfactory nerve before crossing the cribriform plate to merge into the olfactory bulb showed a mild degree of neuropathy with occasional digestion chambers indicative of Wallerian-type degeneration or secondary demyelination (Figure 2.3C), indicative of impaired axonal transport. Occasional lymphocytes were detected in the affected branches of the olfactory, maxillary, glossopharyngeal, and hypoglossal nerves.

Phase II: Neuroinvasion.

24–48 h PI: In the olfactory bulb, immunoreactivity (anti-FLUC or anti-WEEV) showed a high degree of neuronal specificity within CNS tissue (Figure 2.3D and Figure 1.1). Neuronal necrosis was commonly evident in the glomerular, granular, external plexiform and internal plexiform

layers plus the olfactory nerve layer at the ventrum of the bulb. In the areas of microcavitation, there were infiltrations of a few neutrophils, glial cells and lymphocytes (Figure 2.3E–F). Perivascular cuffing was prominent throughout affected areas (Figure 2.3G–H). Also, myeloid cavities of the head showed variable immunoreactivity in lymphoid precursors and monoblasts. Surrounding skeletal muscles showed inconsistent immunoreactivity.

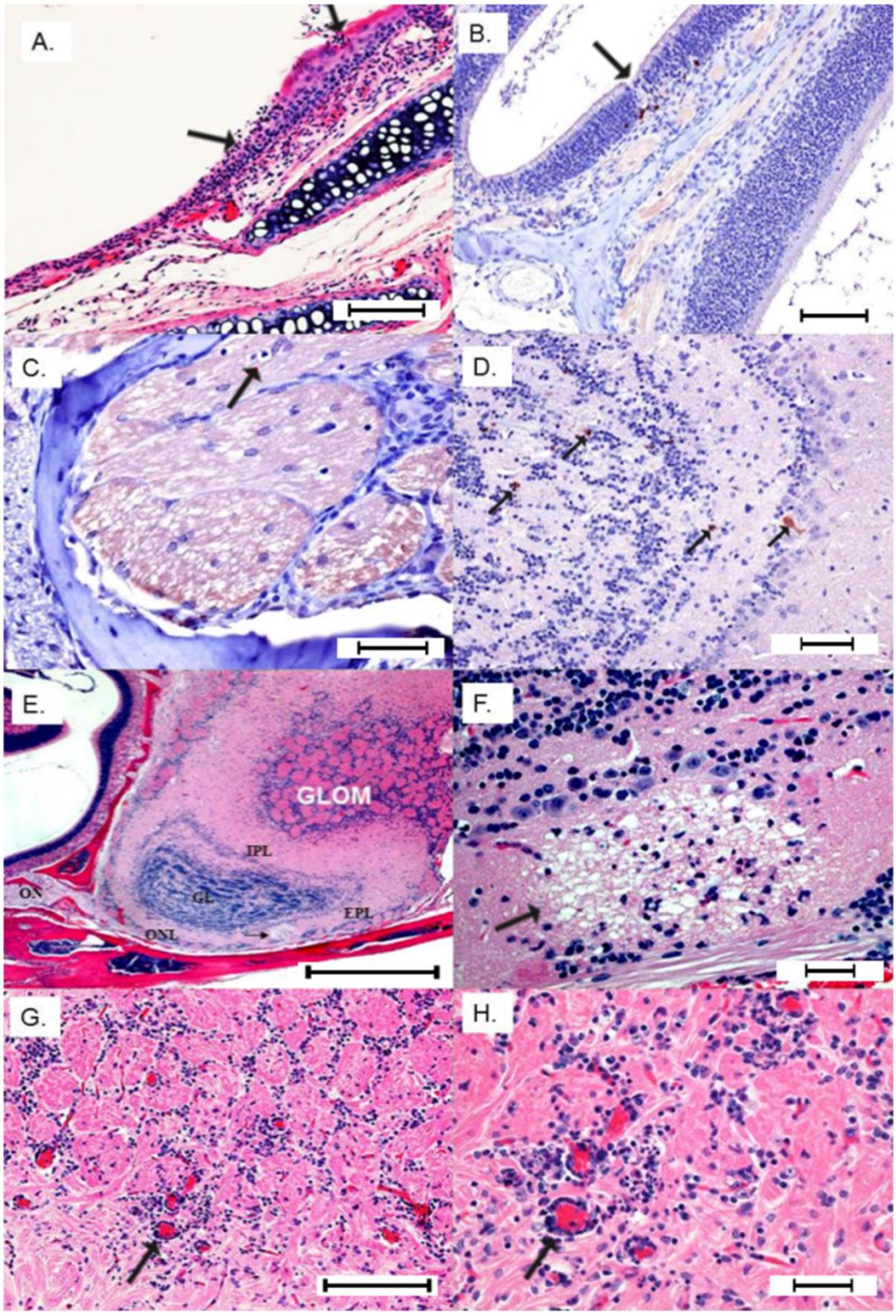

Figure 2.3. I. Extraneural lesions 24 hpi (A,B) and II. Neuroinvasion 48-72 hpi (C-H). I-Extraneural lesions A) Focal erosion/necrosis of the olfactory mucosa with deciliation of the

flanking epithelium and neutrophil infiltration into the mucosa and submucosa (Bar = 100 µm). B) IHC staining for FLUC is highlighted in a few neuropeithelial cells subjacent to a focal loss of olfactory mucosa (Bar = 200 µm). II- Neuroinvasion from olfactory nerve 48–72 hpi. C) Terminal of olfactory nerve shows a digestion chamber (arrow) with occasional lymphocytes infiltrating vacuolated branches (Bar = 100 µm). D) Early immunoreactivity (anti-FLUC) in the main olfactory bulb involving scattered neurons in the external plexiform and granular layers (Bar = 100 µm). E) Sagittal section H&E stain showing the connection between olfactory nerve (ON) and main olfactory bulb layers affected by multifocal necrotizing lesions with associated status spongiosis and infiltration of neutrophils. Glom = glomerular layer; EPI = external plexiform layer; IPL = internal plexiform layer; and ONL = olfactory nerve layer at the ventrum of the olfactory bulb (Bar = 400 µm). F) Neuropil of the olfactory nerve layer shows a large vacuolar lesion (demyelination) with individual neuronal necrosis and infiltration of small numbers of neutrophils (Bar = 100 µm). G) Perivascular cuffs and multifocal gliosis in the glomerular layer 72 hpi (Bar = 200 µm). H) Close-up view of the congested glomerular vessels with pleocellular perivascular cuffs comprising moderate numbers of neutrophils, lymphocytes and glial cells (Bar = 100 µm).

Phase III: CNS dissemination and associated lesions.

48–72 h PI: The severity of the lesions in the olfactory bulb increased and the lesions started to propagate into more caudal regions of the brain (Figure 2.4). Multifocal areas of necrosis along with positive FLUC-immunoreactivity were detected in the anterior olfactory

nucleus, ventral striatum and basal forebrain at the ventrum of the brain. Dorsally, cerebral cortex was multifocally involved along with the pia matter and Virchow-Robin space (fluid-filled canals that surround perforating arteries and veins in the parenchyma of the brain). Other areas that were consistently involved were hippocampus, thalamus, hypothalamus, caudate putamen, mid brain, cerebellar superior peduncle, and pontomedullary region. Cranial nerves also showed focal to multifocal immunoreactivity, especially trigeminal nerve and its ganglia along with optic and cochlear nerves. Trigeminal pathways indicated significant immunopositivity and moderate to severe pathologic alterations, namely chromatolysis, vacuolation and individual neuronal loss (Figure 2.5). To ensure that anti-FLUC staining was truly representative of viral localization, IHC staining of WEEV.McM and WEEV.McM.FLUC antigen were performed to discern any differences in viral distribution and localization to lesions. IHC staining with anti-WEEV polyclonal antibodies showed indistinguishable staining patterns and localization of the lesions (Figures 2.6 and 2.7) compared to anti-FLUC IHC staining (Figure 2.4A and Figure 2.5G,H). Additionally, anti-WEEV IHC revealed that sinus hairs (vibrissae) were affected, supporting trigeminal nerve pathway involvement (Figure 2.8).

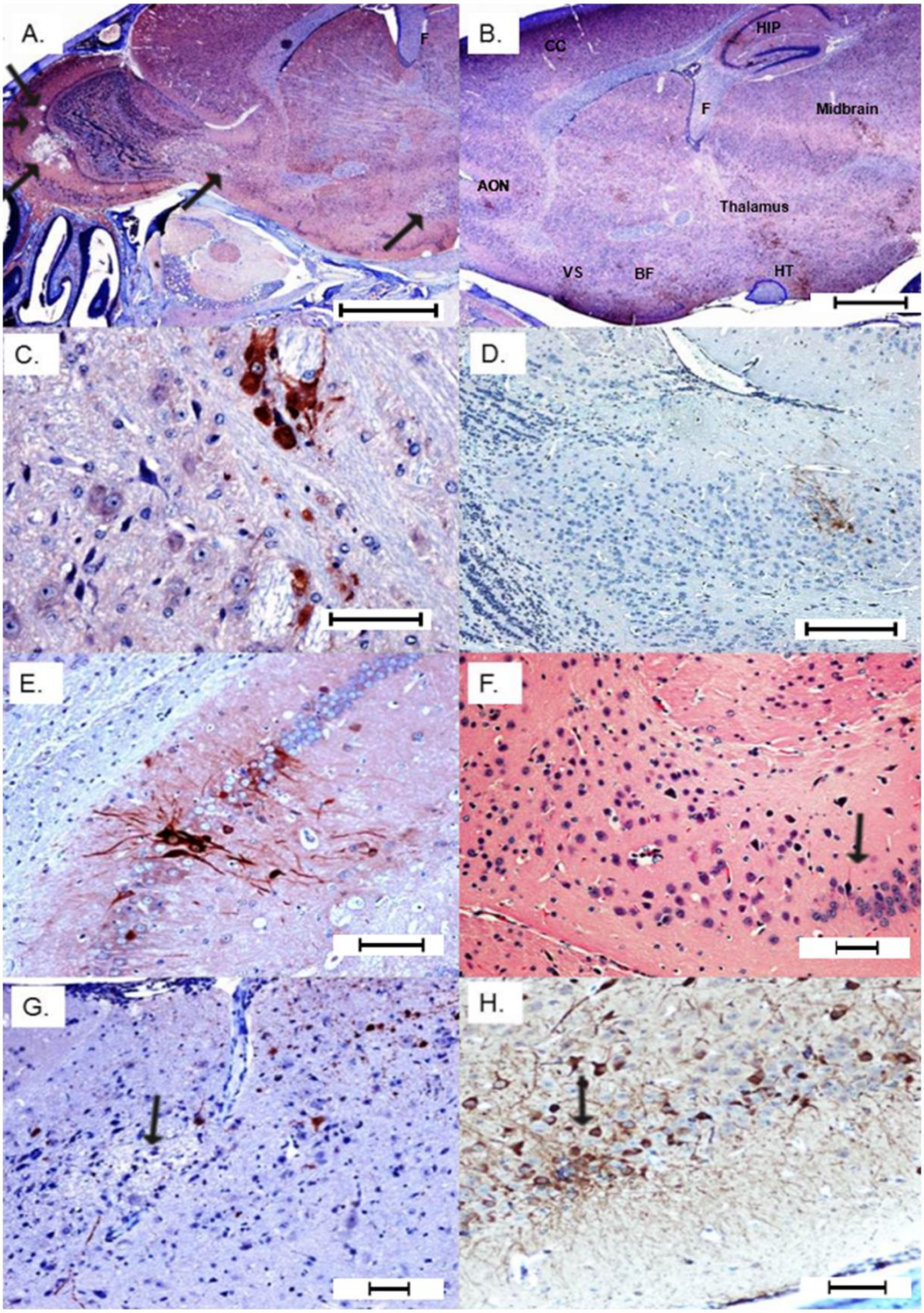

Figure 2.4. Later stage dissemination throughout the brain after intranasal inoculation (72 hpi). A) Expanded view of the olfactory bulb showing progression of virus into caudal

regions of the brain with multifocal necrosis and secondary demyelination (arrows) (Bar = 1000 µm). B) Multifocal demyelination and positive FLUC immunoreactivity in the anterior olfactory nucleus (AON), ventral striatum (VS), basal forebrain (BF) thalamus, hypothalamus, midbrain, hippocampus (HIP), and cerebral cortex (CC). Fornix (F) and optic tract (circled in blue) do not show any immunoreactivity (Bar = 1000 µm). C) Neuronal immunoreactivity in caudal olfactory bulb that shows multifocal demyelinating lesions (Bar = 100 µm). D) Multifocal immunoreactivity in caudal olfactory bulb and anterior olfactory nucleus (Bar = 200 µm). E) Strong immunoreactivity in hippocampus (Bar = 100 µm). F) Hippocampal H&E stain showing focal loss of pyramidal neurons with mild gliosis (Bar = 100 µm). G) Multifocal areas of necrosis and demylelination in the cerebral cortex (Bar = 200 µm). H) Strong immunoreactivity in cerebral neurons and their dendrites, revealing interneuronal spread (Bar = 100 µm). All IHC images within this figure are from anti-FLUC staining. Comparative images using anti-WEEV staining may be found in Figures 2.6-2.7.

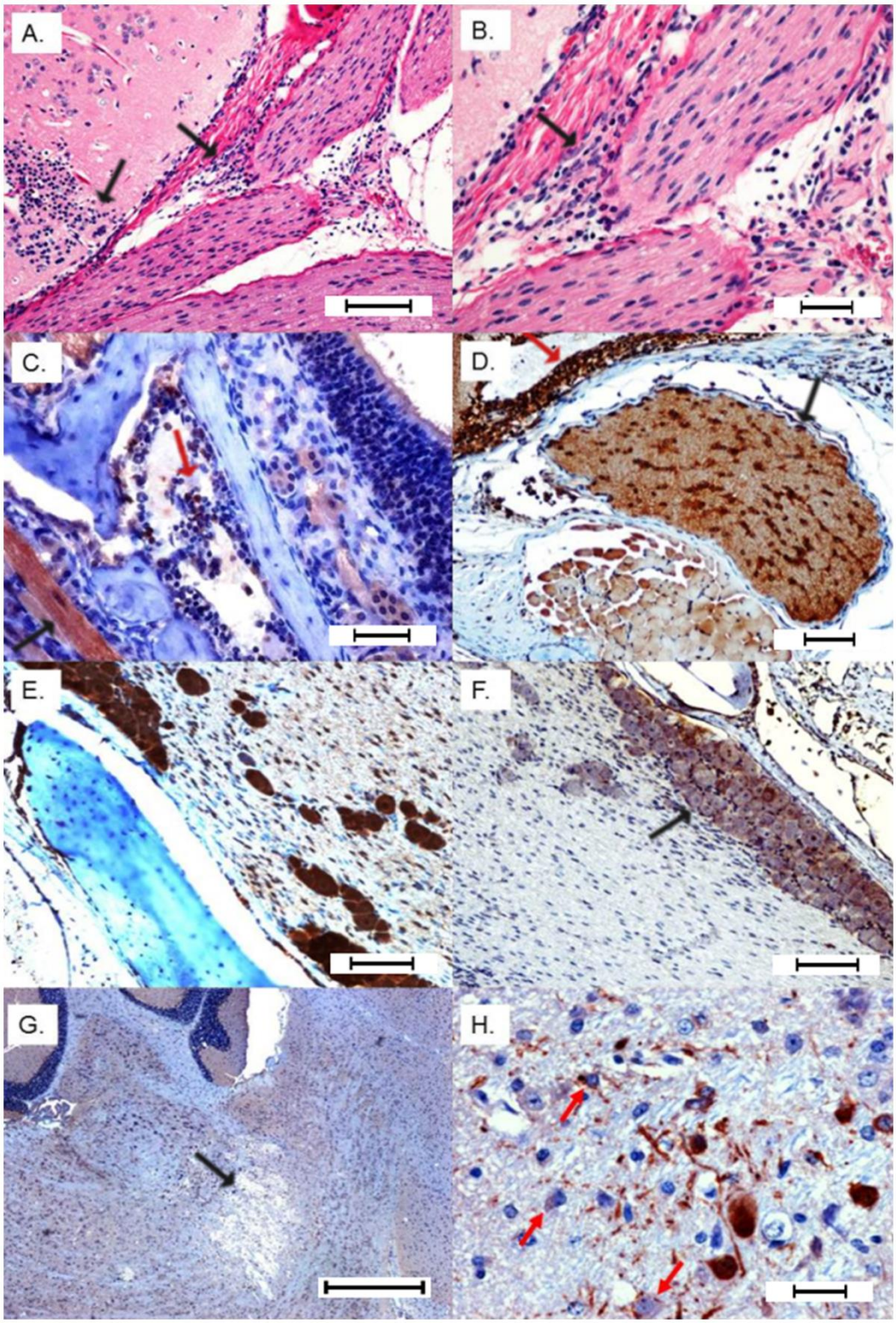

Figure 2.5. Neuroinvasion from trigeminal nerve. A) Cranial nerves including a branch of trigeminal nerve show neutrophilic perineuritis with a large glial nodule extending to the

meninges of the overlying brain section (Bar = 200 µm). B) Close up of epineurium of cranial nerves infiltrated by neutrophils and lymphocytes (Bar = 100 µm). C & D) Strong FLUC immunoreactivity of maxillary nerve, including Schwann cells. Note strong and diffuse immunoreactivity of olfactory neuropeithelium, variable staining of surrounding skeletal muscles and bone marrow elements (Bar = 100 µm). E) Trigeminal ganglion FLUC IHC positivity (Bar = 100 µm). F) Trigeminal FLUC IHC positivity is associated with the overlying meninges and brain tissue (Bar = 100 µm). G) Brainstem demyelinating lesion (potential consequence of trigeminal invasion) (Bar = 400 µm). H) Anti-FLUC IHC staining in the brain stem with interneuronal spread and rare immunoreactivity of glial cells (astrocytes) (Bar = 100 µm). All IHC staining within this figure are from anti-FLUC. Comparison images using anti-WEEV staining may be found in Figures 2.6-2.7.

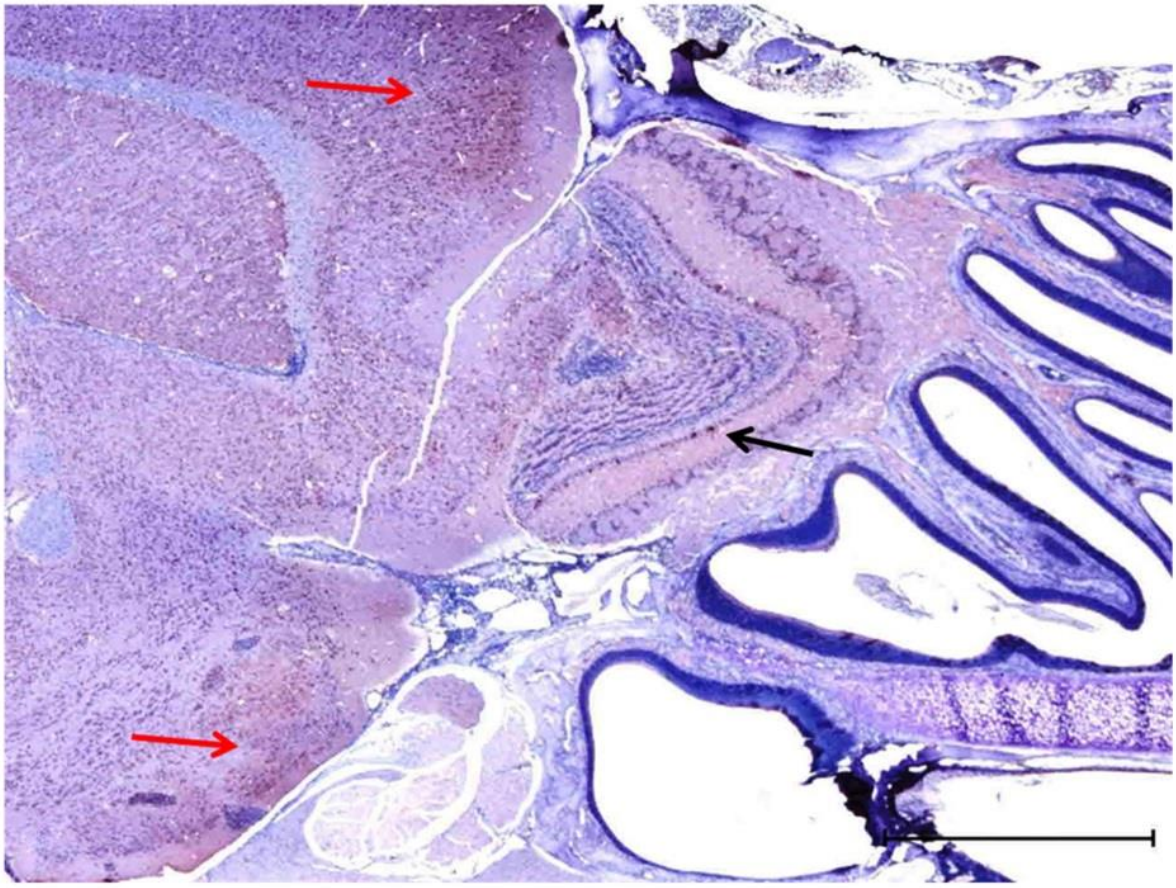

Figure 2.6 Anti-WEEV staining in olfactory bulb. Black arrow shows immunopositivity in the olfactory bulb at 72 hpi. Red arrows show anti-WEEV antigen staining in cortical and lateral olfactory tract.

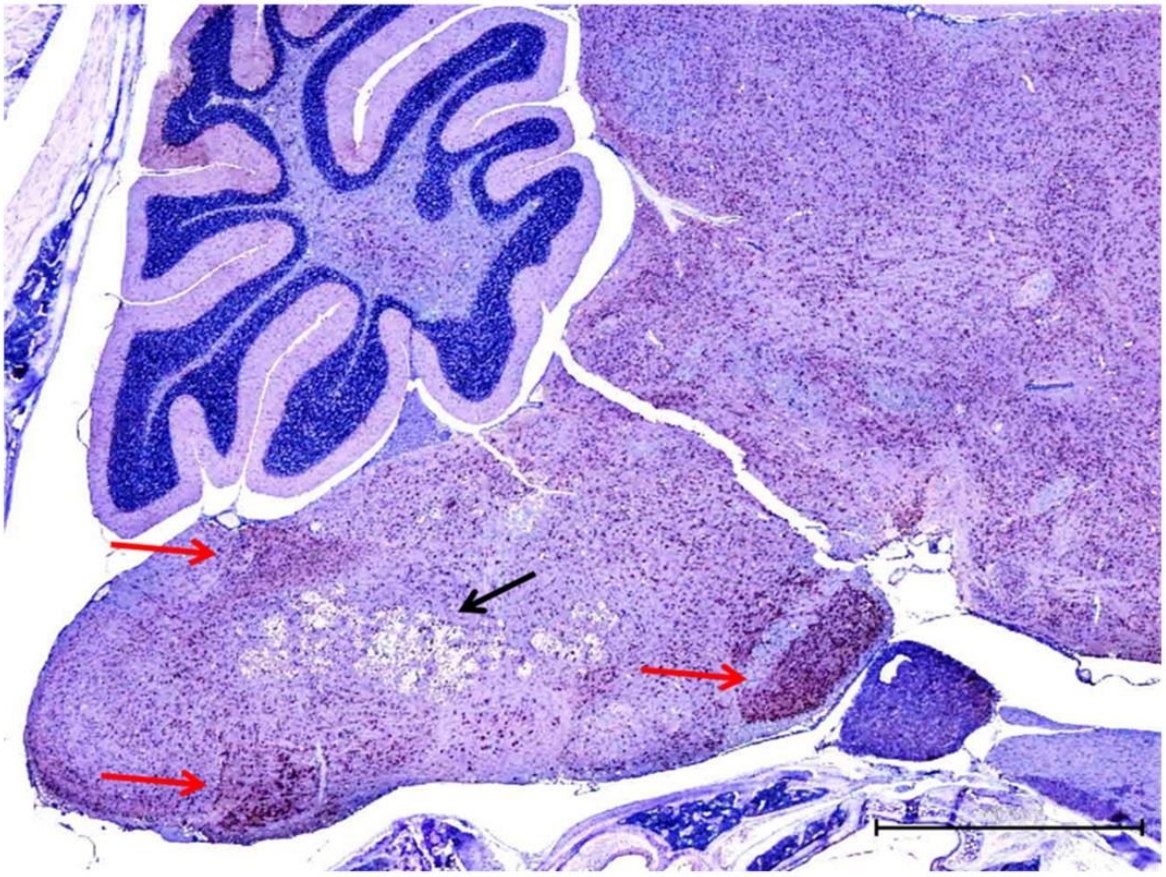

Figure 2.7 Anti-WEEV staining in the brainstem at 72 hpi. Black arrows show WEEV antigen staining at site of a large demyelinating lesion (rarefaction of neuropil). Red arrows show additional staining throughout brainstem.

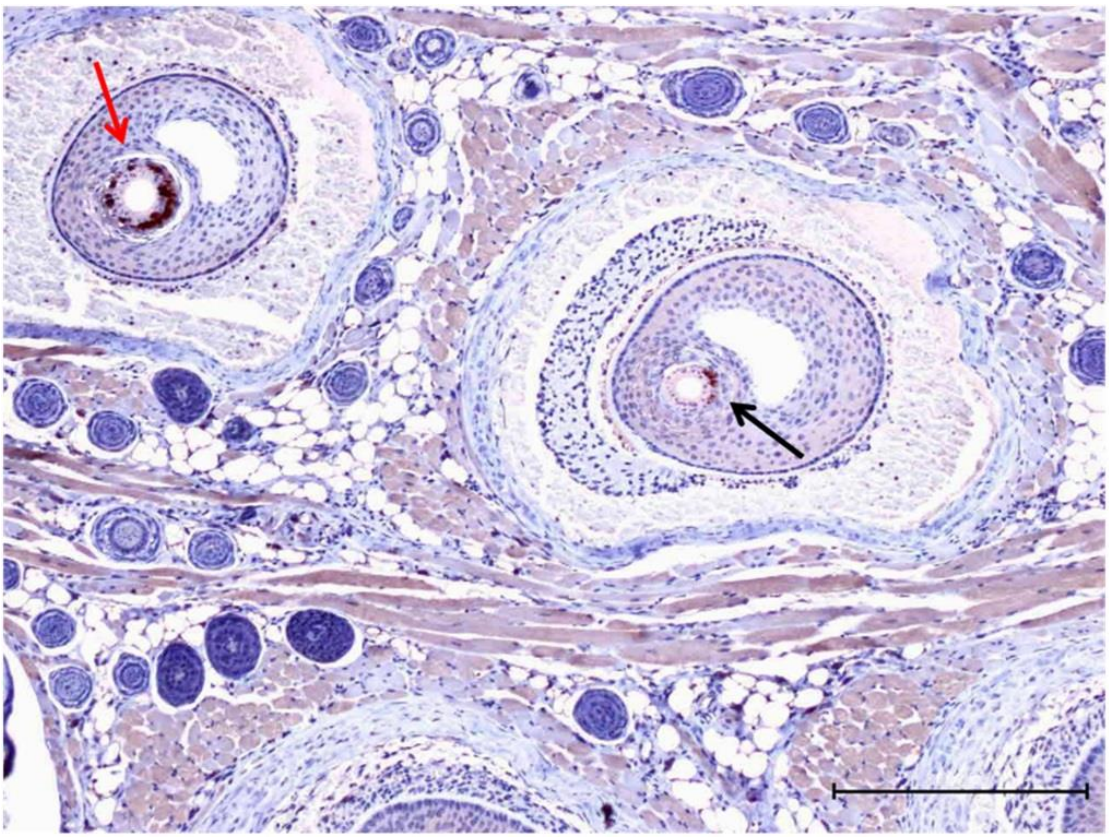

Figure 2.8 WEEV antigen in the sinus hairs at 72 hpi. Red arrow shows markedly WEEV antigen immunopositive sinus hair. Black arrow shows adjacent sinus hair with less intense staining.

Comparison of transgene stability between 3'dsWEEV.McM-fLUC (McFly) and 5'dsWEEV.McM-fLUC (McFire)

Infection via a permissive route, such as intranasal inoculation, did not significantly attenuate luciferase-activity during the progression of CNS disease, thus allowing visualization of neuroinvasion and CNS dissemination by BLM. However, we were unable to visualize CNS infection following footpad inoculation with McFly due to the loss of transgene activity. A previously reported recombinant virus, McFire, was compared to McFly to determine the relative

transgene stability among these two recombinant viruses. Bioluminescence imaging was performed on infected BHK-21 cells and through 8 passages (Figure 2.9A). Expression of 5' double sub-genomic luciferase (McFire) results in lower expression at early time points, but increased retention of FLUC gene (P8 versus P5) compared to 3' double sub-genomic luciferase (McFly). To ensure our observations were not due to replication rate differences between the two viruses, growth curve analysis was performed (Figure 2.9B). There were no significant replication rate differences observed between the two viruses. Next, we analyzed images acquired from each passage for luciferase activity (Figure 2.9C). Uninfected wells were used to control for background. McFly showed increased luciferase activity relative to McFire in P1 (p value = < 0.0001) and P2 (p value = < 0.05), but was not found to be significantly different than McFire in P3. McFire showed higher luciferase activity relative to McFly in P4-5 (p value = <0.005 and <0.05, respectively). P6 and P7 did not demonstrate statistically significant different luciferase intensities between the two viruses (McFly and McFire), but examination of imaging data shows marked differences in transgene activity. P8 was the first passage in which transgene activity appeared to be completely lost from McFire.

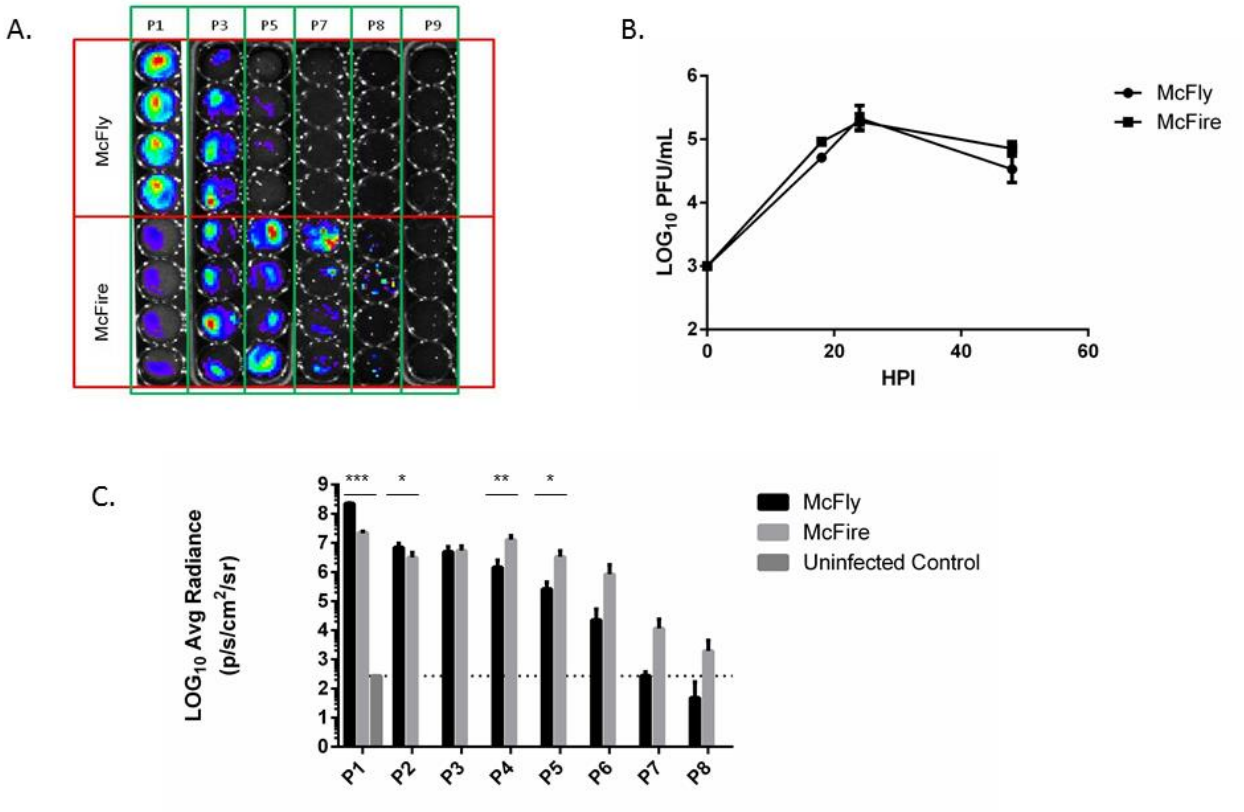

Figure 2.9 Retention of transgene activity by recombinant WEEV is dependent on the genomic location of the duplicated subgenomic promoter. A) McFly or McFire were used to inoculate BHK-21 cells at an m.o.i. of 0.1 (1000 PFU/well) in 4 wells per passage. All wells within a single column are standardized to that column for visual comparison between viruses during each passage. B) Growth curve analysis of McFly and Mcfire viruses sampled from supernatants of wells similar to those imaged in panel A. Notice comparable growth kinetics between the two viruses. C) Quantitative analysis of images from panel A, including passages not shown in Panel A. *** p=<0.0001, ** p=<0.005, * p=<0.05. Dotted-line indicates average background luminescence in control wells for easier comparison to far right bars. Notice the increased expression from McFly early, passages 1 and 2. McFire

showed increased expression compared to McFly from P4-P8, although P6-P8 measurements were not statistically different.

Neuroinvasion following footpad inoculation

To determine if the improved transgene retention of McFire would allow visualization of CNS infection following peripheral inoculation, CD-1 mice were inoculated in the footpad and imaged daily. All mice with increased luciferase activity in the head region compared to control animals (uninfected) became ill and required euthanization. During whole-animal imaging, luciferase activity within the head was easily discernible in affected mice compared to mice which had no apparent CNS disease (Figure 2.10). Surprisingly, there were no additional sites of extra-neural virus replication other than the inoculation site (footpad) (Figure 2.10).

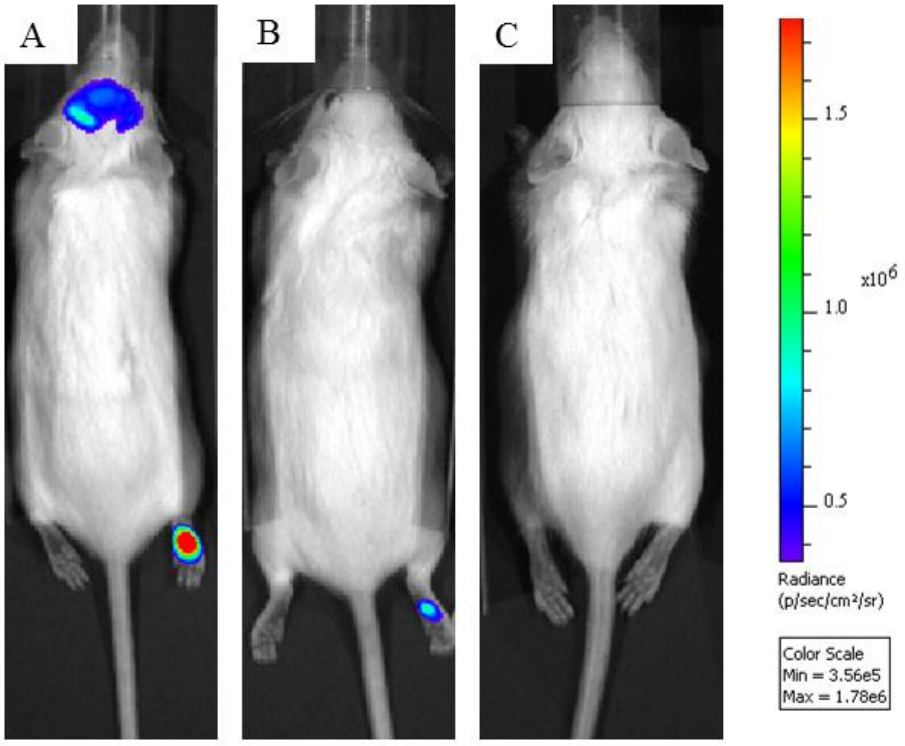

Figure 2.10 Whole-animal imaging showing CNS infection with McFire following footpad inoculation. CD-1 mice were challenged with McFire (10^4 PFU into footpad) and were

imaged at 5dpi. A) Mouse with neurological signs of disease and luciferase activity within the brain region and inoculation site. B) Mouse with no neurological signs of disease and luciferase activity only at inoculation site. Notice the lack of additional sites of extra-neural virus replication other than the footpad in all mice. C) Uninfected control mouse.

WEEV invaded the brain by 48-72hpi, inducing moderate to severe meningoencephalitis where meninges and corresponding parenchyma showed moderate vascular congestion and infiltration of pleocellular exudate. WEEV antigen immunoreactive mononuclear cells seeded the perivascular areas in the connective tissue surrounding circumventricular organs (namely, neurohypophysis, median eminence, pineal gland, and area postrema (Figures 2.11-2.13). Bilaterally symmetrical neurons seemed to be the key targest of the virus, mainly in the caudal pyriform cortex, superior and inferior colliculi, substantia nigra, ventral mammalian nucleus, cerebellar peduncle and hind-brain (Figure 2.14). Apoptosis and neuropil edema became evident in the aforementioned areas, but was most noticeable in the parenchyma that surrounds the circumventricular organs by 72-96 hpi. Many neurons were apoptotic and occasional vessels in the most affected areas were cuffed by small numbers of mixed inflammatory cells including macrophages, lymphocytes and fewer neutrophils. Glial cells also appeared to be infected, but to a lesser degree than neurons. Both astrocytes and oligodendroglial cells showed moderate WEEV antigen immunoreactivity in the midbrain. Strong WEEV antigen immunoreactivity was observed in the hindbrain by 7 dpi. Besides the brain, retinal ganglion neuronal cell bodies showed slight immunoreactivity along with scattered immunoreactivity of the retinal ganglion axons. Cranial nerves also showed strong immunoreactivity especially cochlear, trigeminal and optic nerves. Olfactory nerve was virtually unaffected.

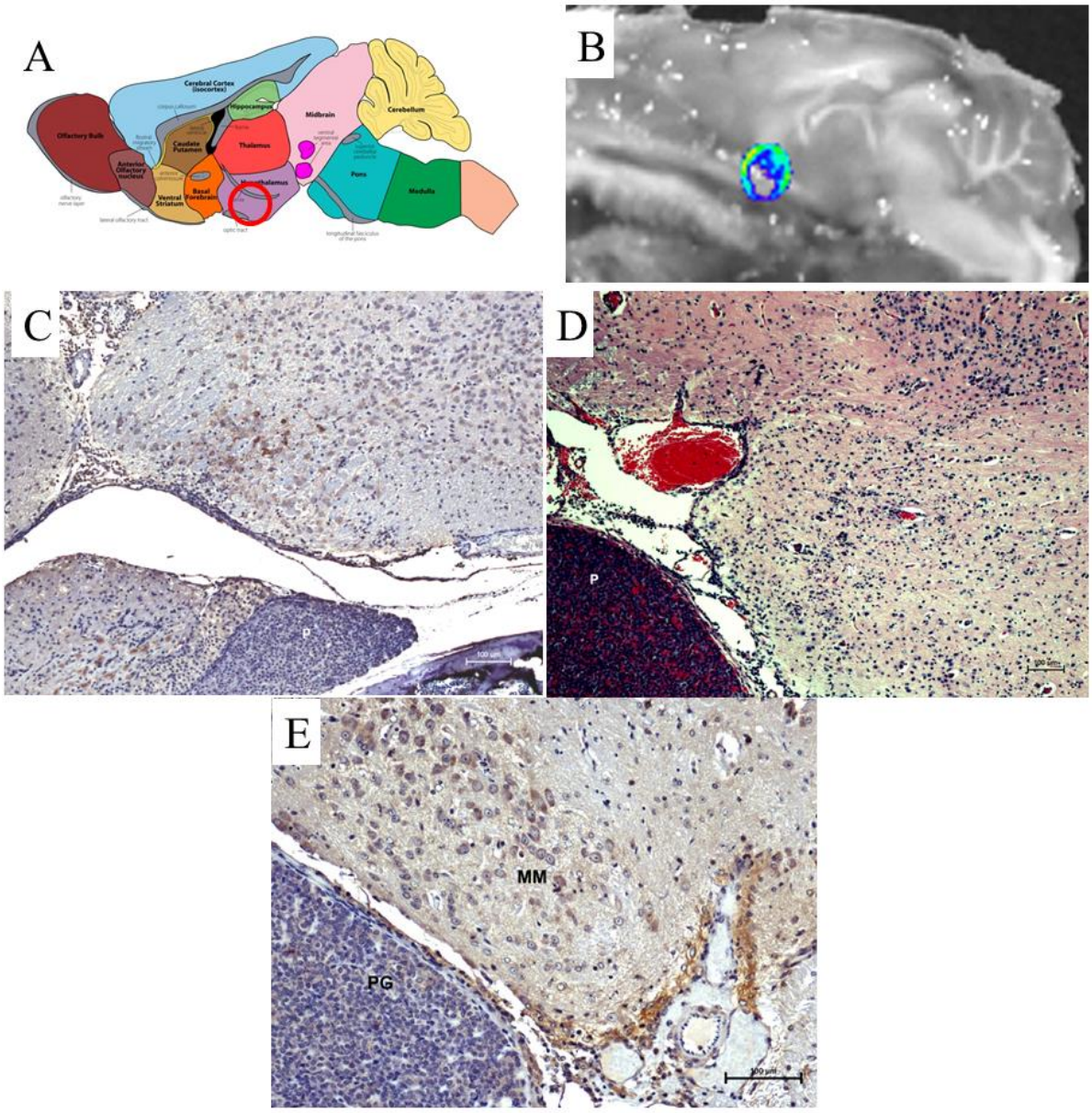

Figure 2.11 Hypothalamic route of CNS entry for WEEV. A) Diagram of mouse brain in sagittal-view. Red circle indicates region where luciferase activity was observed in CD-1 mice at 3dpi. B) *Ex vivo* imaging of sagittally bisected head of CD-1 mouse at 3 dpi showing luciferase activity within the hypothalamic region. C-E) Anti-WEEV antigen IHC or hemotoxylin and eosin staining of bisected head in panel B showing affected areas. C) IHC staining (brown) of hypothalamic region with nearby pituitary gland. Notice the lack of

staining in the anterior pituitary (P). D) Hemotoxylin and eosin staining of median eminence region. Notice necrotic morphology (N) among nuclei in the median eminence. Anterior pituitary appears unaffected. E) IHC staining (brown) of medial mammillary nucleus (MM) region. Notice the lack of staining in the anterior pituitary gland (PG).

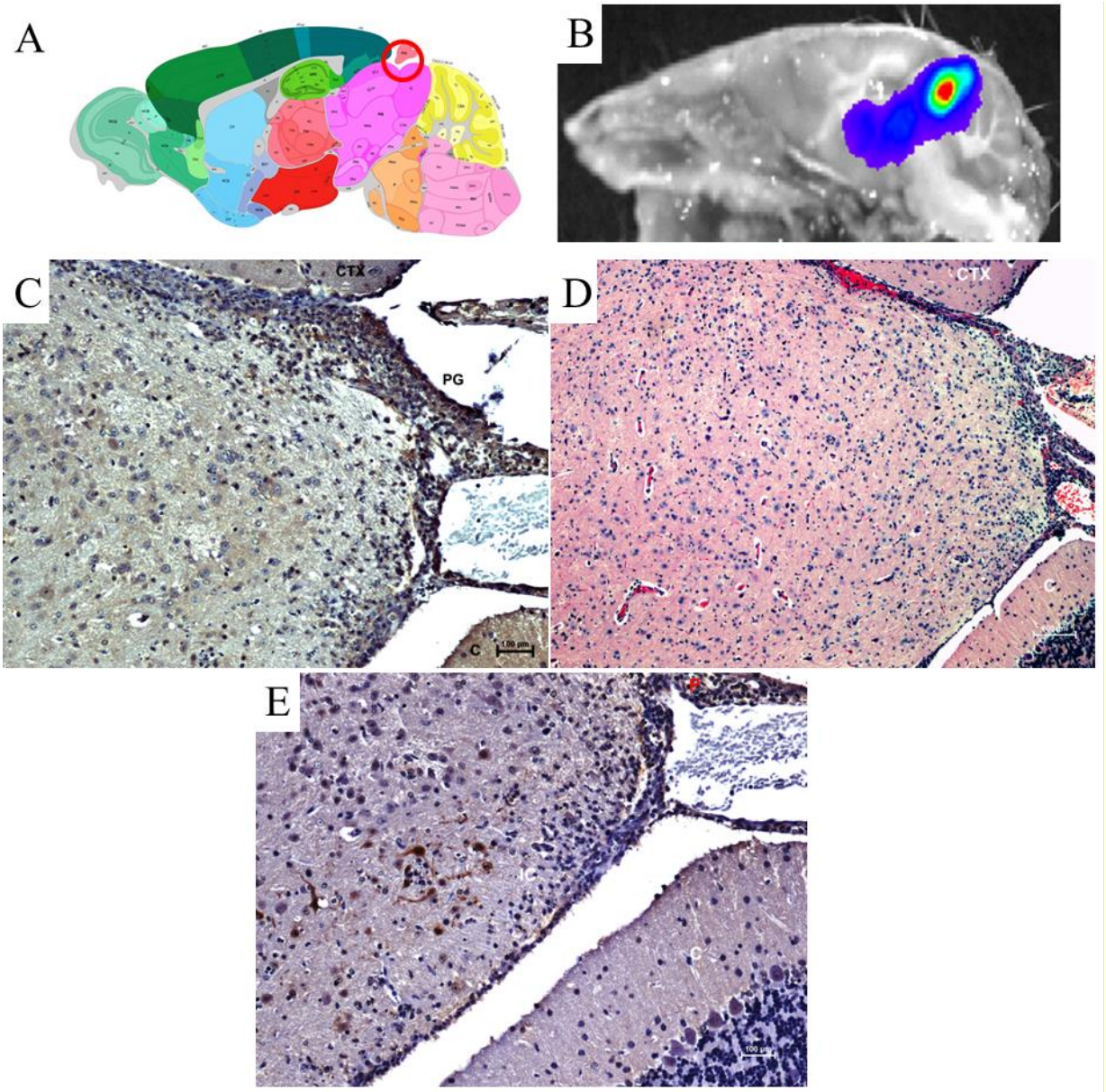

Figure 2.12 Pineal gland route of CNS entry for WEEV. A) Diagram of mouse brain in sagittal-view. Red circle indicates region where luciferase activity was observed in CD-1

mice at 3dpi. B) *Ex vivo* imaging of sagittally bisected head of CD-1 mouse at 3 DPI showing luciferase activity within the hypothalamic region. C-E) Anti-WEEV antigen IHC or hemotoxylin and eosin staining of bisected head in panel B showing affected areas. C) IHC staining (brown) of inferior colliculus and pineal gland region. Notice strong staining in the pineal gland (PG) and nearby neurons of the inferior colliculus. D) Hemotoxylin and eosin staining of same region. Notice necrotic morphology among nuclei in the inferior colliculus along with gliosis and increased numbers of leukocytes. E) IHC staining (brown) of another section of the inferior colliculus region. Notice the strong staining in the pineal gland (P) and neurons of the inferior colliculus but lack of staining in the cerebellum (C). Coretx (CTX).

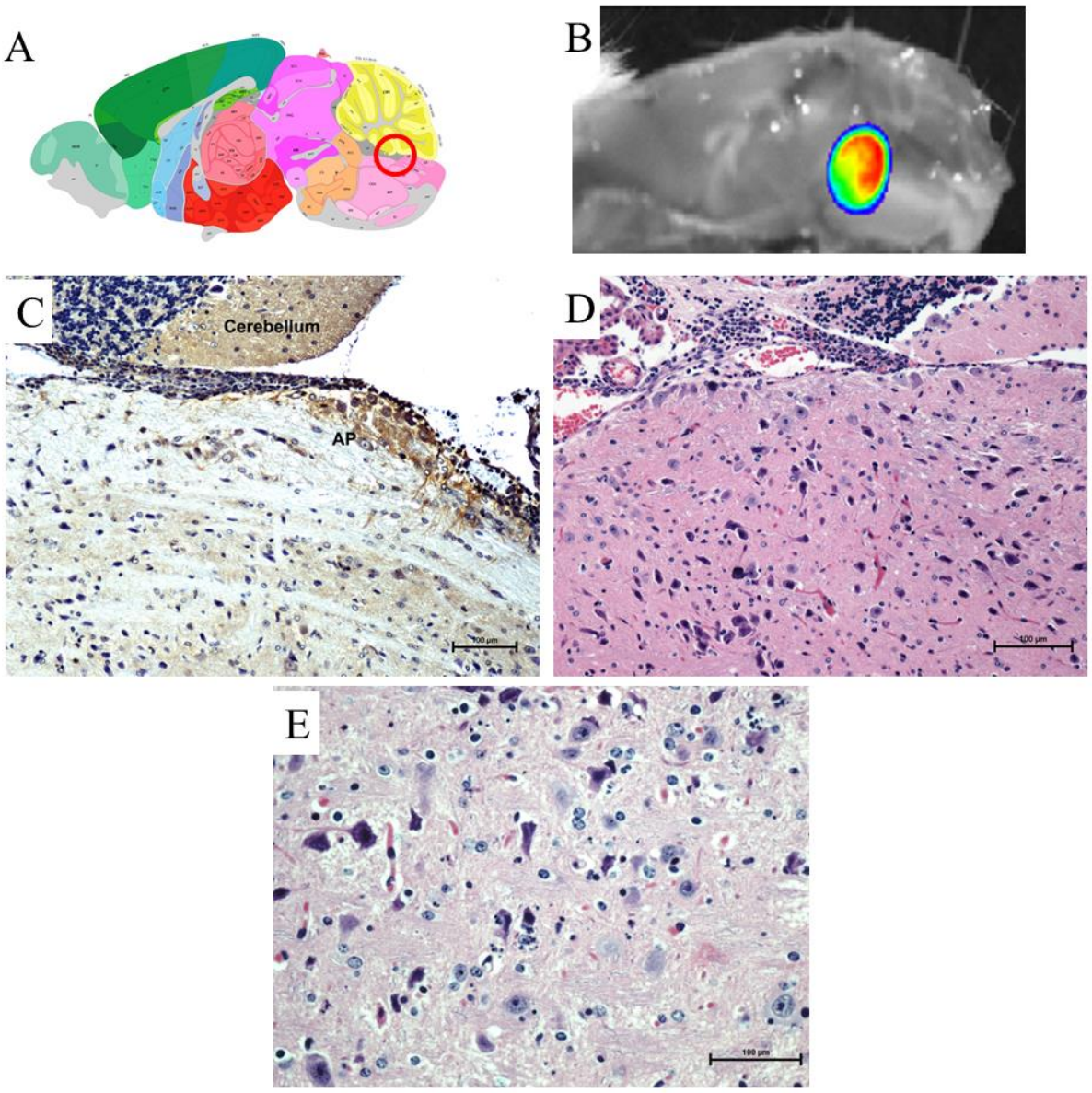

Figure 2.13 Area postrema route of CNS entry for WEEV. A) Diagram of mouse brain in sagittal-view. Red circle indicate region where luciferase activity is observed in CD-1 mice at 3DPI. B) Ex vivo imaging of sagittally bisected head of CD-1 mouse at 3 DPI showing luciferase activity within the area postrema region. C-E) Anti-WEEV antigen IHC or hemotoxylin and eosin staining of bisected head in panel B showing affected areas. C) IHC staining (brown) of area postrema (AP) region. Notice strong staining of neurons and neuronal processes in the area postrema. D) Hemotoxylin and eosin staining of same

region. Notice gliosis and increased numbers of leukocytes. E) Hemotoxylin and eosin staining of hindbrain near area postrema region. Notice the apoptotic nuclei and edema of neuropil.

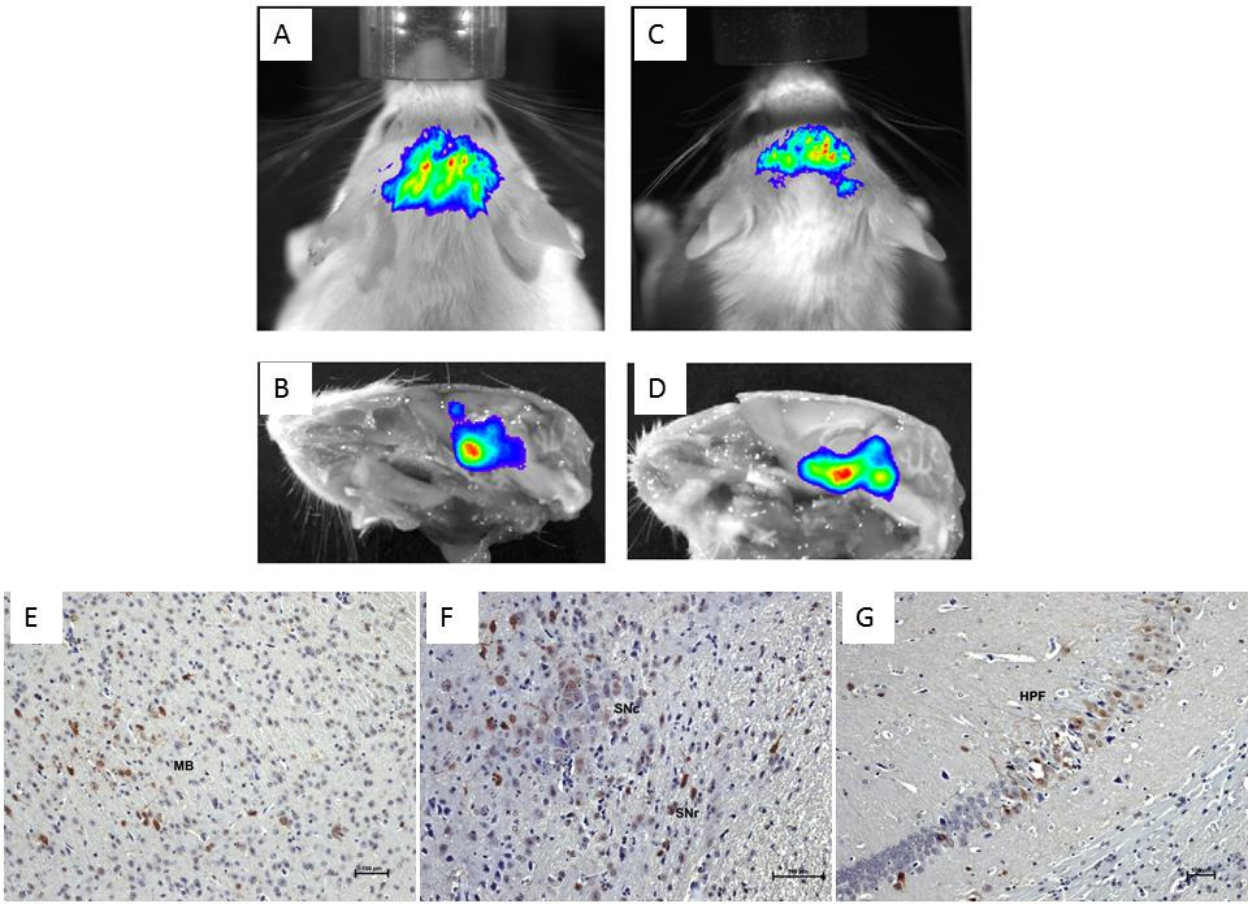

Figure 2.14 Later stages of CNS infection following footpad inoculation. A-D) Two separate CD-1 mice are shown which represent the later stages of CNS infection (5-7 dpi). Images are shown from the intact animal and the subsequent *ex vivo* imaging of the head of that animal. Notice the disseminated infection involving most of the basal ganglia and midbrain and beginning to extend into the cortex. Anti-WEEV antigen IHC staining (brown) of E) midbrain, F) substantia nigra pars compacta (SNc) and pars reticulata (SNr), and G) hippocampal formation showing extensive viral antigen immunoreactivity.

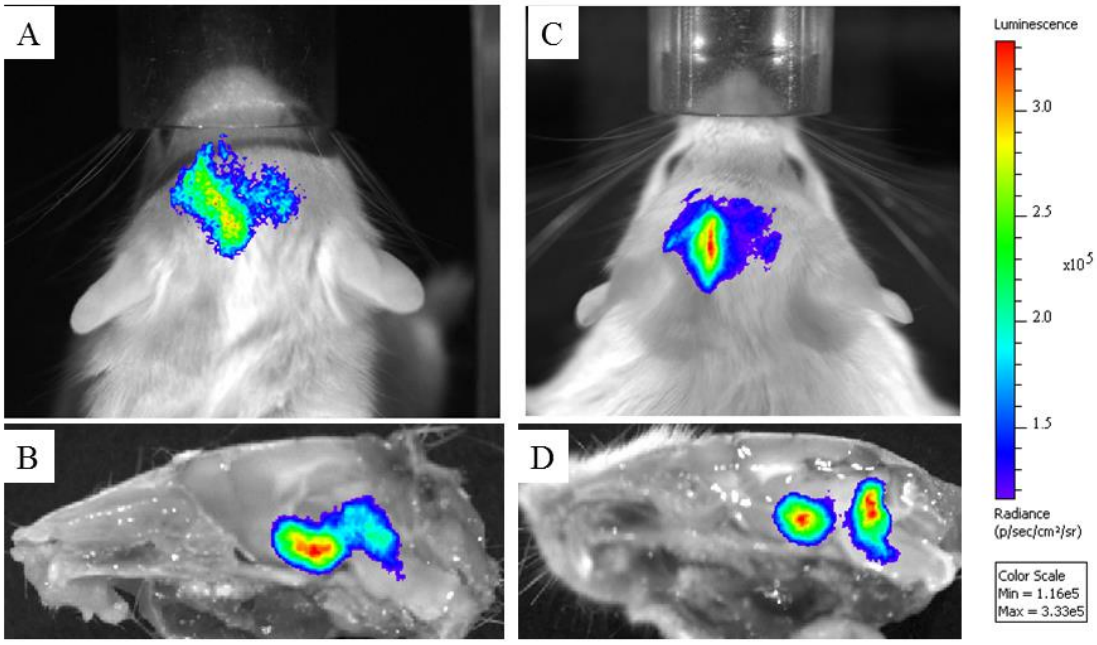

Figure 2.15 *In vivo*/*ex vivo* imaging of McGal-infected Tg-UAS-FLUC mice at 5 dpi (footpad inoculation). (A) *In vivo* image showing luciferase activity markedly pronounced in one hemisphere of the mouse CNS. (B) *Ex vivo* imaging of mouse from panel A. Notice the pattern of luciferase activity which mimics that seen with McFire. Notably, the hypothalamus and midbrain regions are most affected. Panels C and D are an additional example (also from 5 dpi) from a separate animal to demonstrate consistency in luciferase distribution. Again, notice the unilateral nature of the infection.

Discussion

In this report, we have shown that a WEEV-based AES is capable of inducing lethal encephalitic disease in a mouse model. Reporters such as firefly luciferase may be robustly expressed from recombinant virus *in vivo* despite their large coding sequence (1.6 kb). Immunohistochemistry and BLM measurements have shown that WEEV.McM.FLUC retains functional transgene expression throughout CNS dissemination when delivered by the intranasal route. BLM imaging of FLUC activity correlated closely with viral titer within the brain and

provided gross-scale visualization of disease progression. While measurably attenuated in both viral replication kinetics and in the induction of immunological markers of disease, recombinant WEEV.McM.FLUC remained indistinguishable from wild-type virus in terms of histopathological lesions and MTD. This finding supports the use of AES in the assessment of antiviral strategies targeting aerosol exposure. Beyond correlating with viral titers, convenient quantification of reporter signal may provide powerful implications about therapeutic efficacy and mechanism of protection. Therapeutics targeting viral replication, for example, should be capable of significantly decreasing reporter level and distribution. We show in the next chapter that vaccination with liposome-antigen-nucleic acid-complexes provides significant protection from challenge with WEEV.MCM.FLUC and that quantitative analysis of BLM does estimate prophylactic antiviral efficacy. As effective therapeutic strategies become available, BLM imaging could provide an excellent platform with which to rapidly evaluate such strategies.

Ex vivo imaging enhanced correlative histopathological examination as lesions here compared with viral expression levels immediately prior to euthanization. In the case of WEEV, CNS regions associated with viral expression indicated a preference for neuroinvasion through olfactory pathways. When examining the olfactory system, the initial connectivity can be characterized as a tremendous convergence of many olfactory sensory neuron (OSN) dendrites. In the rodent, an estimated 2000 olfactory bulb glomeruli are innervated by 5×10^6 OSN. Each glomerulus possesses an estimated 75 mitral and tufted (MT) neurons that receive information from OSNs. This equates to roughly 1000 OSNs for every MT neuron (Buck and Axel 1991; Buck 1996). Therefore, infection of a proportion of OSNs may result in convergence of advancing infection. The human olfactory system is similar with respect to convergence of axons

onto an individual glomeruli, however, may differ from the rodent with respect to quantity and variety of OSNs.

The neuronal connectivity from the glomerulus is thought to extend into several brain regions. Unlike other sensory systems, the olfactory bulb may send its output directly to olfactory cortex without obligate processing through the thalamus (Shepherd and Greer 1998) although thalamic pathways are also utilized. The connectivity of MT cells was recently detailed in an elegant study utilizing viral tracing techniques (Ghosh, Larson et al. 2011). The virus used to trace the MT cells was a fluorescent reporter-expressing Sindbis virus replicon system. The authors of that study determined that MT cells synapse with a very large set of target neurons, to include neurons of the lateral olfactory tract, but also among other olfactory bulb neurons, including granule cell layer neurons near the mirror symmetric glomerulus (a feature not found in other sensory systems). More research is needed to determine what role the glomerular neuronal connectivity plays in WEEV dissemination. It is conceivable that this architecture would favor increased viral titers within the olfactory bulb and thus lead to more efficient spread into the rest of the CNS. Bilateral communication is also available by means of the anterior commissure. The extensive connectivity of olfactory systems provides broad and bilateral dissemination potential within the brain proper.

The olfactory bulb contains specialized dendrodendritic synapses, in which vesicles are observed within presynaptic and postsynaptic membranes. As synaptic plasticity is dependent in part upon translational machinery present at the synapse, the processes of learning and memory may be intimately tied to encephalitic alphavirus infection. Interestingly, aside from general somatosensation, the trigeminal nerve sends fibers to the neuroepithelium (to detect caustic stimuli). It is conceivable that the observed infection of trigeminal ganglia and brainstem could

have originated from infected neuroepithelia. Such an alternative neuroinvasion mechanism has been reported for VEEV infected animals after ablation of olfactory bulbs (Charles, Walters et al. 1995). CNS infection was associated with trigeminal nerve involvement. The current study shows a similar neuroinvasion for WEEV, including a novel finding of virus localization to the follicular epithelium of vibrissae. Information from vibrissae is delivered via trigeminal nerve first into trigeminal sensory complex of the brain stem. From there the virus spreads to parts of the thalamus and barrel cortex, the most studied pathways from trigeminus to the cortex. WEEV is a naturally-occurring recombinant virus and resembles VEEV in its ability to infect trigeminal nerve-associated neurons and ultimately infect brainstem nuclei. Therefore, WEEV may serve as a relevant model system for higher priority pathogens such as VEEV or EEEV.

The pattern of virus distribution in the brain of peripherally inoculated mice appears to be significantly different from mice challenged intranasally. The rapid onset and consistent involvement of brain regions that correspond to structures where the BBB is absent, with concurrent sparing of neuroepithelium and olfactory bulb, strongly suggests that the main route for CNS invasion occurs via the vascular route. Circumventricular organs are indicated by these studies as the route of CNS entry for WEEV McM strain. Further research is needed to determine if this specific route of CNS entry is common among all strains of WEEV or even among other alphavirus species, such as EEEV. It is conceivable that McM is neuroadapted through passage in neuronal tissue, and that this feature has altered the pathogenesis of the virus from its natural state.

The area postrema, hypothalamus/median eminence, and pineal body are all circumventricular organs, and are characterized by highly vascularized areas that lack a blood-brain barrier. The area postrema is located above the entrance to the central canal of the spinal

cord in the IV cerebral ventricle and differs from other areas of the medulla oblongata in the absence of bundles of myelinated nerve fibers (Siso, Jeffrey et al. 2010). The median eminence, with the hypothalamus-pituitary axis, is located along the ventral floor of the forebrain/midbrain interface. Here, neuroendocrine molecules are secreted by hypothalamic neurons and are received by non-neuronal cells of the anterior pituitary. The pineal body is located along the sagittal-midline axis just rostro-dorsal to the superior colliculus. This neuroendocrine gland is involved in the sleep/wake cycle in vertebrates by its release of melatonin. The specifics regarding the innervation to pineal gland are not well-described and may differ between humans and rodents (Siso, Jeffrey et al. 2010). The two more highly-innervated of the three circumventricular organs are the hypothalamus and area postrema. This may account for the relative prevalence of each during these imaging studies as compared to the pineal body, which was slightly less frequent.

Studies aimed at examining WEEV neuroinvasion or CNS dissemination in the animal model should benefit from the use of bioluminescent imaging. There are no specific antivirals available for alphaviral infection and treatment is limited to supportive care. Studies have demonstrated the limitations of immunoprophylaxis (Ryzhikov, Tkacheva et al. 1991), and while modulators of innate immunity show promise (Julander, Siddharthan et al. 2007; Logue, Phillips et al. 2010), future generations of therapeutics may benefit from a greater understanding of the progression of alphaviral-induced neural disease. BLM may also be useful to test antivirals, prophylactic treatments, and evaluate pathogenesis.

CHAPTER 3: LIPOSOME-ANTIGEN-NUCLEIC ACID COMPLEXES: EVALUATION OF PROTECTION AGAINST LETHAL WEEV OR EEEV INFECTIONS IN MICE

Introduction

Antibody-mediated clearance of alphavirus from the CNS was discussed in Chapter 1 and is an attractive strategy for preventing encephalitic disease from WEEV infection. Antibodies directed to alphavirus envelope glycoproteins can be effective at treating alphavirus infection of the CNS (Schmaljohn, Johnson et al. 1982; Levine, Hardwick et al. 1991; Griffin, Levine et al. 1997; Hunt, Bowen et al. 2011). Importantly, antibodies to SINV E2 or E1 proteins were shown to vary in their degree of cross-reactivity among distinct alphavirus species (Roehrig, Gorski et al. 1982). Anti-SINV E2 antibodies were shown to be highly-neutralizing yet specific only to Sindbis virus antigen, while anti-SINV E1 antibodies were determined to be non-neutralizing yet cross-reactive to WEEV (McM strain) as well as VEEV (strain TC-83) and EEEV (New Jersey strain). Thus, E1 is an excellent vaccine candidate because it might offer broader ("pan-alphavirus") protection against fatal encephalitis. While antibodies targeting alphavirus E1 glycoprotein often fail to neutralize extracellular virus, non-neutralizing antibodies raised to the prototypic alphavirus (SINV) E1 glycoprotein are highly protective in an animal model of infection.

In this study, we examined the protective potential of liposome-antigen-nucleic acid complexes (LANACs) consisting of CLNCs and the recombinant WEEV E1 ectodomain (E1ecto) produced using the baculovirus-insect cell system. We demonstrate that the CLNC component of the LANAC alone has a therapeutic impact on WEEV infection and that cationic liposomes with the ODN/PIC polyvalent-adjuvant formulation provide greater protection than

cationic liposomes containing only a single nucleic acid species (ODN or PIC). We further demonstrate that CLNCs mixed with the recombinant WEEV E1ecto provide effective prophylaxis against homologous and heterologous strains of WEEV (McMillan and Montana-64) as well as cross-protection against a neurovirulent strain of EEEV (Florida-93). This new vaccine formulation is protective against WEEV and EEEV transmitted by a variety of routes, including WEEV-infected mosquito vectors (*Culex tarsalis*), and induces a humoral response that does not include detectable levels of neutralizing antibodies. Taken together, these studies support the use of an adjuvant composed of CLNCs mixed with recombinant WEEV E1ecto as a therapeutic and prophylactic vaccine capable of inducing rapid protection against multiple New World alphaviruses.

Materials and Methods

Virus strains.

WEEV (McMillan and Montana-64 isolates) came from the Arbovirus Reference Collection at the Centers for Disease Control and Prevention, Fort Collins, Colorado, USA. The source (host species) and passage history of the viruses used in this study can be found in Table 3.1. Recombinant luciferase-expressing McMillan virus was generated as previously described (Phillips, Stauft et al. 2013). EEEV strain FL93-939 (Florida-93), a 1993 Florida mosquito isolate passed once in Vero cells (Wang, Petrakova et al. 2007), was obtained from Dr. Richard Bowen (Colorado State University). Viral stocks were produced by infecting Vero cells (ATCC) grown in minimal essential medium (MEM) with 10% fetal calf serum at a multiplicity of infection of ≤0.01 plaque forming units (pfu)/cell. Cell culture supernatants were collected at 48 hours post-

infection (HPI) and stored in aliquots at −80 °C. Virus titers were determined by plaque assay on Vero cells as previously described (Logue, Bosio et al. 2009).

Table 3.1 Viruses used in LANAC studies.

Viral Isolate	Location and date of isolation	Host/passage history
WEEV McMillan	Ontario, Canada, 1941	Human brain/MP2, SMB1, V2
WEEV Montana-64	Montana, USA, 1967	Horse brain/DE1
EEEV Florida-1993	Florida, USA, 1993	*Culiseta melanura* mosquito pool/V1, SMB1

Mouse studies.

Animal use in this study was approved by the Institutional Animal Care and Use Committee at Colorado State University. Care and handling of the mice was consistent with the PHS Policy and Guide for the Care and Use of Laboratory Animals. Outbred, 4-6 week old female CD-1 mice (Charles River, Willington, MA) were allowed to acclimate to the facility for 3–7 days. Subcutaneous (s.c.) and intranasal (i.n.) infections were performed with a dose of 1–5 × 10^4 pfu of virus diluted in PBS. The s.c. inoculations were administered in the right footpad of the mouse. The i.n. inoculations were performed by alternately dripping inocula onto the nostrils of lightly anesthetized mice until a volume of 20 µl was applied. The inocula were titrated by plaque assay on Vero cells to confirm dosages. All mice were observed twice daily for signs of morbidity. Moribund mice were euthanized by CO_2 inhalation and the day of euthanization was taken as the day of death to calculate mean times to death (MTD). Survivorship was followed for a period of 28 days (initial studies).

Preparation and administration of CLNCs and LANAC.

Cationic liposomes (100 mM DOTIM lipid+cholesterol) in 10% sucrose were provided by Dr. Steven Dow (Colorado State University). CLNCs were prepared essentially as described (Logue, Phillips et al. 2010) with the only modification being the addition of PIC. Briefly, liposomes were diluted 1:5 in sterile Tris-buffered 5% dextrose water (pH 7.4). Poly (I:C), ODN 1826 CpG DNA

(InvivoGen, San Diego, CA), or both nucleic acid species were then added to a final concentration of 0.1 mg/ml, causing spontaneous formation of liposome-nucleic acid-complexes (Fig. 3.1A). For therapeutic studies (treatment after viral inoculation), a single dose of CLNCs was administered to mice (n=10) 24 hours after s.c. inoculation with 10^4 pfu of WEEV Montana-64, or immediately after s.c. inoculation with 10^4 PFU of WEEV McMillan.

For vaccination studies, a recombinant HIis-tagged version of WEEV E1ecto was produced in the baculovirus-insect cell expression system and purified by immobilized metal affinity chromatography, as previously described (Toth, Geisler et al. 2011; Phillips, Stauft et al. 2013). Purified E1ecto was added to formed CLNC complexes at a final concentration of 50 µg/mL (10 µg/200 µL dose) unless otherwise noted (as during initial dosage evaluation studies)(Figure 3.2). The antigen was allowed to associate with liposome complexes for 15 minutes with mixing by inversion and the resulting liposome-antigen-nucleic-acid-complexes (LANACs) were used to vaccinate mice (n=10). Each dose of vaccine consisted of 200µL of LANAC delivered via s.c. injection dorsal to the cervical spine. The primary vaccination was followed by a boost dose of the same vaccine two weeks later. The immunized mice were challenged at 2, 3, 7, 9, or 11 weeks after the booster dose by i.n. or s.c. inoculation with WEEV McMillan, WEEV Montana-64, or EEEV Florida-93. Control animals received only CLNCs mixed with a sham antigen prepared by mock affinity purification of the cell-free medium from expreSF+® cells infected with an isogenic, empty baculovirus vector. Additional controls included mice that were neither treated nor virus-inoculated to determine background luminescence during *in vivo* imaging studies.

In vivo imaging and quantitation of luciferase activity

Mice were vaccinated with E1ecto- or sham-LANACs using the prime-boost strategy described above. Two weeks after the booster, animals were challenged by i.n. infection with 10^4 pfu of a WEEV McMillan recombinant encoding luciferase and imaged at 24 and 48 HPI using IVIS 200, as previously described (Phillips, Stauft et al. 2013). Luciferase activity for each acquired image was quantified using Living Image 3.0 software (Caliper Life Science, CA, USA).

Virus titration of mouse brain tissue

Whole brains from each treatment group were collected at 72 HPI (n=4) from mice used for the imaging studies, as previously described (Phillips, Stauft et al. 2013). Samples were removed after a 5 min PBS perfusion by cardiac puncture to ensure all systemic blood was removed. Brains were placed in pre-weighed 1 ml green bead tubes (Roche, Switzerland) containing 0.5 ml MEM and processed as previously described (Logue, Phillips et al. 2010).

Plaque reduction neutralization titer

BHK-21 cells (ATCC) were maintained in MEM supplemented with 10% heat-inactivated fetal bovine serum, 2mM glutamine and 100 U/mL of penicillin and 100 µg/mL of streptomycin and used to seed 24-well plates. Plaque reduction neutralization titers (PRNTs) were measured by incubating virus samples with serial dilutions of serum, inoculating samples into each well, and incubating the plates at 37°C in 5% CO_2 for 1 hour. The inocula were aspirated and the cells were overlaid with growth medium-agar. After being incubated at 37°C in 5% CO_2 for 3 days, plaques were visualized using 3-(4,5-dimethylthiazol-2-yl)-2,5-diphenyl-2H-tetrazolium bromide (MTT). Positive controls consisting of virus that was not pretreated with serum were including in each assay. Sera assayed in these PRNTs included sera collected 3 weeks after the booster dose from mice immunized with E1ecto LANACs, negative control serum, and positive control serum from mice that had survived

footpad infection with luciferase-expressing WEEV McMillan. PRNT endpoints were calculated using probit analysis, as previously described (Cutchins, Warren et al. 1960). A 50% plaque reduction (PRNT50) was used as the neutralizing end point and the PRNT50 titer was expressed as the reciprocal of the highest dilution of test serum able to neutralize 50% of the input virus.

Mouse serum antibody profile assay

For isotype ELISA, polyvinylchloride plates were coated overnight at 4° C with 100 µl of E1ecto antigen diluted to 2 µg/ml in PBS (pH 7). Plates were washed twice with PBS containing 0.25% TWEEN-20 (PBS-TW) and twice more with PBS. Plates were blocked with 200 µl of SuperBlock T20 (Thermo Scientific) for 1 hour at room temperature then washed as described above. Serum samples were diluted 1:100 in PBS and 2-fold serial dilutions were added to the plates, followed by 1 hour incubation at room temperature. Isotype-specific detection was performed by 1 hour incubation with monoclonal antibodies to IgG1 (clone X56, HRP conjugate), IgG2a (R19-15, HRP), IgG2b (R12-3, biotinylated conjugate), IgG3 (R40-82, biotinylated), IgM (11/41, HRP) or IgA (C10-1, biotinylated) diluted 1:500 in PBS. Wells with biotinylated antibodies were incubated for an additional hour with HRP-streptavidin (Rockland) at 1:1000 in PBS. ABTS substrate (KPL) was added, incubated for 15 min, and absorbance at 405 nm was recorded. Endpoint titers were calculated as the reciprocal of the greatest dilution that was 0.200 O.D. greater than the negative control.

Cell-based assay for viral replication inhibition by antibody activity

Luciferase-expressing WEEV was used to infect SY5Y neuroblastoma cells (ATCC CRL-2266) for one hour in a 24 well plate at a multiplicity of infection (M.O.I.) of 0.01 and the infected cells were washed 3 times with cold PBS. Sera from immunized mice, negative controls, or positive control mice that had survived previous challenge were diluted 1:200 in growth medium, added to each well,

and images were acquired at 24 and 48 HPI. Supernatants were collected and used to quantify infectious virus by plaque assay.

Mosquito studies

Female *Culex tarsalis* (Bakersfield strain) were reared at the insectary facility of the Arthropod-borne and Infectious Diseases Laboratory at Colorado State University and moved into BSL-3 insectary as adults. At 1 week post-emergence, mosquitoes were intra-thoracically inoculated with 10^2 PFU of WEEV McMillan in a total volume of 69 nL. Mosquitoes were held for 7 days at 28°C and 75% humidity before being used to challenge. WEEV E1ecto LANACs- (n=5) or sham-LANACs-vaccinated mice (n=5) were exposed to 6-12 infected mosquitoes per mouse at 2 weeks after the booster. A representative sample of blood-engorged mosquitoes was collected from each treatment group (E1ecto-LANAC n=9, sham-LANACs n=13), and individual whole mosquitoes were homogenized and viral titrations performed.

Statistical analyses

All titration data were $\log_{10}$-transformed and compared using unpaired Student's t test. Analysis was conducted using statistical analysis software (SAS) version 9.2. Survival curves were subjected to Kaplan-Meier (log rank test) analysis using Prism version 6.00 for Windows (GraphPad). Quantitative analysis of bioluminescence in the assessment of vaccine efficacy was conducted using two-tailed t-test.

Results

Therapeutic efficacy of CLNCs

The therapeutic efficacy of liposomes containing PIC and/or ODN (Fig. 3.1A) was assessed in mice that had been infected with either the Montana-64 or McMillan strain of

WEEV. Montana-64 has a longer MTD in CD-1 mice and is more suitable for modeling human disease following epizootic outbreaks, as compared to the mouse-adapted, highly virulent McMillan strain (Logue, Bosio et al. 2009). Montana-64 is also more sensitive to therapeutic intervention (Phillips, unpublished data). We examined the effect of CLNCs containing ODN, PIC, or both at 24 HPI (Montana-64) or 0 HPI (McMillan) to determine which CLNC formulation provided the best protection in our mouse model. CLNC formulations containing both PIC and ODN, but not those containing only one or the other, significantly increased survival relative to untreated controls following infection with either Montana-64 or McMillan (Fig. 3.1B and C). However, CLNC/ODN/PIC administered at 48 (Montana-64) or 24 (McMillan) HPI had no statistically significant impact on survival relative to untreated controls (data not shown).

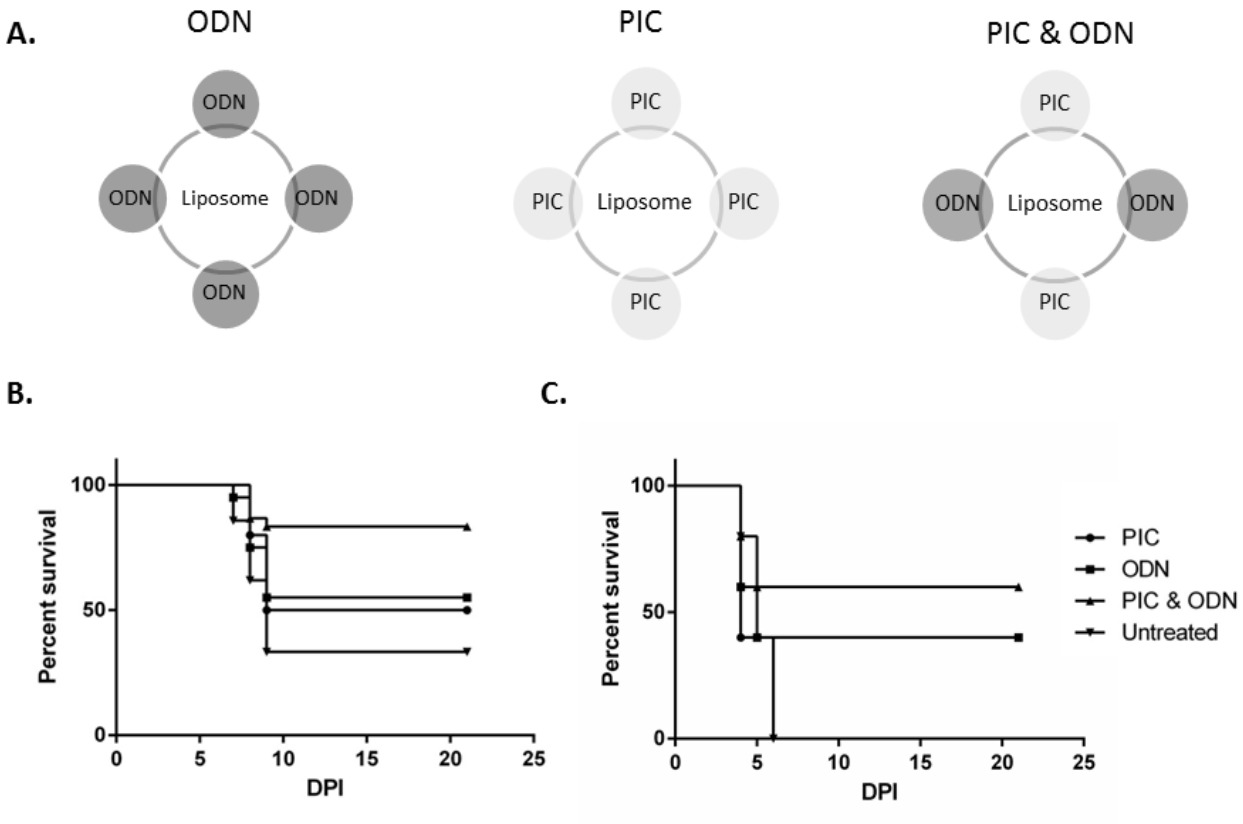

Figure 3.1 Effect of nucleic acid type on therapeutic efficacy of CLNCs. (A) Schematic diagram of liposomes containing ODN, PIC, or both ODN and PIC. (B) Mice (n=10/group) were infected with 10^4 PFU of WEEV Montana-64 and then treated with liposomes containing ODN, PIC, or both ODN and PIC at 24 HPI. Liposomes containing PIC and ODN provided significant protection (p=0.0154) compared to untreated control mice. (C) Same as (B) except WEEV McMillan was used and liposome treatments were performed immediately after infection (0 HPI). Liposomes containing PIC and ODN provided significant protection (p=0.0488) compared to untreated control mice.

Protective efficacy of LANACs containing WEEV E1ecto

We subsequently assessed the ability of LANACs composed of CLNC/ODN/PIC and recombinant WEEV McMillan E1ecto to protect mice against WEEV Montana-64 or McMillan. The protective efficacy of this formulation was first examined by immunizing mice with LANACs containing varying amounts of E1ecto (10, 1, or 0.1 µg) followed by s.c. challenge with Montana-64 (least virulent strain used in these studies). LANACs containing 10 µg of E1ecto provided 100% protection against challenge with WEEV Montana-64 at two weeks after the booster (Fig. 3.3).

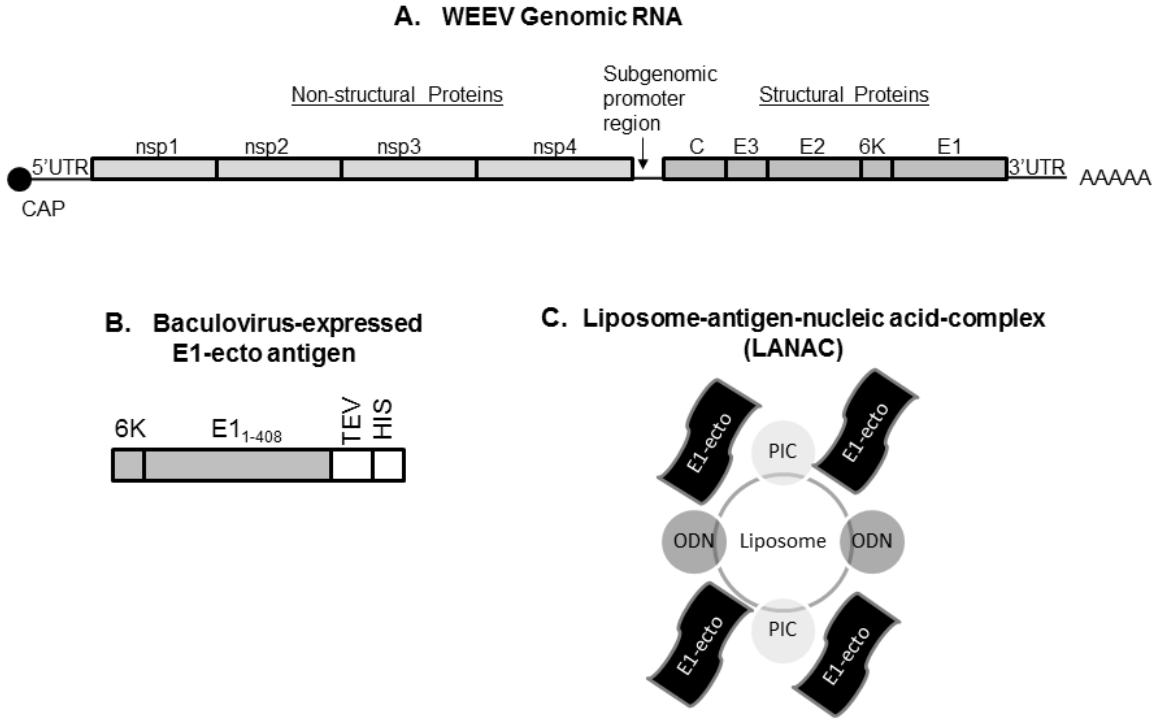

Figure 3.2 Diagram of WEEV genome, E1ecto construct, and LANACs. (A) The WEEV genome contains a 5' untranslated region (5'UTR), nonstructural polyprotein gene (nsP1-nsP2-nsP3-nsP4), subgenomic promoter sequence, structural polyprotein gene (capsid-E3-

E2-6K-E1), and a 3' untranslated region (3'UTR). (B) The E1ecto construct encoded full-length WEEV (McMillan) 6K protein, the first 408 amino acids of WEEV (McMillan) E1 protein, a tobacco etch virus protease cleavage site (TEV), and an 8X histidine purification tag. E1ecto was produced using the baculovirus-insect cell system. (C) E1ecto or a sham preparation (see Materials and Methods) were mixed with PIC and ODN- containing liposomes to form E1ecto- or sham-LANACs that were used for vaccination experiments.

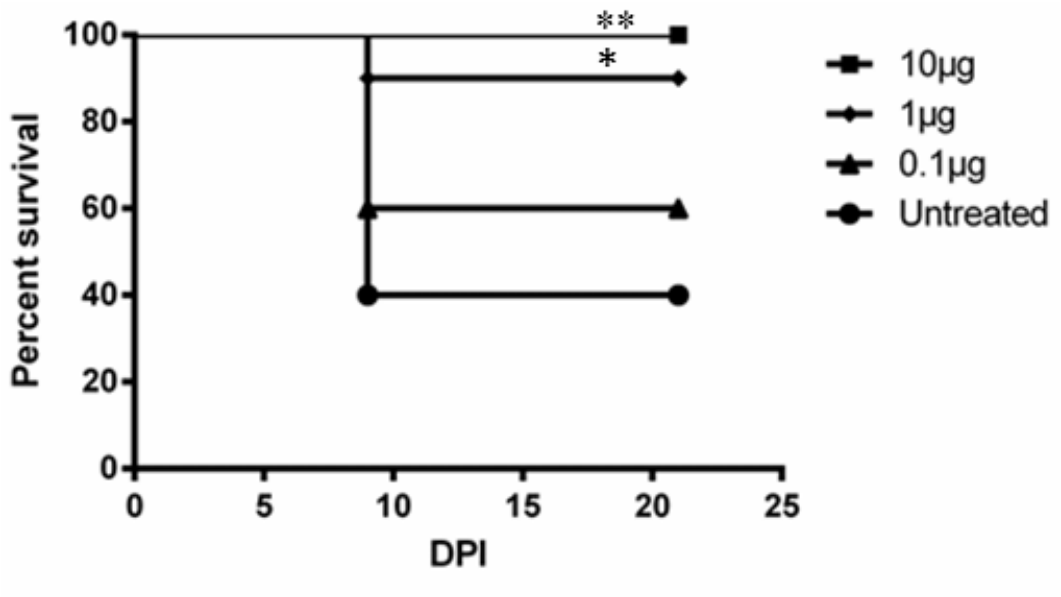

Figure 3.3 Effect of E1ecto antigen dose on mouse survival. Mice (n=10/group) were vaccinated with LANACs containing 0.1, 1.0, or 10µg of E1ecto using a prime-boost protocol, then challenged by s.c. inoculation with 10^4 PFU of WEEV Montana-64. Complete protection was observed using the 10µg antigen dose and this dosage was used for the remainder of the vaccination experiments. ** *p* value = 0.0082 , * *p* value = 0.0461.

Next, we determined the protective efficacy of LANACs containing the optimal 10 µg of E1ecto against the more virulent WEEV McMillan strain. The effects of infection route and longevity of the immune response to the E1ecto-LANACs were examined by challenging

immunized mice by the s.c. or i.n. routes at two different times after the booster. Immunization with the E1ecto-LANACs provided 100% protection against s.c. infection and 60% protection against i.n. infection at two weeks (Fig. 3.4A) and 100% protection against virus administered by either route at 11 weeks (Fig. 3.4B) after the booster dose.

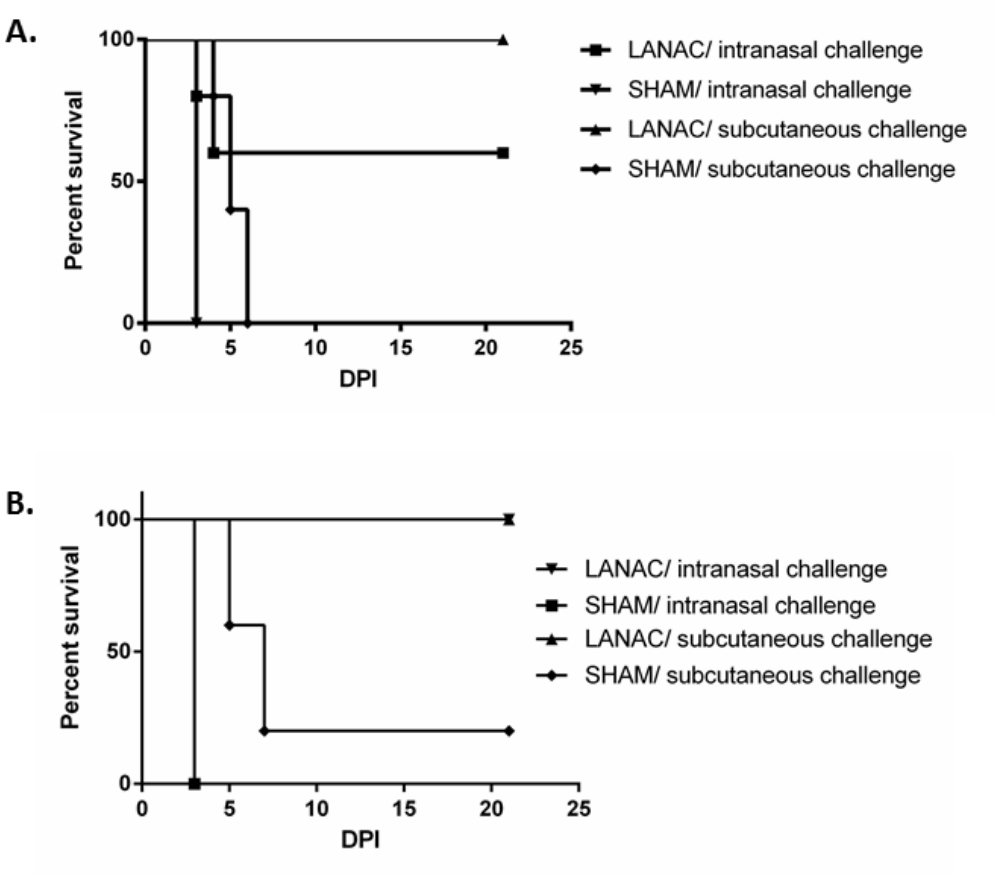

Figure 3.4 LANACs protection against intranasal or subcutaneous challenge with WEEV. (A) Mice (n=10/group) were prime-boost immunized with E1ecto-LANACs (LANAC) or sham-LANACs (SHAM) and challenged with 10^4 PFU of WEEV McMillan two weeks after the booster. The differences in survival among mice immunized with E1ecto- or sham-LANACs were statistically significant ($p < 0.0001$ for s.c.; $p = 0.0359$ for i.n. routes). (B) Same as (A) except the mice were challenged 11 weeks after the booster dose. Again, the

differences in survival among mice immunized with E1ecto- or sham-LANACs were statistically significant ($p<0.001$).

Finally, we examined the protective efficacy of LANACs in mice challenged with WEEV via exposure to infected *Culex tarsalis* mosquitoes at 2 weeks after boost dose of vaccine. The results showed that the E1ecto LANACs provided complete protection (Fig. 3.5A). Plaque assays confirmed that the viral titers of blood-engorged mosquitoes for infecting E1ecto LANAC– or sham-LANAC immunized mice were not significantly different (Fig. 3.5B).

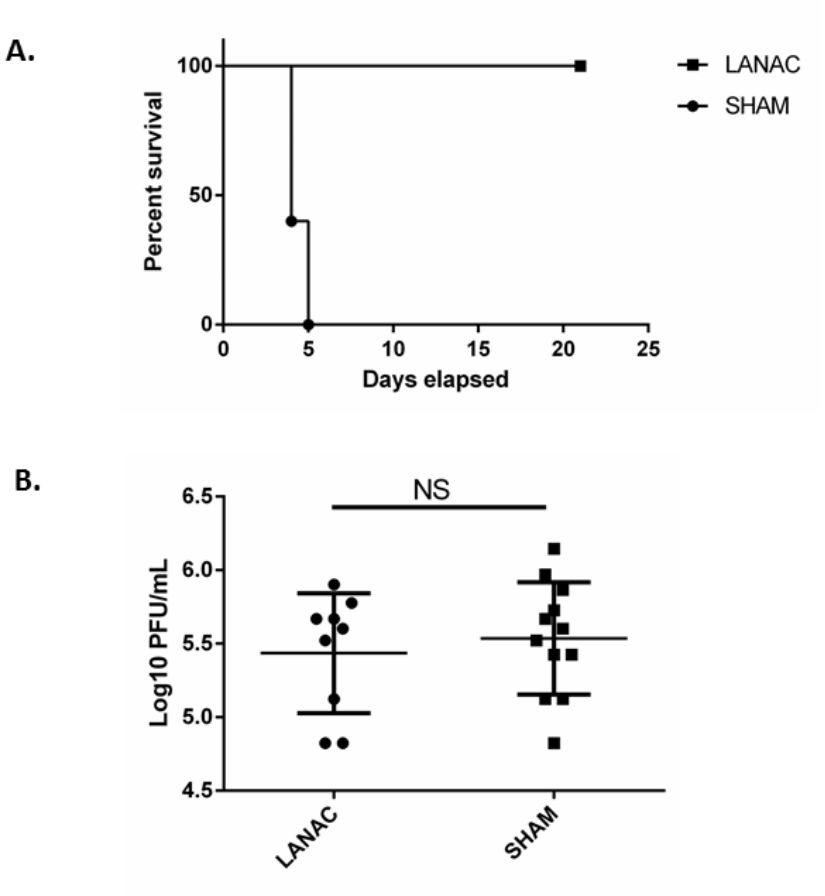

Figure 3.5 LANACs protection against mosquito-delivered WEEV challenge. (A) Mice (n=5/group) were prime-boost vaccinated with E1ecto-LANACs (LANAC) or sham-LANACs (SHAM) and exposed to WEEV McMillan-infected *Culex tarsalis* mosquitoes 2

weeks after boost dose. Survivorship was monitored for 21 DPI. Differences in the survival curves of mice immunized with E1ecto- or sham-LANACs were statistically significant (*p*=0.0295). (B) Infectious virus titers in individual mosquitoes used to infect mice from each treatment group in panel A. Differences were not statistically significant.

Bioluminescence imaging for visualizing effects of LANACs on virus replication

We also used imaging to examine non- or E1ecto LANACs-immunized mice after i.n. challenge at 2 weeks after the booster dose with a luciferase-expressing form of WEEV. The results revealed a significant reduction in the bioluminescence signal observed in the LANACs-immunized animals, as compared to non-immunized controls at both 24 and 48 HPI (Fig. 3.6A and 3.6B). In fact, there was no difference in the levels of bioluminescence observed in the immunized animals and uninfected controls (Fig. 3.6B red line indicates level of uninfected animal background luminescence). These findings were extended by measuring viral infectivity in homogenates of brains removed from euthanized animals at 72 HPI at (Fig. 3.6C). The immunized mouse brain homogenates produced no detectable plaques, indicating a viral titer lower than the detection limit of our plaque assay (6.6 PFU/mL). In contrast, we observed titers of ~10^7-10^8 PFU/g tissue in the non-immunized mouse brain homogenates, which was consistent with our previous results (Phillips, Stauft et al. 2013).

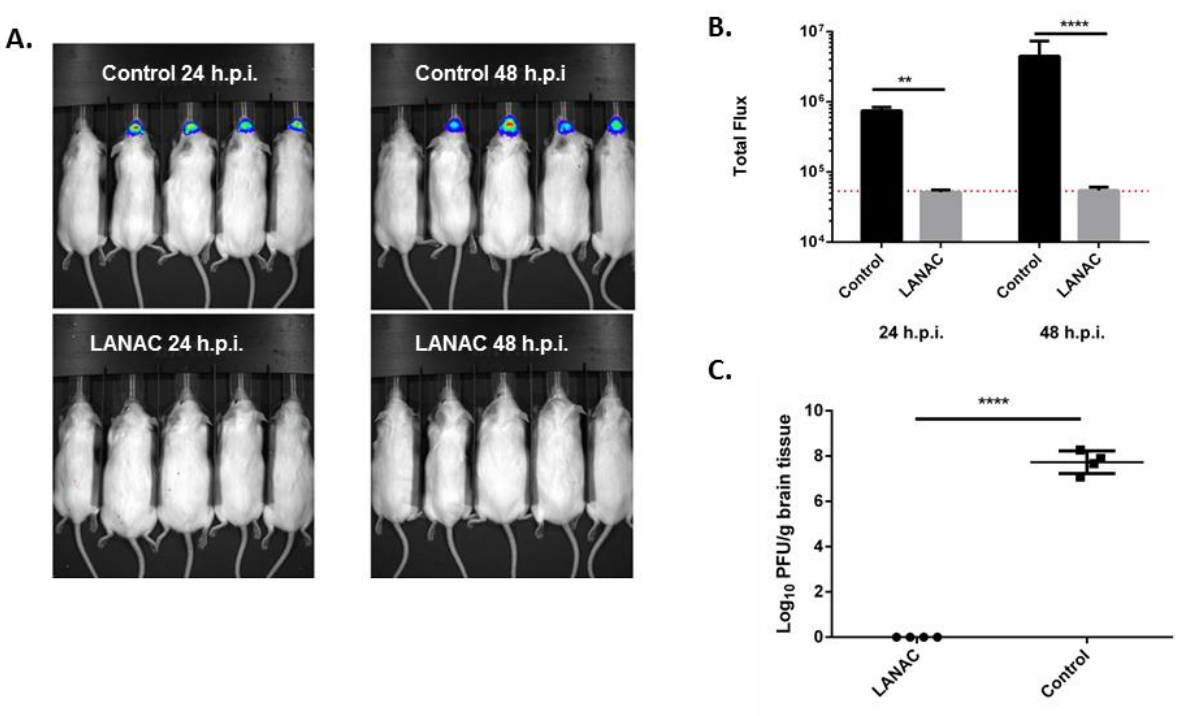

Figure 3.6 . ***In vivo*** **bioluminescence imaging of the protective effects of LANACs. (A) Non-immunized and E1ecto-LANACs-immunized mice (n=4/group) were challenged by i.n. inoculation with 10^4 PFU of recombinant luciferase-expressing WEEV McMillan, and then imaged at 24 and 48 HPI. In each image, the first mouse on the left is an uninfected control to establish background bioluminescence. (B) Bioluminescence quantitation of (A). Each bar represents the average bioluminescence signal -/+ standard deviation for each treatment group. Differences between the two treatment groups were significant (*****p*<0.01, **** *p*<0.0001). (C) Infectious virus titers in homogenates of brains isolated from animals used in panel A at 72 HPI. Differences between the two treatment groups were statistically significant (*******p*<0.0001).**

Neutralizing and antiviral activities of serum from LANACs-immunized mice

The viral neutralization titers of sera from 1) E1ecto LANACs-immunized, 2) non-immunized (normal), and 3) untreated mice that survived experimental s.c. challenge with recombinant McMillan (survivor) were measured using standard PRNT assays. Like the normal sera, the LANACs-immunized mouse sera had no detectable neutralizing activity ($PRNT_{50}$ of <40), while the survivor sera had a $PRNT_{50}$ of 200 (Fig. 3.7A). We extended these results by imaging Vero cells 24 hr after being infected with the luciferase-expressing WEEV McMillan strain and treated (1 HPI) with a 1:200 dilution of sera. The results of this assay showed that sera from the LANACs-immunized mice significantly reduced the bioluminescence signal, as compared to the negative control serum (Fig. 3.7B and C). The LANACs-immunized mouse sera also significantly reduced the amount of infectious virus produced by the infected cells (Fig. 3.7D), as compared to normal sera. Therefore, although the E1ecto LANACs-immunized mouse sera had no detectable virus neutralizing activity, the sera nevertheless had significant antiviral activity.

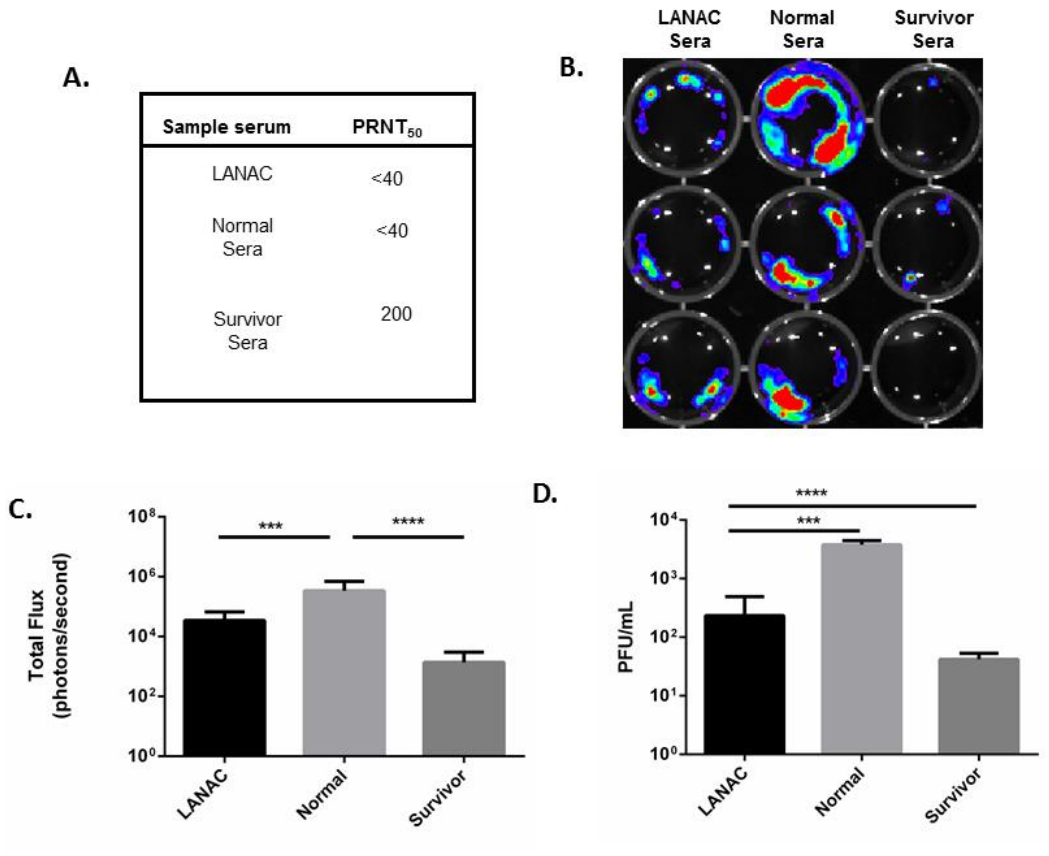

Figure 3.7 Neutralizing and passive protection activity of serum from LANACs-immunized mice. (A) PRNTs of sera from E1ecto-LANAC-vaccinated mice (LANAC), non-immunized, uninfected mouse sera (normal), or sera from mice which had survived s.c. challenge with WEEV (survivor). (B) SY5Y cells were infected with recombinant luciferase-expressing WEEV and treated after 1 hour with 1/200 dilution of sera. Cells were imaged at 24 (shown) and 48 HPI. (C) Quantitation of bioluminescence shown in (B). Each bar represents the average -/+ standard deviation of the indicated treatment group. Sera from E1ecto-LANAC-vaccinated mice significantly reduced luciferase activity (p value =0.007) compared to normal (normal) control sera. (D) Infectious virus titers present in cell culture medium of each treatment group shown in (B). Sera from LANAC-

vaccinated mice significantly reduced virus titers compared to normal (uninfected) control sera (p value =0.007).

Antibody profiling

To further characterize antigen-specific humoral responses induced by immunization, sera collected at 2 weeks following the first (prime) and second (prime-boost) doses of LANACs or bovine serum albumin (BSA) were assayed for relative isotype abundance by ELISAs (Figure 3.8A). Sera from uninfected, unvaccinated animals were used as controls. The results showed that animals that were vaccinated or boosted with LANACs produced E1ecto-specific IgG, whereas unimmunized and BSA-immunized animals did not. In addition, primed animals produced primarily IgG1, whereas prime-boosted animals produced IgG2a and IgG2b, indicating isotype switching. Immunization did not induce appreciable levels of IgG3. The geometric mean titers (GMTs) of both IgG1 and IgG2b LANACs-immunized (prime boost) mouse sera were >10,000 (Fig. 3.8B). There was more animal to animal variability in the IgG2a titers, with 4/10 animals failing to produce a GMT >250.

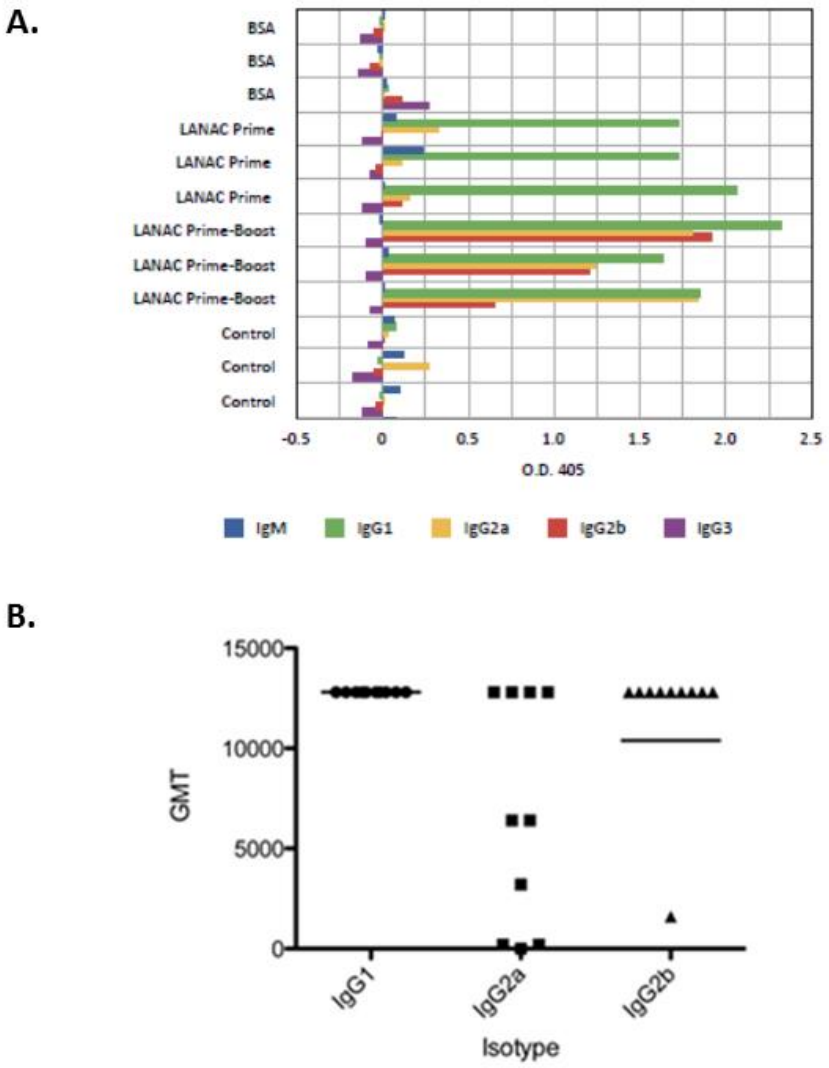

Figure 3.8 Humoral immune response to LANACs immunization. (A) E1ecto antigen specific ELISA. Serum samples collected 3 weeks after boost, each of four groups, were assayed for relative antibody isotype abundance. The groups were (1) mice immunized with LANACs containing bovine serum albumin (LANAC BSA), (2) mice vaccinated once with LANACs containing E1ecto (LANAC Prime), (3) mice vaccinated and boosted with LANACs containing E1ecto (LANAC Prime-Boost), and (4) pre-immune serum (control). (B) Geometric mean titers (GMT) of antibody isotypes from E1ecto LANAC prime-boost serum.

Cross-protection E1ecto LANAC vaccine against EEEV

Finally, we examined the ability of WEEV E1ecto LANACs immunization to protect mice against EEEV challenge. Mice were prime-boost immunized with either sham-LANACs or WEEV E1ecto LANACs and challenged at 9 weeks after the booster by s.c. or i.n. inoculation with EEEV (Florida-93; Fig. 3.9). Mice immunized with the WEEV E1ecto LANACs survived the EEEV challenge via either route at significantly higher levels (p value = < 0.0001) than the sham-LANAC vaccinated controls. In fact, 9/10 CD-1 mice from each group immunized with the WEEV E1ecto LANACs survived EEEV (Florida-93) challenge, with only one from each group euthanized at 9 days post-challenge due to neurological deficits, while all 10 mice immunized with the sham-LANACs were euthanized at days 6 or 7 due to obvious neurological deficits. These results show that the LANACs formulation containing the recombinant WEEV E1ecto provided strong cross-protection against the heterologous alphavirus, EEEV.

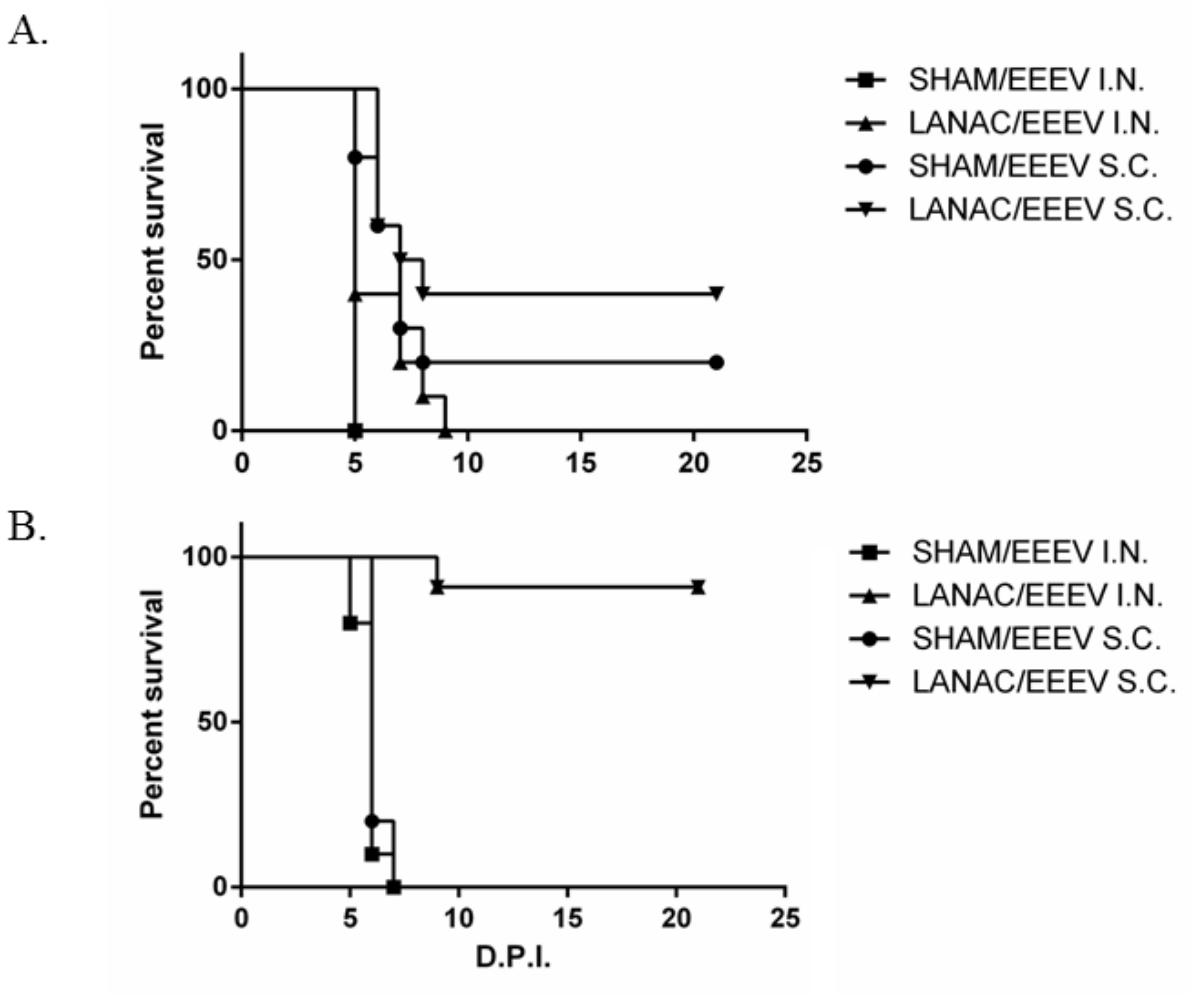

Figure 3.9 Protection by LANACs vaccination against EEEV challenge. CD-1 mice were immunized with E1ecto-LANACs (LANAC) or sham-LANACs (SHAM), then challenged 2 weeks (A) or 9 weeks (B) after the booster with 10^4 PFU of EEEV (Florida-93) by either s.c. or i.n. routes. The survival curve for each 9 week post-vaccinated group was analyzed and found to be significantly different from the sham-immunized control group (*p* value = < 0.0001 for both s.c. and i.n. routes).

Discussion

We describe a new LANACs formulation that is effective in providing prophylactic protection against both WEEV and EEEV, two distinct alphaviruses that cause serious human disease. The CLNC component of the LANACs also exhibited therapeutic efficacy out to 24 hours after WEEV infection, most likely through innate immune system stimulation, with induction of antiviral activity occurring even when the CLNCs are administered after infection. In contrast, the recombinant E1ecto antigen component of the LANACs may provide an epitope framework with which the host may mount a humoral immune response providing specific and long-term protection against alphaviral disease.

It is not surprising that the CLNC component of our LANACs worked therapeutically against WEEV; CLNCs can rapidly induce potent, non-specific antiviral activity across a wide-range of viral infections (Gowen, Fairman et al. 2006; Morrey, Motter et al. 2008; Logue, Phillips et al. 2010). We previously reported that CLDCs (liposome-ODN-complexes) protect against s.c. challenge with WEEV in the CD-1 mouse model when administered 24 hours before infection (Logue, Phillips et al. 2010). The findings presented here extend our previous results and indicate that cationic liposososmes-ODN-PIC complexes can be used therapeutically against WEEV when administered within the first day of infection.

More surprising, were our results indicating that CLNCs containing both PIC and ODN had stronger antiviral effects than CLNCs containing only PIC or only ODN. This additive effect might be due to the stimulation of separate innate immune pathways by these molecules. PIC binds TLR3, which can activate MyD88-dependent and independent pathways, whereas ODN binds TLR9, which uses a MyD88-dependent pathway. Furthermore, PIC can activate the

cytosolic sensors MDA-5 and RIG-I (Kato, Sato et al. 2005; Gitlin, Barchet et al. 2006), triggering IPS-1-dependent pathways (Zou, Kawai et al. 2013).

Of particular importance was the cross-protection of the WEEV McMillan E1ecto component of LANACs. We purposefully chose this protein antigen for our LANACs formulation for several reasons. First, although E2 protein is the major neutralizing antigen, E1 is highly-conserved among distinct alphaviral species (Hahn, Lustig et al. 1988; Netolitzky, Schmaltz et al. 2000) and antibody to E1 is protective (Schmaljohn, Johnson et al. 1982). Second, the E1 of WEEV is a recent ancestor of the E1 from a Sindbis-like virus, which in addition to VEEV E1 protein has been shown to induce cross-reactive and cross-protective antibodies (Mathews and Roehrig 1982; Schmaljohn, Johnson et al. 1982; Stec, Waddell et al. 1986). Given WEEV evolutionary history, WEEV E1ecto may be an important antigen for developing immune cross-protection among NWA and OWA species. Finally, monoclonal antibodies against E1 (McMillan strain) are alphavirus group reactive (Hunt and Roehrig 1985; Roehrig 1993; Roehrig and Bolin 1997). The insect cell-derived McMillan E1ecto antigen presented to mice in the LANACs context (CLNC/ODN/PIC) may explain why our study differs with a previous study in which mice immunized with recombinant bacteria-derived WEEV E1 antigen exhibited minimal protection from challenge with two WEEV strains (Strizki and Repik 1995). Gauchi et al (2010) used a DNA vaccine approach to immunize mice with WEEV E1 and demonstrated protection from challenge with a low-virulence WEEV strain but not with a high-virulence WEEV strain (Das, Gares et al. 2004; Gauci, Wu et al. 2010). In both studies, WEEV challenge occurred at 2-3 weeks after boost. Our studies showed that development of maximal protection to highly virulent WEEV and EEEV strains occurred at 9-11 weeks after boost.

Interestingly, mice that were prime-boost immunized with LANACs containing WEEV E1 antigen and challenged 2 weeks after boost with EEEV (Florida-93) were poorly protected.

Although E1ecto LANACs induced a strong humoral immune response, no detectable neutralizing activity was found in serum from immunized animals. How, then, might the antibodies protect against fatal CNS infection? One possibility is that the antibodies bind to E1 protein at the surface of infected cells and disrupt E2-E1 interactions such as the formation of E2-E1 dimer-trimer complexes (glycoprotein spikes) necessary for virus budding from infected cell. It is interesting to speculate that the host-cell plasma membrane may maintain its integrity by virtue of antibody binding to E1. It is notable that antibodies to alphavirus glycoprotein can restore membrane potential, host protein synthesis, and interferon responsiveness of neurons (Griffin, Levine et al. 1997; Burdeinick-Kerr, Wind et al. 2007).

Metcalf et al. (2013) reported that viral antigen-specific antibody-secreting cells (ASC) become enriched within the brain following infection with Sindbis virus (Metcalf, Baxter et al. 2013), and that these Sindbis-specific ASCs are maximally enriched (as a percentage of total ASCs within the brain) at 8-9 weeks after inoculation. Such a timeline corresponds well with our observation that 9 weeks is required after boost before vaccine efficacy is realized in cross-protection experiments. It could be that E1ecto-specific ASCs require 9 weeks in order to attain effective enrichment within the CNS.

In summary, our data support the use of CLNCs as alphavirus therapeutics and highlight the utility of LANACs consisting of CLNCs and WEEV E1ecto as a vaccine against WEEV and EEEV. Future studies are are supported which aim to more precisely determine the mechanism of protection. An investigation of the effectiveness of our WEEV E1ecto-LANACs formulation

to protect mice against other alphaviruses, including VEEV and Chikungunya virus are logical next steps. I remain optimistic that this approach has potential as a broad-spectrum alphavirus vaccine.

CHAPTER 4: SUMMARY

The application of *in vivo* imaging technology to the study of WEEV infection of mice has yielded some expected and unexpected results. The intranasal challenge route appears to allow virus to enter the CNS through olfactory pathways, as expected. However, following footpad inoculation, virus entry into the CNS takes a very different course, involving cicumventricular organs. The absence of BBB protections may render these sites more susceptible to infection. Neuronal cells present in these areas are in direct contact with circulating blood. Infection spreads rapidly throughout the brain after initial infection of CNS tissue. Given this later point, investigations solely using traditional methods such as histopathological examination, may have not been able to definitive identify when virus had initially reached the CNS. The convenience of visualizing viral replication within the CNS of intact animals using BLM technology promises to lessen the burden on researchers by visualizing infection within the intact animal and may lessen the number of animals required.

With respect to treatment strategies against encephalitic alphavirus infections, these studies have shown that immunoactivation with adjuvants alone can impart some protection. Further, multiple-ligand adjuvants, such as ODN-PIC, impart high immunogenicity to the antigens used in these studies. Antigens based on WEEV McM E1 glycoprotein, when formulated into LANACs, induce highly protective adaptive immune responses against multiple strains of WEEV and at least one strain of EEEV. These findings may provide a new avenue for research aimed at developing pan-alphavirus treatment strategies.

Future directions for this work may include the development of a novel system in which virus can be tracked within the infected vector, transmitted through hematophagous feeding

activity by the vector, and further tracked as infection spreads through the CNS of the vertebrate host. Injection of bioluminescent substrates into the vector is typically lethal to the vector. Additionally, bioluminescent substrates do not circulate through a vasculature as in vertebrates, resulting in localized areas of high intensity luciferase activity. Ideally, a virus which can induce fluorescent reporters in the vector and bioluminescence reporters in the vertebrate, are desired. One such method could involve the development of a transcription factor-expressing virus and transgenic vectors and transgenic vertebrates. As shown in Chapter II, Gal4-expressing recombinant WEEV (McGal) can be used to detect and track experimental infection of Tg UAS-FLUC mice. It is interesting to speculate that if a comparable transgenic mosquito was produced, one in which FLUC was replaced by the preferred reporter type for vector studies (fluorescence), the infection cycle from mosquito to vertebrate could be conveniently detected and tracked. That is to say that the same virus could induce the expression of the reporter optimal for each system by expression of a moderately sized (>700 nucleotides) transgene (Gal-4)

A better understanding of WEEV pathogenesis and an improved treatment strategy are the major features of this dissertation. Through these findings, perhaps others may derive critical information pertinent to their own research pursuits. It would be difficult to believe that WEEV is the only virus known to enter the CNS through circumventricular organs. In the future, perhaps reporter viruses can be generated to represent the other encephalitic viruses for which the route of CNS entry is still a mystery.

REFERENCES

Abbott, N. J., A. A. Patabendige, et al. (2010). "Structure and function of the blood-brain barrier." Neurobiol Dis **37**(1): 13-25.

Afonso, P. V., S. Ozden, et al. (2008). "Alteration of blood-brain barrier integrity by retroviral infection." PLoS Pathog **4**(11): 14.

Antoine, A. F., C. Montpellier, et al. (2007). "The alphavirus 6K protein activates endogenous ionic conductances when expressed in Xenopus oocytes." J Membr Biol **215**(1): 37-48.

Atasheva, S., A. Fish, et al. (2010). "Venezuelan equine Encephalitis virus capsid protein forms a tetrameric complex with CRM1 and importin alpha/beta that obstructs nuclear pore complex function." J.Virol. **84**(9): 4158-4171.

Bennett, R. S., C. M. Cress, et al. (2008). "La Crosse virus infectivity, pathogenesis, and immunogenicity in mice and monkeys." Virol J **5**(25): 5-25.

Bergmann, C. C., T. E. Lane, et al. (2006). "Coronavirus infection of the central nervous system: host-virus stand-off." Nat Rev Microbiol **4**(2): 121-132.

Bonthius, D. J. (2012). "Lymphocytic choriomeningitis virus: an underrecognized cause of neurologic disease in the fetus, child, and adult." Semin Pediatr Neurol **19**(3): 89-95.

Boothpur, R. and D. C. Brennan (2010). "Human polyoma viruses and disease with emphasis on clinical BK and JC." J Clin Virol **47**(4): 306-312.

Brault, A. C., B. D. Foy, et al. (2004). "Infection patterns of o'nyong nyong virus in the malaria-transmitting mosquito, Anopheles gambiae." Insect Molecular Biology **13**(6): 625-635.

Buchanan, R. and D. J. Bonthius (2012). "Measles virus and associated central nervous system sequelae." Semin Pediatr Neurol **19**(3): 107-114.

Buck, L. and R. Axel (1991). "A NOVEL MULTIGENE FAMILY MAY ENCODE ODORANT RECEPTORS - A MOLECULAR-BASIS FOR ODOR RECOGNITION." Cell **65**(1): 175-187.

Buck, L. B. (1996). "Information coding in the vertebrate olfactory system." Annual Review of Neuroscience **19**: 517-544.

Burdeinick-Kerr, R., J. Wind, et al. (2007). "Synergistic roles of antibody and interferon in noncytolytic clearance of Sindbis virus from different regions of the central nervous system." J Virol **81**(11): 5628-5636.

Caley, I. J., M. R. Betts, et al. (1997). "Humoral, mucosal, and cellular immunity in response to a human immunodeficiency virus type 1 immunogen expressed by a Venezuelan equine encephalitis virus vaccine vector." J Virol. 1997 Apr;71(4):3031-8.

Calisher, C. H. (1994). "MEDICALLY IMPORTANT ARBOVIRUSES OF THE UNITED-STATES AND CANADA." Clinical Microbiology Reviews **7**(1): 89-116.

Carpentier, P. A., B. R. Williams, et al. (2007). "Distinct roles of protein kinase R and toll-like receptor 3 in the activation of astrocytes by viral stimuli." Glia **55**(3): 239-252.

Casiraghi, C., K. Dorovini-Zis, et al. (2011). "Epstein-Barr virus infection of human brain microvessel endothelial cells: a novel role in multiple sclerosis." J Neuroimmunol **230**(1-2): 173-177.

Chapagain, M. L., S. Verma, et al. (2007). "Polyomavirus JC infects human brain microvascular endothelial cells independent of serotonin receptor 2A." Virology **364**(1): 55-63.

Charles, P. C., E. Walters, et al. (1995). "MECHANISM OF NEUROINVASION OF VENEZUELAN EQUINE ENCEPHALITIS-VIRUS IN THE MOUSE." Virology **208**(2): 662-671.

Contag, C. H., S. D. Spilman, et al. (1997). "Visualizing gene expression in living mammals using a bioluminescent reporter." Photochemistry and Photobiology **66**(4): 523-531.

Cook, S. H. and D. E. Griffin (2003). "Luciferase Imaging of neurotropic viral infection in intact animals." Journal of Virology **77**(9): 5333-5338.

Cross, R. K. (1983). "Identification of a unique guanine-7-methyltransferase in Semliki Forest virus (SFV) infected cell extracts." Virology **130**(2): 452-463.
Cutchins, E., J. Warren, et al. (1960). "The antibody response to smallpox vaccination as measured by a tissue culture plaque method." J Immunol **85**: 275-283.
Das, D., S. L. Gares, et al. (2004). "Evaluation of a Western Equine Encephalitis recombinant E1 protein for protective immunity and diagnostics." Antiviral Research **64**(2): 85-92.
Dash, A. P., R. Bhatia, et al. (2013). "Emerging and re-emerging arboviral diseases in Southeast Asia." J Vector Borne Dis **50**(2): 77-84.
Dayan, G. H. and S. Rubin (2008). "Mumps outbreaks in vaccinated populations: are available mumps vaccines effective enough to prevent outbreaks?" Clin Infect Dis **47**(11): 1458-1467.
Del Piero, F., P. A. Wilkins, et al. (2001). "Clinical, pathologic, immunohistochemical, and virologic findings of eastern equine encephalomyelitis in two horses." Veterinary Pathology **38**(4): 451-456.
Deshmane, S. L., S. Kremlev, et al. (2009). "Monocyte chemoattractant protein-1 (MCP-1): an overview." J Interferon Cytokine Res **29**(6): 313-326.
Detje, C. N., T. Meyer, et al. (2009). "Local type I IFN receptor signaling protects against virus spread within the central nervous system." J Immunol **182**(4): 2297-2304.
Diefenbach, R. J., M. Miranda-Saksena, et al. (2008). "Transport and egress of herpes simplex virus in neurons." Rev Med Virol **18**(1): 35-51.
Dourmashkin, R. R. (1997). "What caused the 1918-30 epidemic of encephalitis lethargica?" J R Soc Med **90**(9): 515-520.
Dropulic, B. and C. L. Masters (1990). "Entry of neurotropic arboviruses into the central nervous system: an in vitro study using mouse brain endothelium." J Infect Dis **161**(4): 685-691.
Dups, J., D. Middleton, et al. (2012). "A new model for Hendra virus encephalitis in the mouse." PLoS One **7**(7): 10.
Dyer, J. L., R. Wallace, et al. (2013). "Rabies surveillance in the United States during 2012." J Am Vet Med Assoc **243**(6): 805-815.
Engler, R. J., J. A. Mangiafico, et al. (1992). "Venezuelan equine encephalitis-specific immunoglobulin responses: live attenuated TC-83 versus inactivated C-84 vaccine." J Med Virol **38**(4): 305-310.
Esolen, L. M., K. Takahashi, et al. (1995). "Brain endothelial cell infection in children with acute fatal measles." J Clin Invest **96**(5): 2478-2481.
Finley, K. H., W. A. Longshore, et al. (1955). "WESTERN EQUINE AND ST LOUIS ENCEPHALITIS - PRELIMINARY REPORT OF A CLINICAL FOLLOW-UP STUDY IN CALIFORNIA." Neurology **5**(4): 223-235.
Fish, K. N., C. Soderberg-Naucler, et al. (1998). "Human cytomegalovirus persistently infects aortic endothelial cells." J Virol **72**(7): 5661-5668.
Fletcher, N. F., G. K. Wilson, et al. (2012). "Hepatitis C virus infects the endothelial cells of the blood-brain barrier." Gastroenterology **142**(3): 634-643.
Fogg, C. N., J. L. Americo, et al. (2007). "Adjuvant-enhanced antibody responses to recombinant proteins correlates with protection of mice and monkeys to orthopoxvirus challenges." Vaccine **25**(15): 2787-2799.
Forrester, N. L., J. L. Kenney, et al. (2008). "Western Equine Encephalitis submergence: lack of evidence for a decline in virus virulence." Virology **380**(2): 170-172.
Foy, B. D., K. C. Kobylinski, et al. (2011). "Probable non-vector-borne transmission of Zika virus, Colorado, USA." Emerg Infect Dis **17**(5): 880-882.
Foy, B. D., K. M. Myles, et al. (2004). "Development of a new Sindbis virus transducing system and its characterization in three Culicine mosquitoes and two Lepidopteran species." Insect Molecular Biology **13**(1): 89-100.

Foy, B. D. and K. E. Olson (2008). "Alphavirus transducing systems." Transgenesis and the Management of Vector-Borne Disease **627**: 19-34.
Gaedigk-Nitschko, K. and M. J. Schlesinger (1990). "The Sindbis virus 6K protein can be detected in virions and is acylated with fatty acids." Virology **175**(1): 274-281.
Gardner, C. L., C. W. Burke, et al. (2008). "Eastern and Venezuelan equine encephalitis viruses differ in their ability to infect dendritic cells and macrophages: impact of altered cell tropism on pathogenesis." J Virol. 2008 Nov;82(21):10634-46. Epub 2008 Sep 3.
Gardner, C. L., G. D. Ebel, et al. (2011). "Heparan sulfate binding by natural eastern equine encephalitis viruses promotes neurovirulence." Proc Natl Acad Sci U S A **108**(38): 16026-16031.
Garoff, H., D. Huylebroeck, et al. (1990). "The signal sequence of the p62 protein of Semliki Forest virus is involved in initiation but not in completing chain translocation." J Cell Biol **111**(3): 867-876.
Gauci, P. J., J. Q. Wu, et al. (2010). "Identification of Western equine encephalitis virus structural proteins that confer protection after DNA vaccination." Clin Vaccine Immunol **17**(1): 176-179.
Ghosh, S., S. D. Larson, et al. (2011). "Sensory maps in the olfactory cortex defined by long-range viral tracing of single neurons." Nature **472**(7342): 217-220.
Gitlin, L., W. Barchet, et al. (2006). "Essential role of mda-5 in type I IFN responses to polyriboinosinic:polyribocytidylic acid and encephalomyocarditis picornavirus." Proc Natl Acad Sci U S A **103**(22): 8459-8464.
Gomez de Cedron, M., N. Ehsani, et al. (1999). "RNA helicase activity of Semliki Forest virus replicase protein NSP2." FEBS Lett **448**(1): 19-22.
Gowen, B. B., J. Fairman, et al. (2006). "Protective immunity against acute phleboviral infection elicited through immunostimulatory cationic liposome-DNA complexes." Antiviral Res **69**(3): 165-172.
Gralinski, L. E., S. L. Ashley, et al. (2009). "Mouse adenovirus type 1-induced breakdown of the blood-brain barrier." J Virol **83**(18): 9398-9410.
Griffin, D., B. Levine, et al. (1997). "The role of antibody in recovery from alphavirus encephalitis." Immunol Rev **159**: 155-161.
Griffin, D. E. (2005). "Neuronal cell death in alphavirus encephalomyelitis." Role of Apoptosis in Infection **289**: 57-77.
Griffin, D. E., A. P. Byrnes, et al. (2004). "Emergence and virulence of encephalitogenic arboviruses." Archives of Virology: 21-33.
Griffin, D. E. and R. T. Johnson (1977). "Role of the immune response in recovery from Sindbis virus encephalitis in mice." J Immunol **118**(3): 1070-1075.
Hafezi, W. and V. Hoerr (2013). "In Vivo Visualization of Encephalitic Lesions in Herpes Simplex Virus Type 1 (HSV-1) Infected Mice by Magnetic Resonance Imaging (MRI)." Methods Mol Biol: 601-606_618.
Hahn, C. S., S. Lustig, et al. (1988). "WESTERN EQUINE ENCEPHALITIS-VIRUS IS A RECOMBINANT VIRUS." Proceedings of the National Academy of Sciences of the United States of America **85**(16): 5997-6001.
Hahn, C. S., S. Lustig, et al. (1988). "Western equine encephalitis virus is a recombinant virus." Proc Natl Acad Sci U S A **85**(16): 5997-6001.
Hahn, Y. S., A. Grakoui, et al. (1989). "Mapping of RNA- temperature-sensitive mutants of Sindbis virus: complementation group F mutants have lesions in nsP4." J Virol **63**(3): 1194-1202.
Hahn, Y. S., E. G. Strauss, et al. (1989). "Mapping of RNA- temperature-sensitive mutants of Sindbis virus: assignment of complementation groups A, B, and G to nonstructural proteins." J Virol **63**(7): 3142-3150.
Hardy, J. L. (1987). "The ecology of western equine encephalomyelitis virus in the Central Valley of California, 1945-1985." Am J Trop Med Hyg **37**(3 Suppl): 18S-32S.

Havlikova, S., M. Lickova, et al. (2013). "Non-viraemic transmission of tick-borne viruses." Acta Virol **57**(2): 123-129.
Heidner, H. W., K. L. McKnight, et al. (1994). "Lethality of PE2 incorporation into Sindbis virus can be suppressed by second-site mutations in E3 and E2." J Virol **68**(4): 2683-2692.
Higgs, S., K. E. Olson, et al. (1995). "MOSQUITO SENSITIVITY TO A SCORPION NEUROTOXIN EXPRESSED USING AN INFECTIOUS SINDBIS-VIRUS VECTOR." Insect Molecular Biology **4**(2): 97-103.
Higgs, S., A. M. Powers, et al. (1993). "ALPHAVIRUS EXPRESSION SYSTEMS - APPLICATIONS TO MOSQUITO VECTOR STUDIES." Parasitology Today **9**(12): 444-452.
Hobson, D. E. (2012). "Asymmetry in parkinsonism, spreading pathogens and the nose." Parkinsonism & Related Disorders **18**(1): 1-9.
Hollidge, B. S., F. Gonzalez-Scarano, et al. (2010). "Arboviral encephalitides: transmission, emergence, and pathogenesis." J Neuroimmune Pharmacol **5**(3): 428-442.
Hopkins, T. A., H. H. Seliger, et al. (1967). "The chemiluminescence of firefly luciferin. A model for the bioluminescent reaction and identification of the product excited state." J Am Chem Soc **89**(26): 7148-7150.
Howe, H. A. and D. Bodian (1942). Neural Mechanisms in Poliomyelitis. New York, Commonwealth Fund.
Hunt, A. R., R. A. Bowen, et al. (2011). "Treatment of mice with human monoclonal antibody 24 h after lethal aerosol challenge with virulent Venezuelan equine encephalitis virus prevents disease but not infection." Virology **414**(2): 146-152.
Hunt, A. R., R. A. Bowen, et al. (2011). "Treatment of mice with human monoclonal antibody 24h after lethal aerosol challenge with virulent Venezuelan equine encephalitis virus prevents disease but not infection." Virology **414**(2): 146-152.
Hunt, A. R. and J. T. Roehrig (1985). "Biochemical and biological characteristics of epitopes on the E1 glycoprotein of western equine encephalitis virus." Virology **142**(2): 334-346.
Inoue, Y., S. Kiryu, et al. (2009). "Comparison of subcutaneous and intraperitoneal injection of D-luciferin for in vivo bioluminescence imaging." Eur J Nucl Med Mol Imaging **36**(5): 771-779.
Jang, H., D. A. Boltz, et al. (2009). "Viral parkinsonism." Biochim Biophys Acta **7**: 714-721.
Johnson, D. C., M. J. Schlesinger, et al. (1981). "Fluorescence photobleaching recovery measurements reveal differences in envelopment of Sindbis and vesicular stomatitis viruses." Cell **23**(2): 423-431.
Johnson, R. T. (1983). "Pathogenesis of La Crosse virus in mice." Prog Clin Biol Res **123**: 139-144.
Jose, J., J. E. Snyder, et al. (2009). "A structural and functional perspective of alphavirus replication and assembly." Future Microbiol **4**(7): 837-856.
Julander, J. G., V. Siddharthan, et al. (2007). "Effect of exogenous interferon and an interferon inducer on western equine encephalitis virus disease in a hamster model." Virology **360**(2): 454-460.
Kail, M., M. Hollinshead, et al. (1991). "The cytoplasmic domain of alphavirus E2 glycoprotein contains a short linear recognition signal required for viral budding." Embo J **10**(9): 2343-2351.
Kamer, G. and P. Argos (1984). "Primary structural comparison of RNA-dependent polymerases from plant, animal and bacterial viruses." Nucleic Acids Res **12**(18): 7269-7282.
Karabatsos, N., Ed. (1985). INTERNATIONAL CATALOGUE OF ARBOVIRUSES INCLUDING CERTAIN OTHER VIRUSES OF VERTEBRATES. Fort Collins, CO, American Journal of Tropical Medicine and Hygiene.
Kasturi, S. P., I. Skountzou, et al. (2011). "Programming the magnitude and persistence of antibody responses with innate immunity." Nature **470**(7335): 543-547.
Kato, H., S. Sato, et al. (2005). "Cell type-specific involvement of RIG-I in antiviral response." Immunity **23**(1): 19-28.
Kaul, M., G. A. Garden, et al. (2001). "Pathways to neuronal injury and apoptosis in HIV-associated dementia." Nature **410**(6831): 988-994.

Kawai, T. and S. Akira (2007). "Antiviral signaling through pattern recognition receptors." J Biochem **141**(2): 137-145.
Kidner, T. B., D. L. Morton, et al. (2012). "Combined intralesional Bacille Calmette-Guerin (BCG) and topical imiquimod for in-transit melanoma." J Immunother **35**(9): 716-720.
Koyuncu, O. O., I. B. Hogue, et al. (2013). "Virus infections in the nervous system." Cell Host Microbe **13**(4): 379-393.
Kramer, M. F., W. J. Cook, et al. (2003). "Latent herpes simplex virus infection of sensory neurons alters neuronal gene expression." J Virol **77**(17): 9533-9541.
Kramer, T., T. M. Greco, et al. (2012). "Kinesin-3 mediates axonal sorting and directional transport of alphaherpesvirus particles in neurons." Cell Host Microbe **12**(6): 806-814.
Kumar, H., S. Koyama, et al. (2008). "Cutting edge: cooperation of IPS-1- and TRIF-dependent pathways in poly IC-enhanced antibody production and cytotoxic T cell responses." J Immunol **180**(2): 683-687.
Laakkonen, P., M. Hyvonen, et al. (1994). "Expression of Semliki Forest virus nsP1-specific methyltransferase in insect cells and in Escherichia coli." J Virol **68**(11): 7418-7425.
Lai, C. Y., Y. C. Ou, et al. (2012). "Endothelial Japanese encephalitis virus infection enhances migration and adhesion of leukocytes to brain microvascular endothelia via MEK-dependent expression of ICAM1 and the CINC and RANTES chemokines." J Neurochem **123**(2): 250-261.
Langmuir, A. D. (1963). "The surveillance of communicable diseases of national importance." N Engl J Med **268**: 182-192.
Lemm, J. A., T. Rumenapf, et al. (1994). "Polypeptide requirements for assembly of functional Sindbis virus replication complexes: a model for the temporal regulation of minus- and plus-strand RNA synthesis." Embo J **13**(12): 2925-2934.
Levine, B., J. M. Hardwick, et al. (1991). "Antibody-mediated clearance of alphavirus infection from neurons." Science **254**(5033): 856-860.
Liljestrom, P. and H. Garoff (1991). "A NEW GENERATION OF ANIMAL-CELL EXPRESSION VECTORS BASED ON THE SEMLIKI FOREST VIRUS REPLICON." Bio-Technology **9**(12): 1356-1361.
Linger, B. R., L. Kunovska, et al. (2004). "Sindbis virus nucleocapsid assembly: RNA folding promotes capsid protein dimerization." Rna **10**(1): 128-138.
Liu, C., D. W. Voth, et al. (1970). "A comparative study of the pathogenesis of western equine and eastern equine encephalomyelitis viral infections in mice by intracerebral and subcutaneous inoculations." J Infect Dis **122**(1): 53-63.
Liu, N. and D. T. Brown (1993). "Phosphorylation and dephosphorylation events play critical roles in Sindbis virus maturation." Virology **196**(2): 703-711.
Liu, N. and D. T. Brown (1993). "Transient translocation of the cytoplasmic (endo) domain of a type I membrane glycoprotein into cellular membranes." J Cell Biol **120**(4): 877-883.
Liu, Q. H., D. A. Williams, et al. (2000). "HIV-1 gp120 and chemokines activate ion channels in primary macrophages through CCR5 and CXCR4 stimulation." Proc Natl Acad Sci U S A **97**(9): 4832-4837.
Logue, C. H., C. F. Bosio, et al. (2009). "Virulence variation among isolates of western equine encephalitis virus in an outbred mouse model." J Gen Virol **90**(Pt 8): 1848-1858.
Logue, C. H., A. T. Phillips, et al. (2010). "Treatment with cationic liposome-DNA complexes (CLDCs) protects mice from lethal Western equine encephalitis virus (WEEV) challenge." Antiviral Research **87**(2): 195-203.
Luker, G. D., J. P. Bardill, et al. (2002). "Noninvasive bioluminescence imaging of herpes simplex virus type 1 infection and therapy in living mice." Journal of Virology **76**(23): 12149-12161.
Lycke, E., B. Hamark, et al. (1988). "Herpes simplex virus infection of the human sensory neuron. An electron microscopy study." Arch Virol **101**(1-2): 87-104.

Malet, H., B. Coutard, et al. (2009). "The crystal structures of Chikungunya and Venezuelan equine encephalitis virus nsP3 macro domains define a conserved adenosine binding pocket." J Virol **83**(13): 6534-6545.
Margolis, T. P., Y. Imai, et al. (2007). "Herpes simplex virus type 2 (HSV-2) establishes latent infection in a different population of ganglionic neurons than HSV-1: role of latency-associated transcripts." J Virol **81**(4): 1872-1878.
Martin, K. A., R. Wyatt, et al. (1997). "CD4-independent binding of SIV gp120 to rhesus CCR5." Science **278**(5342): 1470-1473.
Mathews, J. H. and J. T. Roehrig (1982). "Determination of the protective epitopes on the glycoproteins of Venezuelan equine encephalomyelitis virus by passive transfer of monoclonal antibodies." J Immunol **129**(6): 2763-2767.
Mattson, M. P. (2004). "Infectious agents and age-related neurodegenerative disorders." Ageing Res Rev **3**(1): 105-120.
McGavern, D. B. and S. S. Kang (2011). "Illuminating viral infections in the nervous system." Nat Rev Immunol **11**(5): 318-329.
Metcalf, T. U., V. K. Baxter, et al. (2013). "Recruitment and retention of B cells in the central nervous system in response to alphavirus encephalomyelitis." J Virol **87**(5): 2420-2429.
Metz, S. W. and G. P. Pijlman (2011). "Arbovirus vaccines; opportunities for the baculovirus-insect cell expression system." J Invertebr Pathol **107**(30): 002.
Meyer, K. F., C. M. Haring, et al. (1931). "THE ETIOLOGY OF EPIZOOTIC ENCEPHALOMYELITIS OF HORSES IN THE SAN JOAQUIN VALLEY, 1930." Science **74**(1913): 227-228.
Mi, S. and V. Stollar (1991). "Expression of Sindbis virus nsP1 and methyltransferase activity in Escherichia coli." Virology **184**(1): 423-427.
Monath, T. P., C. B. Cropp, et al. (1983). "Mode of entry of a neurotropic arbovirus into the central nervous system. Reinvestigation of an old controversy." Lab Invest **48**(4): 399-410.
Mori, I., Y. Nishiyama, et al. (2005). "Olfactory transmission of neurotropic viruses." J Neurovirol **11**(2): 129-137.
Morrey, J. D., N. E. Motter, et al. (2008). "Efficacy of cationic lipid-DNA complexes (CLDC) on hepatitis B virus in transgenic mice." Antiviral Res **79**(1): 71-79.
Mossel, E. C., J. P. Ledermann, et al. (2013). "Molecular determinants of mouse neurovirulence and mosquito infection for Western equine encephalitis virus." PLoS One **8**(3): 27.
Mulder, D. W., M. Parrott, et al. (1951). "Sequelae of western equine encephalitis." Neurology **1**(4): 318-327.
Munster, V. J., J. B. Prescott, et al. (2012). "Rapid Nipah virus entry into the central nervous system of hamsters via the olfactory route." Sci Rep **2**(736): 15.
Nagata, L. P., W. G. Hu, et al. (2006). "Infectivity variation and genetic diversity among strains of Western equine encephalitis virus." Journal of General Virology **87**: 2353-2361.
Netolitzky, D. J., F. L. Schmaltz, et al. (2000). "Complete genomic RNA sequence of western equine encephalitis virus and expression of the structural genes." J Gen Virol **81**(Pt 1): 151-159.
Ohka, S., N. Matsuda, et al. (2004). "Receptor (CD155)-dependent endocytosis of poliovirus and retrograde axonal transport of the endosome." J Virol **78**(13): 7186-7198.
Okamoto, Y., L. A. Vricella, et al. (2012). "Immature CD4+CD8+ thymocytes are preferentially infected by measles virus in human thymic organ cultures." PLoS One **7**(9): 24.
Olitsky, P. K., R. W. Schlesinger, et al. (1943). "INDUCED RESISTANCE OF THE CENTRAL NERVOUS SYSTEM TO EXPERIMENTAL INFECTION WITH EQUINE ENCEPHALOMYELITIS VIRUS: II. SEROTHERAPY IN WESTERN VIRUS INFECTION." The Journal of Experimental Medicine **77**(4): 359-374.

Olson, K. E., K. M. Myles, et al. (2000). "Development of a Sindbis virus expression system that efficiently expresses green fluorescent protein in midguts of Aedes aegypti following per os infection." Insect Molecular Biology **9**(1): 57-65.
Paessler, S. and S. C. Weaver (2009). "Vaccines for Venezuelan equine encephalitis." Vaccine **5**(27): 095.
Palmer, R. J. and K. H. Finley (1956). "Sequelae of encephalitis; report of a study after the California epidemic." Calif Med **84**(2): 98-100.
Park, C. H., M. Ishinaka, et al. (2002). "The invasion routes of neurovirulent A/Hong Kong/483/97 (H5N1) influenza virus into the central nervous system after respiratory infection in mice." Arch Virol **147**(7): 1425-1436.
Park, E. and D. E. Griffin (2009). "The nsP3 macro domain is important for Sindbis virus replication in neurons and neurovirulence in mice." Virology **388**(2): 305-314.
Patterson, M., A. Poussard, et al. (2011). "Rapid, non-invasive imaging of alphaviral brain infection: reducing animal numbers and morbidity to identify efficacy of potential vaccines and antivirals." Vaccine **29**(50): 9345-9351.
Patterson, M., A. Poussard, et al. (2011). "Rapid, non-invasive imaging of alphaviral brain infection: reducing animal numbers and morbidity to identify efficacy of potential vaccines and antivirals." Vaccine **29**(50): 9345-9351.
Phillips, A. T., C. B. Stauft, et al. (2013). "Bioluminescent imaging and histopathologic characterization of WEEV neuroinvasion in outbred CD-1 mice." PLoS One **8**(1): 2.
Phillpotts, R. J. (2006). "Venezuelan equine encephalitis virus complex-specific monoclonal antibody provides broad protection, in murine models, against airborne challenge with viruses from serogroups I, II and III." Virus Res **120**(1-2): 107-112.
Phillpotts, R. J., L. D. Jones, et al. (2002). "Monoclonal antibody protects mice against infection and disease when given either before or up to 24 h after airborne challenge with virulent Venezuelan equine encephalitis virus." Vaccine **20**(11-12): 1497-1504.
Pichler, A., J. L. Prior, et al. (2008). "Generation of a highly inducible Gal4-->Fluc universal reporter mouse for in vivo bioluminescence imaging." Proc Natl Acad Sci U S A **105**(41): 15932-15937.
Pienaar, I. S. and P. F. Chinnery (2013). "Existing and emerging mitochondrial-targeting therapies for altering Parkinson's disease severity and progression." Pharmacol Ther **137**(1): 1-21.
Pinto, L. H., L. J. Holsinger, et al. (1992). "Influenza virus M2 protein has ion channel activity." Cell **69**(3): 517-528.
Pittman, P. R. (1999). Immunization of persons at risk of exposure to eastern equine encephalitis virus: continued assessment of the safety and effectiveness of eastern equine encephalitis vaccine, inactivated, TSI-GSD 104 (Protocol No IND 266:FY99–11). Ft Detrick, MD, The United States Army Medical Research Institute for infectious diseases.
Powers, A. M., K. I. Kamrud, et al. (1996). "Molecularly engineered resistance to California serogroup virus replication in mosquito cells and mosquitoes." Proceedings of the National Academy of Sciences of the United States of America **93**(9): 4187-4191.
Racaniello, V. R. (2006). "One hundred years of poliovirus pathogenesis." Virology **344**(1): 9-16.
Raju, R. and H. V. Huang (1991). "Analysis of Sindbis virus promoter recognition in vivo, using novel vectors with two subgenomic mRNA promoters." J Virol **65**(5): 2501-2510.
RaymsKeller, A., A. M. Powers, et al. (1995). "Replication and expression of a recombinant Sindbis virus in mosquitoes." Insect Molecular Biology **4**(4): 245-251.
Reed, D. S., T. Larsen, et al. (2005). "Aerosol exposure to western equine encephalitis virus causes fever and encephalitis in cynomolgus macaques." J Infect Dis **192**(7): 1173-1182.
Reese, S. M., E. C. Mossel, et al. (2010). "Identification of super-infected Aedes triseriatus mosquitoes collected as eggs from the field and partial characterization of the infecting La Crosse viruses." Virol J **7**(76): 7-76.

Reid, A. H., S. McCall, et al. (2001). "Experimenting on the past: the enigma of von Economo's encephalitis lethargica." J Neuropathol Exp Neurol **60**(7): 663-670.
Reisen, W. K., Y. Fang, et al. (2008). "Limited interdecadal variation in mosquito (Diptera : Culicidae) and avian host competence for western equine encephalomyelitis virus (Togaviridae : Alphavirus)." American Journal of Tropical Medicine and Hygiene **78**(4): 681-686.
Reisen, W. K., J. L. Hardy, et al. (1995). "LANDSCAPE ECOLOGY OF ARBOVIRUSES IN SOUTHERN CALIFORNIA - PATTERNS IN THE EPIZOOTIC DISSEMINATION OF WESTERN EQUINE ENCEPHALOMYELITIS AND ST-LOUIS ENCEPHALITIS VIRUSES IN COACHELLA VALLEY, 1991-1992." Journal of Medical Entomology **32**(3): 267-275.
Reisler, R. B., P. H. Gibbs, et al. (2012). "Immune interference in the setting of same-day administration of two similar inactivated alphavirus vaccines: eastern equine and western equine encephalitis." Vaccine **30**(50): 7271-7277.
Ren, R. and V. R. Racaniello (1992). "Human poliovirus receptor gene expression and poliovirus tissue tropism in transgenic mice." J Virol **66**(1): 296-304.
Richardson-Burns, S. M., D. J. Kominsky, et al. (2002). "Reovirus-induced neuronal apoptosis is mediated by caspase 3 and is associated with the activation of death receptors." J Neurovirol **8**(5): 365-380.
Rikkonen, M., J. Peranen, et al. (1994). "ATPase and GTPase activities associated with Semliki Forest virus nonstructural protein nsP2." J Virol **68**(9): 5804-5810.
Roberson, E. C., J. E. Tully, et al. (2012). "Influenza induces endoplasmic reticulum stress, caspase-12-dependent apoptosis, and c-Jun N-terminal kinase-mediated transforming growth factor-beta release in lung epithelial cells." Am J Respir Cell Mol Biol **46**(5): 573-581.
Roehrig, J. T. (1993). "Immunogens of encephalitis viruses." Vet Microbiol **37**(3-4): 273-284.
Roehrig, J. T. and R. A. Bolin (1997). "Monoclonal antibodies capable of distinguishing epizootic from enzootic varieties of subtype 1 Venezuelan equine encephalitis viruses in a rapid indirect immunofluorescence assay." J Clin Microbiol **35**(7): 1887-1890.
Roehrig, J. T., D. Gorski, et al. (1982). "Properties of monoclonal antibodies directed against the glycoproteins of Sindbis virus." J Gen Virol **59**(Pt 2): 421-425.
Roy, C. J., D. S. Reed, et al. (2009). "Pathogenesis of aerosolized Eastern Equine Encephalitis virus infection in guinea pigs." Virology Journal **6**: 13.
Ruzek, D., J. Salat, et al. (2011). "Breakdown of the blood-brain barrier during tick-borne encephalitis in mice is not dependent on CD8+ T-cells." PLoS One **6**(5): 23.
Ryman, K. D., C. L. Gardner, et al. (2007). "Heparan sulfate binding can contribute to the neurovirulence of neuroadapted and nonneuroadapted Sindbis viruses." J Virol. 2007 Apr;81(7):3563-73. Epub 2007 Jan 10.
Ryman, K. D., C. L. Gardner, et al. (2007). "Early restriction of alphavirus replication and dissemination contributes to age-dependent attenuation of systemic hyperinflammatory disease." J Gen Virol. 2007 Feb;88(Pt 2):518-29.
Ryzhikov, A., N. Tkacheva, et al. (1991). "Venezuelan equine encephalitis virus propagation in the olfactory tract of normal and immunized mice." Biomed Sci. **2**(6): 607-614.
Ryzhikov, A. B., E. I. Ryabchikova, et al. (1995). "Spread of Venezuelan equine encephalitis virus in mice olfactory tract." Archives of Virology **140**(12): 2243-2254.
Salminen, A., J. M. Wahlberg, et al. (1992). "Membrane fusion process of Semliki Forest virus. II: Cleavage-dependent reorganization of the spike protein complex controls virus entry." J Cell Biol **116**(2): 349-357.
Savini, G., N. J. MacLachlan, et al. (2008). "Vaccines against bluetongue in Europe." Comp Immunol Microbiol Infect Dis **31**(2-3): 101-120.

Schapira, A. H., V. M. Mann, et al. (1990). "Anatomic and disease specificity of NADH CoQ1 reductase (complex I) deficiency in Parkinson's disease." J Neurochem **55**(6): 2142-2145.
Schapira, A. H. V., J. M. Cooper, et al. (1989). "MITOCHONDRIAL COMPLEX I DEFICIENCY IN PARKINSON'S DISEASE." The Lancet **333**(8649): 1269.
Scherbik, S. V. and M. A. Brinton (2010). "Virus-induced Ca2+ influx extends survival of west nile virus-infected cells." J Virol **84**(17): 8721-8731.
Schmaljohn, A. L., E. D. Johnson, et al. (1982). "Non-neutralizing monoclonal antibodies can prevent lethal alphavirus encephalitis." Nature **297**(5861): 70-72.
Schneider-Schaulies, J., V. Meulen, et al. (2003). "Measles infection of the central nervous system." J Neurovirol **9**(2): 247-252.
Schultz, D. R., J. S. Barthal, et al. (1977). "WESTERN EQUINE ENCEPHALITIS WITH RAPID ONSET OF PARKINSONISM." Neurology **27**(11): 1095-1096.
Schweighardt, B. and W. J. Atwood (2001). "Virus receptors in the human central nervous system." J Neurovirol **7**(3): 187-195.
Shepherd, G. M. and C. A. Greer (1998). Olfactory Bulb. The Synaptic Organization of the Brain. New York, Oxford University Press**:** 159-204.
Shirako, Y. and J. H. Strauss (1994). "Regulation of Sindbis virus RNA replication: uncleaved P123 and nsP4 function in minus-strand RNA synthesis, whereas cleaved products from P123 are required for efficient plus-strand RNA synthesis." J Virol **68**(3): 1874-1885.
Silva da Costa, L., A. P. Pereira da Silva, et al. (2012). "Mitochondrial bioenergetic alterations in mouse neuroblastoma cells infected with Sindbis virus: implications to viral replication and neuronal death." PLoS One **7**(4): 2.
Siso, S., M. Jeffrey, et al. (2010). "Sensory circumventricular organs in health and disease." Acta Neuropathol **120**(6): 689-705.
Sloat, B. R. and Z. Cui (2006). "Nasal immunization with anthrax protective antigen protein adjuvanted with polyriboinosinic-polyribocytidylic acid induced strong mucosal and systemic immunities." Pharm Res **23**(6): 1217-1226.
Smith, G. (2012). "Herpesvirus transport to the nervous system and back again." Annu Rev Microbiol **66**: 153-176.
Sokolov, A. A. and M. Reincke (2012). "Herpes simplex encephalitis affecting the entire limbic system." Mayo Clin Proc **87**(9): 023.
Solomon, T., P. Lewthwaite, et al. (2010). "Virology, epidemiology, pathogenesis, and control of enterovirus 71." Lancet Infect Dis **10**(11): 778-790.
Stauft, C. B. (2012) "WESTERN EQUINE ENCEPHALITIS VIRUS: DEVELOPMENT AND APPLICATION OF A NEW WORLD ALPHAVIRUS TRANSDUCING SYSTEM." Colorado State University, 156.
Stec, D. S., A. Waddell, et al. (1986). "Antibody-selected variation and reversion in Sindbis virus neutralization epitopes." J Virol **57**(3): 715-720.
Steele, K. E., D. S. Reed, et al. (2007). ALPHAVIRUS ENCEPHALITIDES. Medical Aspects of Biological Warfare. Z. F. Dembek. Washington D.C., Borden Institute.
Strauss, E. G., R. J. De Groot, et al. (1992). "Identification of the active site residues in the nsP2 proteinase of Sindbis virus." Virology **191**(2): 932-940.
Strauss, J. H., E. G. Strauss, et al. (1995). "Budding of alphaviruses." Trends Microbiol **3**(9): 346-350.
Strizki, J. M. and P. M. Repik (1995). "Differential reactivity of immune sera from human vaccinees with field strains of eastern equine encephalitis virus." Am J Trop Med Hyg **53**(5): 564-570.
Tewari, K., B. J. Flynn, et al. (2010). "Poly(I:C) is an effective adjuvant for antibody and multi-functional CD4+ T cell responses to Plasmodium falciparum circumsporozoite protein (CSP) and alphaDEC-CSP in non human primates." Vaccine **28**(45): 7256-7266.

Tirabassi, R. S., R. A. Townley, et al. (1998). "Molecular mechanisms of neurotropic herpesvirus invasion and spread in the CNS." Neurosci Biobehav Rev **22**(6): 709-720.
Toth, A. M., C. Geisler, et al. (2011). "Factors affecting recombinant Western equine encephalitis virus glycoprotein production in the baculovirus system." Protein Expr Purif **80**(2): 274-282.
Trevelyan, B., M. Smallman-Raynor, et al. (2005). "The Spatial Dynamics of Poliomyelitis in the United States: From Epidemic Emergence to Vaccine-Induced Retreat, 1910-1971." Ann Assoc Am Geogr **95**(2): 269-293.
Tsunoda, I. and R. S. Fujinami (2010). "Neuropathogenesis of Theiler's murine encephalomyelitis virus infection, an animal model for multiple sclerosis." J Neuroimmune Pharmacol **5**(3): 355-369.
Tuittila, M. and A. E. Hinkkanen (2003). "Amino acid mutations in the replicase protein nsP3 of Semliki Forest virus cumulatively affect neurovirulence." J Gen Virol **84**(Pt 6): 1525-1533.
Ugolini, G. (2011). "Rabies virus as a transneuronal tracer of neuronal connections." Adv Virus Res **79**: 165-202.
Vanlandingham, D. L., K. Tsetarkin, et al. (2005). "Development and characterization of a double subgenomic chikungunya virus infectious clone to expess heterologous genes in Aedes aegypti mosqutioes." American Journal of Tropical Medicine and Hygiene **73**(6): 309-309.
Vasiljeva, L., A. Merits, et al. (2000). "Identification of a novel function of the alphavirus capping apparatus. RNA 5'-triphosphatase activity of Nsp2." J Biol Chem **275**(23): 17281-17287.
Verma, S., M. Kumar, et al. (2010). "Reversal of West Nile virus-induced blood-brain barrier disruption and tight junction proteins degradation by matrix metalloproteinases inhibitor." Virology **397**(1): 130-138.
Vogel, P., D. Abplanalp, et al. (1996). "Venezuelan equine encephalitis in BALB/c mice - Kinetic analysis of central nervous system infection following aerosol or subcutaneous inoculation." Archives of Pathology & Laboratory Medicine **120**(2): 164-172.
von Hunolstein, C., S. Mariotti, et al. (2001). "The adjuvant effect of synthetic oligodeoxynucleotide containing CpG motif converts the anti-Haemophilus influenzae type b glycoconjugates into efficient anti-polysaccharide and anti-carrier polyvalent vaccines." Vaccine **19**(23-24): 3058-3066.
Wang, E., O. Petrakova, et al. (2007). "Chimeric Sindbis/eastern equine encephalitis vaccine candidates are highly attenuated and immunogenic in mice." Vaccine **25**(43): 7573-7581.
Wang, T., T. Town, et al. (2004). "Toll-like receptor 3 mediates West Nile virus entry into the brain causing lethal encephalitis." Nat Med **10**(12): 1366-1373.
Watanabe, M., K. Suyama, et al. (2013). "Mumps virus-associated acute encephalopathy: case report and review of the literature." J Child Neurol **28**(2): 243-245.
Weaver, S. C. and A. D. Barrett (2004). "Transmission cycles, host range, evolution and emergence of arboviral disease." Nat Rev Microbiol **2**(10): 789-801.
Weiss, B., U. Geigenmuller-Gnirke, et al. (1994). "Interactions between Sindbis virus RNAs and a 68 amino acid derivative of the viral capsid protein further defines the capsid binding site." Nucleic Acids Res **22**(5): 780-786.
Weiss, B., H. Nitschko, et al. (1989). "Evidence for specificity in the encapsidation of Sindbis virus RNAs." J Virol **63**(12): 5310-5318.
Whitehead, S. S., J. E. Blaney, et al. (2007). "Prospects for a dengue virus vaccine." Nat Rev Microbiol **5**(7): 518-528.
Wong, A. D., M. Ye, et al. (2013). The blood-brain barrier: an engineering perspective, Front Neuroeng.
Woodman, D. R., A. T. McManus, et al. (1975). "EXTENSION OF MEAN TIME TO DEATH OF MICE WITH A LETHAL INFECTION OF VENEZUELAN EQUINE ENCEPHALOMYELITIS VIRUS BY ANTITHYMOCYTE-SERUM TREATMENT." Infection and Immunity **12**(5): 1006-1011.

Wu, J. Q., N. D. Barabe, et al. (2007). "Complete protection of mice against a lethal dose challenge of western equine encephalitis virus after immunization with an adenovirus-vectored vaccine." Vaccine **25**(22): 4368-4375.

Wust, C. J., J. A. Nicholas, et al. (1989). "Monoclonal antibodies that cross-react with the E1 glycoprotein of different alphavirus serogroups: characterization including passive protection in vivo." Virus Res **13**(2): 101-112.

Xie, H., I. Gursel, et al. (2005). "CpG oligodeoxynucleotides adsorbed onto polylactide-co-glycolide microparticles improve the immunogenicity and protective activity of the licensed anthrax vaccine." Infect Immun **73**(2): 828-833.

Xu, Z., R. Waeckerlin, et al. (2012). "West Nile virus infection causes endocytosis of a specific subset of tight junction membrane proteins." PLoS One **7**(5): 24.

Zaichick, S. V., K. P. Bohannon, et al. (2013). "The herpesvirus VP1/2 protein is an effector of dynein-mediated capsid transport and neuroinvasion." Cell Host Microbe **13**(2): 193-203.

Zaitseva, M., S. M. Kapnick, et al. (2009). "Application of Bioluminescence Imaging to the Prediction of Lethality in Vaccinia Virus-Infected Mice." Journal of Virology **83**(20): 10437-10447.

Zhang, Y., C. W. Burke, et al. (2007). "Identification and characterization of interferon-induced proteins that inhibit alphavirus replication." J Virol. 2007 Oct;81(20):11246-55. Epub 2007 Aug 8.

Zhao, H. and H. Garoff (1992). "Role of cell surface spikes in alphavirus budding." J Virol **66**(12): 7089-7095.

Zichis, J. and H. J. Shaughnessy (1945). "Successful Treatment of Experimental Western Equine Encephalomyelitis with Hyperimmune Rabbit Serum." Am J Public Health Nations Health **35**(8): 815-823.

Ziegler, S. A., J. Nuckols, et al. (2011). "In Vivo Imaging of Chikungunya Virus in Mice and Aedes Mosquitoes Using a Renilla Luciferase Clone." Vector-Borne and Zoonotic Diseases **11**(11): 1471-1477.

Zou, J., T. Kawai, et al. (2013). "Poly IC triggers a cathepsin D- and IPS-1-dependent pathway to enhance cytokine production and mediate dendritic cell necroptosis." Immunity **38**(4): 717-728.